

## **DELIVERY OF MICROENCAPSULATED CELLS TO THE CNS OF DOGS**

THE DELIVERY OF MICROENCAPSULATED NON-AUTOLOGOUS CELLS TO  
THE CENTRAL NERVOUS SYSTEM OF DOGS

By

SUSAN C. BARSOUM, B.Sc

A Thesis

Submitted to the School of Graduate Studies

In Partial Fulfillment of the Requirements

For the Degree

Master of Science

McMaster University

©Copyright by Susan C. Barsoum, September, 1999

MASTER OF SCIENCE (1999)  
(Biology)

McMaster University  
Hamilton, Ontario

TITLE: The Delivery of Microencapsulated Non-Autologous Cells to the Central  
Nervous System of Dogs

AUTHOR: Susan C. Barsoum, B.Sc.

SUPERVISOR: Dr. P.L. Chang

NUMBER OF PAGES: xi, 176

## ABSTRACT

Treatment for neurological diseases has been limited by the presence of the protective blood-brain barrier. Recent studies from our laboratory have shown that direct intraventricular implantation of microcapsules containing genetically modified cells can effectively deliver the transgene product to the mouse brain, thereby circumventing the blood-brain barrier. In this thesis, the experiments were aimed at scaling up the murine experiments to determine if direct implantation of alginate-poly-L-lysine-alginate microcapsules to the central nervous system of dogs was a feasible means of treating the large animal brain.

In the first two experiments reported here, microcapsules containing cells genetically modified to secrete human growth hormone were injected into the central nervous system of dogs. Two routes of delivery were examined, intraventricular brain surgery and injection into the spinal intrathecal space (cisterna magna). While empty capsules within the central nervous system were benign, microcapsules containing cells induced an acute inflammatory response in the brain and spinal cord tissue, irrespective of the route of delivery. Human growth hormone was detected transiently in four of six dogs, but the data were interpreted with caution due to extraneous variables such as compromised microcapsules in two of the dogs and previous systemic treatment in six of the other dogs.

In the last experiment, microcapsules containing cells genetically modified to secrete the lysosomal enzyme  $\alpha$ -L-iduronidase were implanted into the lateral ventricles of a dog with Mucopolysaccharidosis type I in an attempt to correct the characteristic neuronal pathology. An immune response ensued and appeared to abolish any possible effect of the microcapsule treatment.

The experiments presented here demonstrate the challenges and obstacles that need to be overcome to effectively scale up therapies from rodent experiments to large animals. The data also shed light on the immunological complications that may arise with invasive and repeated treatment in the central nervous system of large animals.

## ACKNOWLEDGEMENTS

I would like to thank Dr. P. Chang for taking me on as a Master's student. I would also like to thank my committee members, Dr. D. Harnish, Dr. K. Delaney and Dr. H. Szechtman, for their constant support and insight into my project. Many sincere thanks also go to Drs. K. Delaney, J. Kwiecien and A. Fletch for sharing their time, wisdom and expertise so generously with me. Also to the CAF staff, especially Tracy and Kelley, and the fine staff in EM, I would like to say thanks for your patience and exceptional technical assistance. I am also very grateful to the team at the University of Toronto, Dr. N. Milgram, Dr. W. MacKay, Heather Callahan, Antonio Medonca and Dr. W. Williams, for their partnership, time and intellectual input. Thanks also go to Dr. Coblentz for his time and assistance with the CT scans.

To Nicole MacDonald, Kelly Robinson, Lisa Kockeritz, Vanessa Williamson and Jeremy Van Raamsdonk, I would like to express my sincere thanks for your friendship, the fun times, support and encouragement throughout the last two years. Thanks to Colin, Nong and Gonzalo for your helpful discussions and advice. And to my family and friends outside the lab – Mom, Dad, Kristin, Amir, Henry, Nancy, Janina, Jonathan, Debs, Sam, Nabila, Mark, Eva, Moshe, Paul, Small Group and M.A.C – thank you all for your unconditional friendships, consistent encouragement, wisdom, prayers and love. I don't know what I would have done without you all!

## TABLE OF CONTENTS

THE DELIVERY OF MICROENCAPSULATED NON-AUTOLOGOUS CELLS TO THE CENTRAL NERVOUS SYSTEM OF DOGS -----	i
ABSTRACT -----	iii
AKNOWLEDGEMENTS -----	v
TABLE OF CONTENTS -----	vi
LIST OF FIGURES AND TABLES -----	x
LIST OF ABBREVIATIONS -----	xi
1.0 INTRODUCTION	
1.1.0 Somatic Gene Therapy -----	1
1.1.1 Gene Therapy for the Central Nervous System -----	1
1.1.1.0 Delivery -----	2
1.1.2 Viral Vectors -----	2
1.1.2.1 Retroviral Vectors -----	4
1.1.2.2 Adenoviral Vectors -----	5
1.1.2.3 Adeno-Associated Viral Vectors -----	6
1.1.2.4 Herpes Simplex Virus Type I Vectors -----	7
1.1.3 Non-autologous Somatic Gene Therapy -----	7
1.1.3.1 Microencapsulation -----	8
1.1.3.2 Microencapsulation in the Central Nervous System	9
1.2 The Cerebral Ventricular System	
1.2.0 Anatomy -----	11
1.2.1 Visualization -----	12
1.2.2 Cerebrospinal Fluid (CSF) -----	12
1.3 The Immune and Central Nervous Systems	
1.3.0 Inflammation -----	15
1.3.1 Immunologic Privilege -----	15
1.3.1.1 Blood-Brain Barrier (BBB) -----	16
1.3.1.2 Endothelial Adhesion Molecules at the BBB	17
1.3.1.3 Major Histocompatibility Complexes in CNS	18
1.3.1.4 Lymphatic Drainage-----	18
1.4 Mucopolysaccharidoses	
1.4.0 Background -----	19
1.4.1 MPS I (Hurler's Syndrome)	
1.4.1.0 Clinical Features -----	19
1.4.1.1 "Hurler Corrective Factor" -----	20

1.4.1.2	Pathology -----	21
1.4.1.3	Neuropathology -----	22
1.4.1.4	Neurological Consequences -----	23
1.4.1.5	Animal Models-----	24
1.4.2	Other MPSs and Their Animal Models -----	26
1.4.3	Treatment	
1.4.3.0	Bone Marrow Transplantation (BMT) -----	28
1.4.3.1	Enzyme Replacement Therapy -----	30
1.4.3.2	Gene Therapy -----	31
1.4.3.2.0	Retroviral Techniques -----	31
1.4.3.2.1	Adenoviral Techniques -----	33
1.4.3.2.2	Adeno-Associated Virus Techniques-----	33
1.4.3.2.3	Microencapsulation Techniques -	34
1.5	Rationale for Current Experiments -----	35
2.0	MATERIALS AND METHODS	
2.1	<i>In Vitro</i> Procedures -----	39
2.1.0	Cell Lines -----	39
2.1.1	Cell Encapsulation -----	40
2.1.2	Pre-Surgery Microcapsule Preparation -----	41
2.1.3	<i>In Vitro</i> Secretion Analysis -----	41
2.1.4	Cell Number per Capsule -----	41
2.1.5	Cell Viability Analysis -----	42
2.2	<i>In Vivo</i> Procedures	
2.2.0	Animals -----	42
2.2.1	Blood Collection -----	43
2.2.2	Canine Anaesthesia -----	43
2.2.3	Cerebrospinal Fluid Collection -----	43
2.2.4	Spinal Intrathecal Implantation-----	44
2.2.5	Computed Tomography Scan -----	44
2.2.6	Intraventricular Implantation -----	45
2.2.7	Post-Surgical Care -----	46
2.2.8	Neurological Examination -----	46
2.2.9	Euthanasia -----	47
2.3	Quantitative Analysis	
2.3.0	Tissue Processing -----	48
2.3.1	Human Growth Hormone ELISA -----	48
2.3.2	Anti-Human Growth Hormone Antibody Assay -----	49
2.3.3	$\alpha$ -L-Iduronidase Activity Assay -----	50
2.3.4	Anti- $\alpha$ -L-Iduronidase Antibody Assay-----	50
2.3.5	Protein Assay -----	51
2.4	Pathology	
2.4.0	Tissue Processing and Embedding -----	52
2.4.1	Tissue Staining -----	53

2.4.2 Immunohistochemistry -----	54
<b>3.0 DELIVERY OF HUMAN GROWTH HORMONE-SECRETING MICROCAPSULES TO THE CENTRAL NERVOUS SYSTEM OF DOGS</b>	
3.1 Rationale -----	57
3.2 Materials and Methods	
3.2.1 Animals -----	57
3.2.2 CNS Treatment -----	57
3.2.3 Analyses -----	58
3.3 Results	
3.3.1 Post-operative Clinical Assessment -----	59
3.3.2 Post-mortem Analyses -----	59
3.3.3 Microcapsule Cell Viability and Secretion Analysis -----	60
3.3.4 Quantitative Analysis -----	60
3.3.5 Pathology -----	61
<b>4.0 DELIVERY OF MICROCAPSULES WITH VARYING CONTENTS TO THE CENTRAL NERVOUS SYSTEM OF PREVIOUSLY TREATED DOGS</b>	
4.1 Rationale -----	78
4.2 Materials and Methods	
4.2.1 Animals -----	79
4.2.2 Central Nervous System Treatment -----	79
4.2.2.1 Spinal Intrathecal Implantation -----	79
4.2.2.2 Intraventricular Implantation -----	80
4.2.3 Analyses -----	81
4.3 Results	
4.3.1 Clinical Evaluation -----	81
4.3.2 Post-Mortem Analyses	
4.3.2.1 Spinal Intrathecal Implantations -----	82
4.3.2.2 Intraventricular Implantations -----	83
4.3.3 Microcapsule Cell Viability and Secretion Analyses -----	84
4.3.4 Quantitative Analyses -----	85
4.3.5 Pathology	
4.3.5.1 Spinal Intrathecal Implantations -----	86
4.3.5.2 Intraventricular Implantations -----	88
<b>5.0 DELIVERY OF <math>\alpha</math>-L-IDURONIDASE-SECRETING MICROCAPSULES TO THE BRAIN OF A DOG WITH MUCOPOLYSACCHARIDOSIS TYPE I</b>	
5.1 Rationale -----	119
5.2 Materials and Methods	
5.2.1 Animals -----	119
5.2.2 Intraventricular Implantation -----	120

5.2.3 Analyses	-----	120
5.3 Results		
5.3.1 Clinical Evaluation	-----	121
5.3.2 Post-mortem Evaluation	-----	122
5.3.3 Microcapsule Cell Viability and Secretion Analyses	-----	123
5.3.4 Quantitative Analyses	-----	124
5.3.5 Pathology	-----	124
6.0 DISCUSSION	-----	149
6.1 Microcapsule Implantation Techniques	-----	150
6.2 Product Delivery	-----	151
6.3 Immune Response	-----	153
6.4 MPS I	-----	154
6.5 Areas for Further Research	-----	155
6.6 Conclusion	-----	156
APPENDIX A	-----	157
APPENDIX B	-----	161
REFERENCES	-----	166

## LIST OF FIGURES AND TABLES

<b>Table 1-1</b>	Sequential Enzymatic Degradation of Heparan Sulfate -----	37
<b>Table 1-2</b>	Sequential Enzymatic Degradation of Dermatan Sulfate -----	38
<b>Figure 2-1</b>	Surgical Methods -----	55
<b>Table 3-1</b>	Encapsulated Cell Viability and Secretion -----	63
<b>Figure 3-1</b>	Coronal Brain Section (Dana) -----	64
<b>Figure 3-2</b>	Delivery of hGH to the CSF and Plasma -----	66
<b>Figure 3-3</b>	Delivery of hGH to Various Brain Regions -----	68
<b>Figure 3-4</b>	Detection of Antibody to hGH in CSF and Plasma -----	70
<b>Figure 3-5</b>	Histological Sections – Dino -----	72
<b>Figure 3-6</b>	Immunohistochemistry – Dino -----	74
<b>Figure 3-7</b>	Histological Sections – Dana -----	76
<b>Table 4-1</b>	Summary of Previous and Current Microcapsule Implants -----	90
<b>Table 4-2</b>	Encapsulated Cell Viability and Secretion -----	91
<b>Table 4-3</b>	White blood cell and microprotein content -----	92
<b>Figure 4-1</b>	Representative CT Scan from Jewel -----	93
<b>Figure 4-2</b>	Post-mortem Brain Examination (Jewel) -----	95
<b>Figure 4-3</b>	Post-mortem Brain Examination (Smudge) -----	97
<b>Figure 4-4</b>	Microcapsules -----	99
<b>Figure 4-5</b>	Delivery of hGH to the CSF and Plasma -----	101
<b>Figure 4-6</b>	Delivery of hGH to Various Brain Regions -----	103
<b>Figure 4-7</b>	Detection of Antibody to hGH in CSF and Plasma -----	105
<b>Figure 4-8</b>	Histological Sections – Jazz -----	107
<b>Figure 4-9</b>	Histological Sections – Squirt -----	109
<b>Figure 4-10</b>	Histological Sections – Polly -----	111
<b>Figure 4-11</b>	Histological Sections – Jewel -----	113
<b>Figure 4-12</b>	Immunohistochemistry – Jewel -----	115
<b>Figure 4-13</b>	Histological Sections – Smudge -----	117
<b>Figure 5-1</b>	MPS I dog (Quincy) -----	127
<b>Figure 5-2</b>	Pre-surgery CT Scan from Quincy -----	129
<b>Figure 5-3</b>	Post-surgery CT Scan from Quincy -----	131
<b>Figure 5-4</b>	Coronal Brain Section (Quincy) -----	133
<b>Figure 5-5</b>	$\alpha$ -L-Iduronidase Activity in Various Brain Regions -----	135
<b>Figure 5-6</b>	Antibody Against $\alpha$ -L-Iduronidase in CSF and Plasma -----	137
<b>Figure 5-7</b>	Histological Sections - Buick -----	139
<b>Figure 5-8</b>	Histological Sections – Quincy -----	141
<b>Figure 5-9</b>	PAS Staining of Cerebellar Purkinje Cells (Quincy) -----	143
<b>Figure 5-10</b>	Histological Examination of Olivary Nucleus (Quincy) -----	145
<b>Figure 5-11</b>	Toluidine Blue – Neurons (Quincy) -----	147

## LIST OF ABBREVIATIONS

$\alpha$	alpha
APA	alginate-poly-L-lysine-alginate
AAV	adeno-associated virus
$\beta$	beta
BBB	blood-brain barrier
BMT	bone marrow transplantation
CaCl <sub>2</sub>	calcium chloride
CHES	2-(N-Cyclohexylamino)ethanesulfonic acid
CNS	central nervous system
CSF	cerebrospinal fluid
CNTF	ciliary neurotrophic factor
ELISA	enzyme-linked immunosorbent assay
GFAP	glial fibrillary acidic protein
H&E	hematoxylin and eosin
HSV-I	herpes simplex virus type I
hGH	human growth hormone
HCl	hydrochloric acid
HIV	Human Immunodeficiency Virus
4-MU	4-Methylumbelliferyl
MDCK	Madin-Darby Canine Kidney Cells
mg	milligram
$\mu$ l	microlitre
mM	millimolar
M	molar
MPS	Mucopolysaccharidosis
ng	nanograms
PAS	periodic-acid schiff
PLL	poly-L-lysine

## **1.0 INTRODUCTION**

### **1.1.0 Somatic Gene Therapy**

Somatic gene therapy holds great promise for the future treatment of genetic diseases. “Gene therapy” refers to the ultimate goal of providing a gene so that its therapeutic product can be expressed in the appropriate tissue, while the term “somatic” refers to the cells that will be treated, that is, cells that are neither sperm nor egg (Chang, 1995).

DNA is commonly delivered to patients by one of two means, the *in vivo* or the *ex vivo* methods. With the *in vivo* approach, vectors carrying the desired gene (eg. viral vectors) are introduced directly into the body. Alternatively, scientists may remove cells from the patient, transfer the genes *in vitro* and return the genetically modified cells to the individual. This alternative method is referred to as the *ex vivo* approach (Friedmann, 1997). In both cases, the genetically corrected cells belong to the patient who is being treated (autologous), thereby preventing immune rejection of the DNA.

#### **1.1.1 Gene Therapy for the Central Nervous System**

Inherent properties of the central nervous system (CNS) present a unique, protected environment for the brain. These properties have provided interesting challenges for the treatment of neurological disease.

Unlike most cells in the body, neurons have non-proliferative and non-regenerative phenotypes. Unfortunately, this results in poor prognoses for neurological illnesses since neurons that die are normally lost forever (Ridet and Privat, 1995). Gene

therapeutics, therefore, must aim at preventing cell death or finding ways of replacing the function of lost neurons.

After having developed a therapeutic goal, the major challenge in treatment of the nervous system comes from the relative inaccessibility of the brain. The brain is protected from large systemic molecules and daily biochemical fluctuations by the blood-brain barrier (BBB). The physical properties of this barrier will be discussed in more detail in section 1.3.1.1. Briefly, the cerebral capillary endothelial cells are specialized in such a way that large molecules are inhibited from entering the brain environment. While the BBB serves to protect the brain, it contributes a major obstacle for neurological therapeutic intervention, since corrective drugs or enzymes secreted into the blood cannot gain access to the CNS.

Despite the hurdles that the CNS creates for neurological treatment, there have been some major advances in gene therapy techniques that have been applied in various disease models such as Parkinson's disease (Horellou et al., 1994a, 1994b; Raymon et al., 1997; Kang, 1998), Alzheimer's disease (Tuszynski et al., 1996; Zlokovic and Apuzzo, 1997a), amyotrophic lateral sclerosis (ALS) (Aebischer et al., 1996a, 1996b), brain tumours (Kennedy, 1997; Long et al., 1998; Tamura et al., 1998) and the mucopolysaccharidoses (see section 1.4.3.2).

### **1.1.1.0 Delivery**

Several different methods have been developed to by-pass the BBB to deliver genes and/or their therapeutic products to the brain. These techniques include direct

injection or infusion of the therapeutic vector into the brain tissue or cerebral ventricular system. Direct injection is advantageous for localized disorders and good responses have been seen in small animals. However, drawbacks include the invasive nature of brain surgery and limited treatment distribution in large brains due to long diffusion distances (Zlokovic and Apuzzo, 1997b).

Another method developed to circumvent the barrier is transient osmotic opening of the BBB (Kroll and Neuwelt, 1998). The idea here is to administer a hyperosmotic solution thereby transiently shrinking the endothelial cells and loosening their tight junctions. While this may be an effective means of globally treating the CNS, there are obvious risks to exposing the brain to potential systemic toxins, such as excitotoxic amino acids (Zlokovic and Appuzzo, 1997b).

### **1.1.2 Viral Vectors**

Many experimental gene therapy protocols have been exploring the use of viruses as a means of delivering potentially therapeutic genes to cells. They have been considered a worthwhile area of investigation because of their naturally efficient mechanisms of introducing DNA into target cells (Hermens and Verhaagen, 1998). The major areas in viral vector research have focused on the retrovirus, adenovirus, adeno-associated virus and herpes simplex virus systems.

The viral vectors currently being investigated each have their own inherent advantages and disadvantages. While different strategies will be necessary for each therapeutic goal, some of the ideal qualities of a vector for neurological treatment include

(1) the ability to transduce post-mitotic cells, such as neurons, (2) replication defective characteristics to prevent viral spread, (3) non-toxic and non-immunogenic properties and (4) the ability to provide long-term, stable delivery of the therapeutic product (Hermens et al., 1998; Lachmann et al., 1999). The following sections will provide a brief overview of each of the mentioned viral vectors and their potential utility for use in the CNS.

### **1.1.2.1 Retroviral Vectors**

The retrovirus has been a particularly attractive vector for gene therapy purposes owing to its ability to efficiently integrate copies of genes into the chromosomes of the cells they invade. This feature provides the advantage of potential long-term correction passed on to future generations of the infected cells (Friedmann, 1997). However, it should be noted that chromosomal integration carries with it the risk of insertional mutation, that is, the possibility that a transferred gene will insert itself into an inappropriate position on the chromosome thereby disrupting normal cellular activity.

Retroviral vectors have been used in the brain, however their utility is limited by the fact that they are unable to infect non-dividing cells, such as neurons. (Karpati et al., 1996). Although often considered a disadvantage for neurological treatment, this property has been exploited for targeting and treating rapidly dividing brain tumours (Long et al., 1998; Tamura et al., 1998).

The use of retroviruses in the CNS may be expanding with the recent advances in the lentivirus, human immunodeficiency virus (HIV). The HIV is capable of infecting post-mitotic cells, and its utility for CNS treatment was demonstrated with the introduction of  $\beta$ -galactosidase and green fluorescent protein into the striatum or hippocampus of adult rats (Naldini et al., 1996). After 9 months, the average transgene expression levels remained high and no sign of an immune reaction was observed (Blomer et al., 1997). However, strict biosafety procedures are necessary for the production of a safe virus. Research is currently aimed at producing recombinant retroviruses that will combine the efficiency of HIV with the safety features of the more common retroviruses (Naldini and Verma, 1999; Suhr and Gage, 1999).

### **1.1.2.2 Adenoviral Vectors**

The adenovirus is considered a promising vector for neurological treatment owing to its ability to infect non-dividing cells. It has been used in experimental models such as Parkinson's disease, motor neuron degenerative diseases and Alzheimer's disease (Horellou et al., 1997a, 1997b; Barkats et al., 1998). The adenovirus does not insert its genes into the cellular genome and thus avoids the risks of insertional mutation.

An interesting property of adenoviral vectors in terms of CNS treatment is its ability to be transported retrogradely from the site of injection. In an experiment by Ghadge et al. (1995), researchers showed that recombinant adenovirus injected into the muscle could be transported in a retrograde manner through the motor neuron axons to the cell bodies in the spinal cord. This property thus provides a means of infecting

difficult to reach neuronal populations, such as the motor neurons of the spinal cord (Barkats et al., 1998).

The major obstacle to adenoviral usage is its tendency to elicit strong inflammatory reactions both peripherally and in the CNS resulting in short-term delivery as well as cellular damage (Yang et al., 1994a; Byrnes et al., 1995; Barkats et al., 1998; Parr et al., 1998). New generations of adenoviral vectors are being investigated for the purpose of reducing and/or eliminating this destructive property. Increased transgene expression and decreased cellular immune responses have been reported with vectors that have increased deletions in the adenoviral genome (Engelhardt et al., 1994; Yang et al., 1994b; Chen et al., 1997).

### **1.1.2.3 Adeno-Associated Viral Vectors**

Adeno-associated viruses (AAV) are small, non-pathogenic vectors that insert their DNA into the host cells' chromosomes (Karpati et al., 1996). The AAV may be a useful vector for multi-system diseases due to their ability to target a variety of cell types, including neurons, by integration into the hosts' genome (Daly et al., 1999; Samulski et al, 1999).

The AAV has been shown to induce long-term expression in several mammalian brain disorder models including the rodent and primate models of Parkinsons' disease (Kaplitt et al., 1994; During et al., 1998) and the rodent experimental glioma model (Okada et al., 1996). While this vector is considered non-toxic and non-immunogenic

since it has never been associated with any clinical disease, the *in vivo* risks have not been fully characterized (Karpati et al., 1996)

#### **1.1.2.4 Herpes Simplex Virus Type I (HSV-I) Vectors**

The herpes simplex virus type I (HSV-I) is another promising vector for neuronal gene therapy owing to its natural abilities to transduce post-mitotic cells, maintain infection of the host cells despite immune responses and potentially accommodate large or multiple transgenes (Lachmann and Efstathiou, 1999; Laquerre et al., 1999). One of the obstacles for long-term HSV-I usage is the fact that this virus goes into latency, thus preventing expression of the desired genes. To overcome this hurdle, researchers have designed recombinant HSV vectors in which the therapeutic gene is driven by one of the latency promoters (Karpati et al., 1996). The major disadvantage of HSV vectors are their cytotoxic properties, that is, they have been observed to induce fatal encephalitis when the wild type HSV is injected into the brains of animals (Lachmann and Efstathiou, 1999).

#### **1.1.3 Non-autologous Somatic Gene Therapy**

Autologous somatic gene therapy is a labour intensive and costly form of treatment. Further, not all cell types can be easily obtained for transduction, for example, brain cells. For these reasons, researchers have devoted much time to the development of non-autologous methods with the vision of establishing a universal cell line that can be safely developed and delivered to anyone in the general population (Chang, 1995).

### **1.1.3.1 Microencapsulation**

Clearly, a major problem for the vision of non-autologous transplantation of cells is rejection by the immune system/graft rejection. In 1980, Lim and Sun showed that implantation of microencapsulated pancreatic islet cells in diabetic rats corrected the diabetic state and provided the necessary immunoprotection for the cells to remain viable. Encapsulating genetically modified cells within a biocompatible semi-permeable membrane provides protection for the cells from immune mediators while allowing diffusional exchange of necessary nutrients and metabolites with the environment as well as secretion of the gene product (Aebischer et al., 1988; Tai and Sun, 1993; Al Hendy et al., 1996; Chang, 1995).

Different immuno-isolation devices have been developed to maximize cell viability, gene product secretion, biocompatibility and mechanical stability. The most common materials for encapsulation procedures include biocompatible plastics such as polyacrylonitrile-polyvinyl chloride (PAN-PVC) and the seaweed extract alginate (Smidsrod and Skjak-Braek, 1990). These devices range in size from the microcapsule droplets (~500µm diameter) to macrocapsules (centimeters in length) (Lysaght and Aebischer, 1999). The advantages to the larger macrocapsules are that they are more durable than microcapsules and can be retrieved simply. Microcapsules, however, have a greater surface to volume ratio to help in diffusion and can be more easily implanted by injection (Stockley and Chang, 1997).

Both macro- and microcapsules have been used widely in various animal models. Encapsulation technology has been demonstrated as a feasible means of protecting various cell types from the immune system while delivering relevant levels of recombinant gene products to mice, such as growth hormone (Chang et al., 1993; Al-Hendy et al., 1995) and human factor IX (Liu et al., 1993; Hortelano et al., 1996).

Microencapsulation technology is also a valuable tool for neurological treatment since, although grafts in the brain of animals have been reported to survive for longer periods than those in the periphery, rejection eventually occurs unless an immunosuppressant drug is administered (Aebischer et al., 1988). Further, cell grafts may not show prolonged gene expression and may produce tumors (Doering and Chang, 1991; Hoffman et al., 1993).

### **1.1.3.2 Microencapsulation in the Central Nervous System**

The feasibility of encapsulation techniques in the CNS have been demonstrated with the delivery of various gene products in several different animal models.

Cell encapsulation technology has shown particular promise for the treatment of Parkinson's disease as demonstrated in both rodent and primate models of this disorder (Winn et al., 1989a; Aebischer et al., 1991; Winn et al., 1991; Aebischer et al., 1994; Emerich et al., 1996; Sautter et al., 1998). When dopamine secreting cells were encapsulated and implanted into the striatum of rats or monkeys, behavioural improvements, such as reductions in apomorphine-induced rotational behaviour, were observed (Winn et al., 1991; Aebischer et al., 1994a; Emerich et al., 1996). These

experiments as well as others also demonstrated that the encapsulated cells remained viable and able to secrete their products in the brain environment while the capsules produced only minimal tissue damage that diminished with time (Aebischer et al., 1988; Winn et al., 1989b).

Encapsulation technology has also been shown to be useful in the delivery of neurotrophic factors such as nerve growth factor (NGF), glial cell-derived neurotrophic factor (GDNF) and ciliary neurotrophic factor (CNTF) (Hoffman et al., 1993; Emerich et al., 1994b; Lindner et al., 1995; Deglon et al., 1996; Winn et al., 1996). These factors have shown therapeutic benefits in rodent and primate models of Huntington's disease, (Emerich et al., 1996b, 1997), Alzheimer's disease (Emerich et al., 1994a; Kordower et al., 1994) and a mouse model for amyotrophic lateral sclerosis (ALS) (Sagot et al., 1995).

Delivery of therapeutic products in the brains of various animals has demonstrated the potential for the use of encapsulated cells for human treatment. However, several issues still need to be addressed such as the number or volume of devices that will be necessary to provide therapeutic levels of product to the large human brain. Also, many human diseases require long-term treatment and the ability for encapsulated cells to remain viable and effective for long-term periods (years) has yet to be shown (Lindner and Emerich, 1998). Nevertheless, phase I clinical trials have been underway for several years now to assess the safety and efficacy of spinal intrathecal implantations of macrocapsules for the alleviation of pain (Aebischer et al., 1994b) and treatment of ALS (Aebischer et al., 1996a, 1996b; Ponchon et al., 1996).

## **1.2 THE CEREBRAL VENTRICULAR SYSTEM**

### **1.2.0 Anatomy**

The cerebral ventricular system consists of four continuous fluid-filled cavities within the CNS. Developing from the hollow neural tube, the ventricular system forms early in development, with an ependymal cell lining developing later from surrounding germinal matrix cells (Fishman, 1992; Del Bigio, 1995). The ventricular system is comprised of paired lateral ventricles, one within each cerebral hemisphere, a midline third ventricle, a single fourth ventricle and narrow passages which allow these liquid-filled spaces to communicate.

The lateral ventricles are C-shaped cavities frequently divided anatomically into five different regions (Nolte, 1993). The anterior horn commences within the frontal cortex and leads to the body of the ventricle located within the frontal and parietal lobes. The third portion, termed the posterior horn, projects caudally towards the occipital cortex where it turns in a ventral direction to form the inferior horn and atrium. The paired ventricles are bordered laterally by the caudate nucleus (superior border at the inferior horn) and ventrally by the thalamus.

By way of the interventricular foramen, the lateral ventricles are connected to the single, midline third ventricle. Bordered ventrally by the infundibulum and surrounding the intrathalamic adhesion, the third ventricle is continuous with the fourth ventricle by the cerebral aqueduct, passing through the midbrain. The fourth ventricle is bordered by the cerebellum posteriorly, and the pons and medulla anteriorly. From the fourth ventricle, fluid may flow to the subarachnoid space surrounding the outer surface of the

brain and spinal cord via three openings – the median foramen of Magendie and the two lateral foramina of Luschka (Nolte, 1993). Alternatively, the fluid can remain within the ventricular system, flowing from the fourth ventricle through the central canal of the spinal cord.

### **1.2.1 Visualization**

Historically, the ventricular system was visualized in animals with a radiographic technique termed ventriculography. Air was the safest and most frequently used contrast agent and was injected into each lateral ventricle. The ventricles, and any changes in size or lesions, could then be observed through radiographs (Oliver Jr and Conrad, 1975). A similar technique, pneuencephalography, was used in humans (Nolte, 1993) to provide information regarding ventricular shape. In the 1980's these techniques were replaced by the more sensitive computed tomography, or CT scanning. During a CT scan, x-rays are directed through the patient's head at various angles, producing a collection of computer analyzed density profiles. With this technique, even grey and white matter can be distinguished in spite of the small differences in radiodensity. Hence, the cerebral ventricles can be visualized on the basis of density differences between the fluid and brain matter (Nolte, 1993; Martin et al., 1991).

### **1.2.2 Cerebrospinal Fluid (CSF)**

The clear, colourless fluid within the ventricular system and subarachnoid space is referred to as the cerebrospinal fluid (CSF). The CSF is produced by a membranous

vascular tissue termed the choroid plexus located within the lateral, third and fourth ventricles. The CSF is produced at a rate of  $0.18\mu\text{l}/\text{min}/\text{mg}$  choroid plexus or approximately  $0.5\text{L}/\text{day}$  in the human, and  $0.63\mu\text{l}/\text{min}/\text{mg}$  choroid plexus or approximately  $72\text{ml}/\text{day}$  in the dog (Rosenberg, 1990). This fluid is formed by the filtration of blood through the fenestrated capillaries of the choroid plexus, followed by the active transport of ions and passive transport of water. It is composed primarily of water (99%) and ions (sodium, chloride, magnesium, potassium and bicarbonate) with very low protein and cell counts (Fishman, 1992; Rosenberg, 1990). Although the passage of filtrate from the capillary system into the choroid plexus is non-selective, tight junctions between the choroidal epithelial cells prevent unwanted substances, such as proteins, from entering the CSF (Nolte, 1993). Since there is an uninterrupted association between the CSF and the extracellular milieu of the brain, this blood-CSF barrier plays an important part in maintaining a stable environment for the brain (Cserr et al., 1992; Nolte, 1993; Rosenberg, 1990).

The CSF serves a supportive function within the nervous system. By bathing the brain and spinal cord, the CSF produces a buoyant effect, providing cushioning and protection against mechanical or physical injury (Nolte, 1993). Further, it serves to regulate the extracellular environment of the neurons, both by its regulated production and its apparent “sink action” for cellular waste (Del Bigio, 1995). Finally, it is believed that the CSF provides a pathway for drainage to the lymphatic system for the regulation of interstitial fluid volume and immune function (Cserr et al., 1992; Fishman, 1992; Yamada et al., 1991).

The major sites of CSF reabsorption into the venous and lymphatic systems are the arachnoid villi (Nolte, 1993; Rosenberg, 1990). These villi, or granulations, accomplish unidirectional flow of CSF by one-way valves that open only when the CSF pressure is higher than the opposing blood pressure (Rosenberg, 1990). The alternative route for CSF drainage is by way of prolonged subarachnoid space along the olfactory, optic, trigeminal or acoustic cranial nerves (Bradbury and Cserr, 1985; Hart and Fabry, 1995) and along spinal nerve root ganglia (Cserr et al., 1992).

## **1.3 THE IMMUNE AND CENTRAL NERVOUS SYSTEMS**

### **1.3.0 Inflammation**

Inflammation is a process whereby the host's immune system responds to an invasion by a foreign body to eliminate the harmful agent and begin the process of healing and repair (Robbins et al., 1994). The inflammatory response can be classified as acute or chronic, based on the duration and histological features of the reaction. Acute inflammation can be as short as a few minutes or as long as several days. It is characterized by edema and the movement of leukocytes across the endothelial lining of blood vessels into tissue parenchyma (Robbins et al., 1994). The chronic inflammatory reaction may last from weeks to months and is characterized by the presence of T-lymphocytes and macrophages. Although the inflammatory process continues, tissue destruction as well as repair processes may be occurring simultaneously during a chronic reaction (Robbins et al., 1994).

### **1.3.1 Immunologic Privilege**

The brain has classically been defined as a site of "immunologic privilege", that is, protected from typical immune system reactions, such as inflammation. Although recent findings have shown that this privilege is not absolute, the central nervous system is still considered to be a protected environment. Several characteristics of the CNS have contributed to this protective mechanism. The following section will describe the immune privilege status of the brain as well as some of the emerging re-evaluation of CNS – immune system interactions.

### **1.3.1.1 Blood-Brain Barrier (BBB)**

The blood-brain barrier (BBB) is a boundary between the brain and the rest of the body (via the blood) necessary to safeguard the CNS from daily peripheral biochemical fluctuations, thereby providing a stable environment for brain activity. The anatomical basis for such a barrier lies in specific cerebral endothelial cell features. First, the endothelial cells of cerebral blood vessels can be found lined with astrocyte projections, termed glial end-feet. Although the function of end-feet have not been fully elucidated, they are thought to affect capillary permeability (Rowland et al., 1991; Zlokovic and Apuzzo, 1997b).

Unlike peripheral blood vessels, there is little intercellular communication between the endothelial cells of cerebral blood vessels. This can be accounted for by complex high resistance tight junctions, the second feature of cerebral endothelial cells that allows for the maintenance of the BBB (Rowland et al., 1991). Lastly, the BBB can be partially attributed to a scarcity of pinocytotic vesicles thus preventing movement of compounds through the cells. Large molecules will be rejected at the BBB unless specialized transport systems are in place to carry them across, such as those identified for essential amino acids (Hart and Fabry, 1995; Zlokovic and Apuzzo, 1997b)

Since immune mediators are relatively large molecules, the BBB plays a major role in maintaining the status of immunologic privilege by preventing their entry. While this blockade was once believed to be absolute, evidence has emerged that members of the immune system are capable of passing the BBB under specific conditions, such as immune mediated illnesses (Hickey et al., 1991).

### **1.3.1.2 Endothelial Adhesion Molecules at the BBB**

Endothelial adhesion molecules are essential for the passage of lymphocytes from the blood to tissue parenchyma. These selectins, integrins or immunoglobulins are expressed on blood vessel surfaces and may be induced by inflammatory mediators, particularly cytokines (Robbins et al., 1994). By interacting with leukocyte receptors on the activated cells, the leukocytes adhere to the endothelium and can thereby transmigrate and pierce the basement membrane for entry into the tissue (Robbins et al., 1994).

Until recently, it was commonly believed that the immune privileged status of the CNS was partially the result of a lack of endothelial adhesion molecules on cerebral blood vessels. When activated T-cells and monocytes/macrophages were shown to be able to pass through the intact BBB (Hickey et al., 1991; Lassmann, 1997), researchers began to investigate how the penetration might occur. Such studies led to the current understanding that endothelial adhesion molecules are in fact expressed in low quantities at the BBB.

In 1992, Rossler et al. showed that the leukocyte adhesion molecules were expressed at the human BBB in low levels, thus providing a means of entry for lymphocytes. Further, these adhesion molecules were shown to be upregulated in brain tumours or under inflammatory conditions, consistent with the understanding that endothelial adhesion molecules are upregulated by the secretion of proinflammatory cytokines (Rossler et al., 1992; Lassmann, 1997).

### **1.3.1.3 Major Histocompatibility Complexes in the CNS**

Antigen recognition by the T-cell requires presentation of the foreign substance to the T-cell in association with major histocompatibility complexes (MHC) class I or II molecules. Until recently, it was believed that MHC expression, specifically class II, did not occur in the brain and thus antigen presentation could not be achieved. However, it has been shown that several cell types do indeed express class II MHC and can function as antigen presenting cells (McCarron et al., 1990), specifically astrocytes and microglia/macrophages (Hart and Fabry, 1995; Gehrman et al., 1995). A recent study also showed that MHC class I molecules could be induced in functionally impaired neurons suggesting that cytotoxic T-cells might focus their surveillance on these cells (Neumann et al., 1995).

### **1.3.1.4 Lymphatic Drainage**

The final feature that was thought to contribute to immunologic privilege of the CNS was an apparent lack of lymphatic drainage. Like the other features, researchers eventually showed that lymphatic drainage of the CSF does occur as briefly described in section 1.2.2 (Cserr et al., 1992). Although the brain does not house any lymphatic vessels, antigen injected into the brain or CSF can be detected in the deep cervical lymph nodes via the arachnoid villi with antibody production deep cervical lymph nodes and in the spleen (Cserr et al., 1992; Boulton et al., 1996).

## **1.4 MUCOPOLYSACCHARIDOSES**

### **1.4.0 Background**

The mucopolysaccharidoses (MPSs) are a family of lysosomal storage disorders resulting from deficiencies in one of several enzymes necessary for the degradation of mucopolysaccharides (glycosaminoglycans). As a result, undegraded molecules accumulate intracellularly thereby disrupting normal cellular function in various organs. All the MPSs are recessively inherited, exhibit a broad spectrum of clinical features, and appear with a combined frequency of 1 in 1500 live births (Neufeld and Muenzer, 1989).

### **1.4.1 MPS I (Hurler's Syndrome)**

#### **1.4.1.0 Clinical features**

MPS I, or Hurler's Syndrome, was first described by Gertrud Hurler in 1919. With an incidence of about 1 in 100,000 live births (Lowry and Renwick, 1971), it is considered the prototype MPS and the most severe. This disease is a result of a deficiency in the lysosomal enzyme  $\alpha$ -L-iduronidase. Clinical symptoms usually develop during the first year of life and progressive deterioration occurs thereafter with patients rarely living beyond ten years of age (McKusick and Neufeld, 1983). The clinical spectrum is broad, but typical features include corneal clouding, large tongue, enlargement of the liver and spleen, dwarfed stature, stiff joints, mental retardation and a variety of skeletal abnormalities (McKusick and Neufeld, 1983; Scott et al., 1993).

Two other forms of  $\alpha$ -L-iduronidase deficiency also exist – Scheie syndrome and the intermediate Hurler-Scheie syndrome. Scheie syndrome is considered the least severe of the  $\alpha$ -L-iduronidase deficiencies with patients demonstrating normal stature and intelligence. Affected children present with corneal clouding, skeletal abnormalities, joint stiffness and aortic valve disease with few other somatic problems (Meunzer, 1986). Hurler-Scheie syndrome is characterized by normal intelligence and progressive development of somatic MPS symptoms with an onset usually occurring between the ages of three to eight years. Clinical features include corneal opacity, joint stiffness and deafness (Muenzer, 1986).

#### **1.4.1.1 The “Hurler Corrective Factor”**

In the early 1970’s, researchers worked with fibroblasts from Hurler and Hunter (MPS II) patients to characterize the accumulation glycosaminoglycans. In normal cells, the mucopolysaccharide has a half-life of about 8 hours. In contrast, Hurler and Hunter cells showed mucopolysaccharide half-lives of 2-6 days (Neufeld and Fratantoni, 1970). In their classic Science paper, Neufeld and Fratantoni (1970) showed that when fibroblasts from both types of patients were mixed, glycosaminoglycan degradation defects were cancelled out and normal mucopolysaccharide metabolism was achieved. They suggested the presence of a corrective factor released into the media by one cell type that could compensate for the genotypic defect found in the other. The “Hurler corrective factor” was later purified, described and identified as  $\alpha$ -L-iduronidase (Barton and Neufeld, 1971; Bach et al., 1972).

$\alpha$ -L-iduronidase is a lysosomal enzyme of molecular weight 87,000 that cleaves the terminal iduronic acid residues from heparan and dermatan sulfate (Gielsmann, 1995). This enzyme is lacking in MPS I patients as a result of mutations in the  $\alpha$ -L-iduronidase gene, localized to chromosome 4p16.3 (Moskowitz et al, 1992; Scott et al, 1993). More than 50 mutations of the  $\alpha$ -L-iduronidase gene have been identified including mis-sense (mutations leading to insertion of a different amino acid into the protein), non-sense (mutations leading to a premature termination codon) and point mutations (substitution of one base pair for another) (Scott et al., 1993; Russel, 1996; Huang et al, 1997).

#### **1.4.1.2 Pathology**

The consequence of a deficiency in  $\alpha$ -L-iduronidase is the accumulation of undegraded glycosaminoglycans leading to cellular and organ dysfunction. Intracellular vacuolization can be visualized at the light microscope level in the heart, cartilage, tendons, bone, blood vessels, cornea, liver, spleen, kidney and brain (Cervos-Navarro and Urich, 1995). Electron microscopy studies showed that the cellular inclusions were primarily localized to the lysosomes (McKusick and Neufeld, 1983). These inclusions have been shown to contain glycosaminoglycans, specifically heparan and dermatan sulfate (Constantopoulos et al., 1976).

### 1.4.1.3 Neuropathology

Upon whole brain examination of MPS I patients by CT scanning, magnetic resonance imaging (MRI) or at post-mortem, several characteristic features are noted. The leptomeninges appear opaque and thickened, the ventricles often appear dilated (hydrocephalus), the spinal cord is compressed and atrophy of the white matter in the cerebral and cerebellar cortices is observed (Cervos-Navarro and Urich, 1995; Meunzer, 1986; Gabrelli et al., 1992; Tandon et al., 1996).

Histological analysis of CNS tissue reveals increased collagen in the leptomeninges with vacuolated cells, thus accounting for the gross cloudy and thick appearance. Lysosomal inclusions are observed within glial cells, cerebral blood vessels and neurons (Watts et al., 1981). Gliosis is observed in both the grey and white matter of the cerebral cortex while blood vessel walls are thickened and lined with vacuolated pericytes.

Neuronal pathology appears to most severely affect the large cells of the cerebral cortex, brain stem, cerebellum (Purkinje cells), spinal cord and midbrain (Cervos-Navarro and Urich, 1995; Dekaban and Constantopoulos, 1977). Under the light microscope, many neurons appear swollen with their nuclei pushed to the periphery, while some are observed in various stages of degeneration and shrinkage (Dekaban and Constantopoulos, 1977). Electron microscopy reveals the presence of neuronal “zebra bodies”, lamellar inclusions approximately 1 $\mu$ m in diameter resulting from abnormal distribution of lipids (Cervos-Navarro and Urich, 1995; McKusick and Neufeld, 1983; Neufeld and Fratantoni, 1970). Cortical neurons have also been reported to develop large

processes (“meganeurites”) to accommodate the increased intracellular storage (McKusick and Neufeld, 1983; Watts et al., 1981).

Biochemical studies have complemented the histological findings with reports of increased glycosaminoglycans and glycolipid-like material in the leptomeninges, cerebral veins and arteries, and brain tissue (Dekaban et al., 1976; Dekaban and Constantopoulos, 1977; Constantopoulos and Dekaban, 1978).

#### **1.4.1.4 Neurological Consequences**

Mental retardation is one of the defining clinical features of Hurler’s syndrome and is thought to be the direct result of the described neuronal damage. However, secondary anatomical abnormalities, primarily hydrocephalus, may also contribute to the mental and neurological limitations (Watts et al., 1981).

Communicating hydrocephalus has been well documented in MPS I patients in both CT and MRI scanning studies (Gabrielli et al., 1992; Watts et al., 1981). It is thought that the hydrocephalus is either a secondary consequence to cortical atrophy, a result of abnormal CSF production and absorption due to thickened meninges and dysfunction of the arachnoid villi or a combination of these events (Cervos-Navarro and Urich, 1995; Muenzer, 1986; McKusick and Neufeld, 1983). The quality of patients’ lives can be improved with CSF diversion procedures, such as a ventriculoatrial shunt.

### 1.4.1.5 Animal Models

There are currently three animal models of MPS I, two of which are naturally occurring diseases. All models demonstrate clinical, biochemical and pathological similarities to the human disease and have thus provided a means for studying the disorder and potential treatments.

The murine model of MPS I is the most recently described. After having isolated and characterized the murine  $\alpha$ -L-iduronidase cDNA (Clarke et al., 1994), the mouse model was developed by targeted disruption of the gene (Clarke et al., 1997). These mice do not show any detectable  $\alpha$ -L-iduronidase activity and show increased urinary mucopolysaccharide levels. Clinical disease symptoms can be observed such as coarse facial features, and skeletal abnormalities. No corneal clouding is apparent. Additionally, lysosomal pathology can be observed in different cell types of the liver, spleen, bone, kidney, muscle, trachea and brain (Clarke et al., 1997).

The feline MPS I model was first described by Haskins et al. in 1979. The cats showed clinical features including broad facial features, corneal opacity and skeletal abnormalities. Biochemical analysis showed deficient  $\alpha$ -L-iduronidase activity and excess dermatan and heparan sulfate in the urine. Lysosomal vacuolization was observed in the liver, cartilage, muscle, bone marrow leukocytes, fibroblasts and neurons while zebra bodies were also demonstrated in spinal cord neurons (Haskins et al., 1979; Haskins et al., 1983).

Canine MPS I has been the most extensively characterized animal model of the those discovered thus far. This naturally occurring disease was first noted in dogs in

1982 by Shull et al. Attention was brought to this Plott hound population when veterinarians noted the dogs' stunted growth, progressive lameness and visual difficulties. Further clinical examination revealed severe joint disease, excessively long tongues, corneal clouding, skeletal abnormalities and heart disease (Shull et al., 1982). Enlargement of the liver and spleen was not apparent in these dogs.

Like the human disease, the canine model shows a deficiency in  $\alpha$ -L-iduronidase activity and an accumulation of intracellular mucopolysaccharide (Shull et al., 1984; Constantopoulos et al., 1985). The neurologic pathology also shows remarkable similarities to humans with the presence of intralysosomal vacuoles in neurons, astrocytes, blood vessels and leptomeninges. Further, more detailed examination reveals the presence of zebra bodies and neuronal meganeurites which appear more like those described in humans than in the feline model (Constantopoulos et al., 1985; Shull et al., 1987; Walkley et al., 1988).

The canine  $\alpha$ -L-iduronidase cDNA and gene have been cloned and characterized (Stoltzfus et al., 1992; Menon et al., 1992). Since the MPS I dog colony has been bred from one founder, all affected dogs carry the same mutation, that is, a G to A point mutation in intron 1 leading to a premature termination codon at the exon-intron junction (Menon et al., 1992).

## 1.4.2 Other MPSs and their Animal Models

Before a discussion of treatments for MPS disorders, it is worthwhile to briefly summarize the other MPS types and the existence of their animal models, since they too have been vital in the development of therapeutic paradigms.

MPS II, or Hunter Syndrome, is the result of a deficiency in the  $\alpha$ -L-iduronate-2-sulfate sulfatase. This enzyme desulfates iduronate-2-sulfate residues in heparan and dermatan sulfate (Gielsmann, 1995). Like the other mucopolysaccharidoses, MPS II is recessively inherited, but this type is the only MPS that is X-linked. Phenotypical symptoms include hepatosplenomegaly, skeletal abnormalities and heart failure (Whitley et al, 1996). Clinically, MPS II resembles Hurler Syndrome, but can be distinguished from it by less severe mental retardation and the lack of corneal clouding. MPS type II has only been recently described in a Labrador Retriever (Wilkerson et al., 1998) showing clinical and biochemical characteristics akin to an intermediate form of the disease.

MPS III, Sanfilippo Syndrome, is divided into four subtypes, all of which show diminished enzyme activity in the degradation pathway of heparan sulfate. Heparan sulfamidase is deficient in type A,  $\alpha$ -N-acetylglucosaminidase in type B, acetyl-CoA:  $\alpha$ -glucosaminide acetyltransferase in type C and N-acetyl glucosamine-6-sulfatase in type D (Fischer et al., 1998). Severe mental retardation and relatively mild somatic MPS symptoms characterize all MPS III categories (McKusick and Neufeld, 1983). Only MPS type IIIA has been identified in the dog (Fischer et al., 1998). The examined Dachshunds both exhibited neurologic disease without any apparent somatic involvement. Clinical,

pathologic and biochemical features were paralleled to the human disease and a diagnosis was thus applied.

MPS IV, or Morquio A syndrome, is caused by a deficiency of N-acetylgalactosamine-6-sulfate sulfatase which cleaves sulfate residues from sulfated galactose in keratan sulfate (Gielsmann, 1995). MPS VI (Maroteaux Lamy Syndrome) is caused by a deficiency of arylsulfatase B which catalyses the hydrolysis of the sulfate ester in N-acetylgalactosamine-4-sulfate resulting in an inability to metabolize dermatan sulfate and chondroitin-4-sulfate (Gielsmann, 1995). Both MPS IV and VI are characterized by skeletal abnormalities, corneal clouding and the absence of neurologic involvement. Only MPS VI has been described in a feline form (Haskins et al., 1980).

MPS VII, Sly Syndrome, is caused by a deficiency of  $\beta$ -D-glucuronidase, necessary for the hydrolysis of terminal glucuronic acid residues from dermatan, heparan, chondroitin-4 and -6 sulfate (Gielsmann, 1995). Clinically, MPS VII resembles MPS I and II with skeletal abnormalities, hepatosplenomegaly and mental retardation. Also like MPS I, MPS VII has been described in the mouse (Vogler et al., 1990), dog (Haskins et al., 1984; Haskins et al., 1991) and cat (Gitzelmann et al., 1994).

### **1.4.3 Treatment**

The discovery of animal models for the MPSs has provided an excellent platform for the examination of various treatment protocols. The following section will focus on the various treatment strategies used for the different MPS types, with particular emphasis on MPS I.

### **1.4.3.0 Bone Marrow Transplantation (BMT)**

The first bone marrow transplantation (BMT) for Hurler's syndrome took place in April, 1980. A nine month old boy received marrow from his mother and is currently fully engrafted with stable intelligence in the low to normal range (Hobbs et al., 1981; Peters et al., 1998).

Since the initial transplantation, various BMT trials have taken place both clinically and in animal models with varying degrees of success (Shull et al., 1987; Whitley et al., 1993; Poorthuis et al., 1994; Peters et al., 1996; Guffon et al., 1998). Successful BMT engraftment appears to provide long-term correction of enzyme levels. For example, in one clinical trial, 7 patients demonstrated normal levels of  $\alpha$ -L-iduronidase activity while 5 patients demonstrated greater than 50% of normal levels, for up to 6.5 years post unrelated-donor-treatment (Peters et al., 1996). Further, many patients show increased life expectancy since they do not battle typical disease complications such as heart failure or hydrocephalus (Peters et al., 1996, 1998). Animal studies in MPS I dogs and MPS VII mice show reversal of pathology in various organs, including the retina, liver, kidney and heart (Poorthuis, 1994; Breider et al., 1989; Constantopoulos et al., 1989).

Unfortunately, the effects observed within the brain have not been as promising as those seen in the visceral organs. Neuropsychological abilities post-BMT treatment varied widely in human patients (Peters et al., 1996). Additionally, in BMT-treated MPS I dogs or MPS VII mice, little improvement could be seen in CNS symptoms, although in some cases, small amounts of enzyme could be detected within the brain up to nine

months after BMT therapy (Bastedo et al., 1994; Poorthuis et al., 1994; Sands et al., 1993; Shull et al., 1987). Minimal  $\alpha$ -L-iduronidase levels did prove to be somewhat beneficial in the treated MPS I dogs as demonstrated by a reduction of glycosaminoglycans and less lysosomal distention in the brain, as compared to untreated MPS I dogs. However, the effect varied among animals and many neurons maintained their enlarged, vacuolated state (Shull et al., 1987; Shull et al., 1988).

It is unclear how the small amounts of enzyme might gain access to the CNS post-BMT treatment since the mentioned lysosomal enzymes are unable to pass the blood-brain barrier. The first possibility is that the blood-brain barrier may have been injured or compromised, at least transiently, from the pre-transplant total body irradiation, thus altering the permeability towards systemic substances (Shull et al., 1987; Shull et al., 1988). The second hypothesis comes from evidence showing that glial and microglial cells within the brain may be derived from bone marrow precursors (Gehrmann et al., 1995). Thus, a small portion of marrow cells might pass through the blood-brain barrier for that purpose (Shull et al., 1988).

While BMT is the only therapy reported thus far to provide clinical improvement for MPS disorders (Ohashi et al., 1997), several drawbacks have been highlighted. The limitation in terms of CNS treatment remains one of the largest concerns. Additionally, several risks are associated with the pre-therapy total body irradiation, necessary to increase the likelihood of successful engraftment. These risks were exemplified in BMT-treated neonatal MPS VII mice that showed radiation dose-dependent cerebellar and retinal dysplasia as well as long bone growth retardation (Sands et al., 1993). Further, the

procedure is expensive and produces a significant risk of graft vs. host disease and mortality (Whitley et al., 1993; Fairbairn et al., 1996).

#### **1.4.3.1 Enzyme Replacement Therapy**

In an attempt to alleviate the inherent drawbacks of BMT, researchers have been investigating the possibility of direct enzyme injection.

When recombinant human  $\alpha$ -L-iduronidase was injected intravenously into MPS I dogs, the enzyme was rapidly cleared from the blood and found primarily in the liver (Shull et al., 1994). With weekly administration of the enzyme over three months, normal  $\alpha$ -L-iduronidase levels and improvements in cellular vacuolization were achieved in the liver and spleen. Lower, but significant enzyme levels were found in the kidney and lung, but essentially no enzyme could be detected in the heart, cartilage, cornea and brain (Shull et al., 1994). One dog was observed for 13 months and continued to show clinical, biochemical and histological improvement (Kakkis et al., 1996). Significantly, the animals developed antibodies towards the enzyme (human or canine form), and in one case developed an anaphylactoid reaction (Kakkis et al., 1996; Shull et al., 1994).

Enzyme replacement trials in MPS VII mice have been effective in delivering significant levels of  $\beta$ -glucuronidase to various organs including the brain (Sands et al., 1994). Decreased lysosomal storage was also observed in the same organs, although glia and neurons remained distended. The biochemical and histological improvements correlated with several positive clinical effects in the treated MPS VII mice including

increased survival times, behavioural improvements as measured by the Morris Water Maze and improved auditory function (Vogler et al., 1996; O'Connor et al., 1998).

Although the biochemical and histological effects of long term enzyme replacement could be observed in MPS VII treated mice if the enzyme treatment was initiated at six weeks of age (monthly administration), the treatment appeared to be more effective if it was initiated at birth (Sands et al., 1997). This was important particularly in terms of skeletal and CNS improvement. Interestingly, Sands et al. (1997) then showed that combined enzyme replacement therapy with BMT initiated at birth resulted in a more effective therapy paradigm than either treatment alone.

### **1.4.3.2 Gene Therapy**

The recent isolation and description of genes and cDNA sequences of lysosomal enzymes has stimulated the gene therapy research field for the treatment of MPS disorders. The MPS VII mouse model has been the focus of many of these studies, highlighting the promise gene therapy holds for all the MPSs. The following section will review some of the recent advances in gene therapy techniques for MPS with emphasis on the effects in the brain.

#### **1.4.3.2.0 Retroviral Techniques**

Several different studies have reported success in delivering lysosomal enzyme cDNA to various cell types *in vitro* using retroviral vectors (Bielicki et al., 1996; Braun et al., 1996; Fairbairn et al., 1996; Huang et al., 1997; Taylor and Wolfe, 1997a; Ray et al.,

1998). In all cases, the delivered enzyme cleared the intracellular accumulation of the glycosaminoglycan in question. One clinical study for the treatment of MPS II (Hunter syndrome) has developed from these advancements and is currently underway (Whitley et al., 1996).

In an *ex-vivo* experiment where fibroblasts were retrovirally transduced with murine  $\beta$ -glucuronidase and then grafted into the MPS VII mouse brain, high levels of enzyme could be detected within the grafts 2-4 weeks post-transplantation (Taylor and Wolfe, 1997b). Neuronal and glial lysosomal correction were observed in the direct vicinity of the grafts for up to 4 weeks without any evidence of an inflammatory reaction. Although the extent of correction was significant for the mouse brain, further research, perhaps with other cell types, will be necessary to extend this technology to larger brains (Taylor and Wolfe, 1997b).

Gene therapy delivered by hematopoietic stem cells offers the advantage of long-term, *in vivo* production of a therapeutic enzyme (Lutzko et al., 1999a).  $\alpha$ -L-iduronidase has been retrovirally incorporated into such cells (Wolfe et al., 1992; Fairbairn et al., 1996; Huang et al., 1997; Lutzko et al., 1999a). When transduced stem cells were transplanted intravenously into MPS VII mice, only low levels of  $\beta$ -glucuronidase activity could be detected, although dramatic improvements in the liver and spleen were observed (Wolfe et al., 1992). Recently, transduced canine cells were infused into MPS I dogs and fetal pups (Lutzko et al., 1999a, 1999b). Despite high enzyme levels *in vitro*, and good evidence of engraftment, the enzyme could not be detected in any dogs, possibly due to silencing of the vectors.

#### **1.4.3.2.1 Adenoviral Techniques**

Intravenous injection of recombinant adenovirus expressing human  $\beta$ -glucuronidase into MPS VII mice resulted in enzyme delivery to the liver and spleen leading to pathological and biochemical correction for at least 35 days (Ohashi et al., 1997). In another study, correction was observed in the liver and kidney for 16 weeks when immunosuppression was administered (Stein et al., 1999).

CNS correction using the adenovirus has been attempted by direct injection into the brain parenchyma of MPS VII mice (Ghodsi et al., 1998; Stein et al., 1999). Although injections were unilateral, enzyme activity and cellular correction could be detected in both cerebral hemispheres. Similarly, injection of the adenovirus into the lateral ventricles or cisterna magna resulted in detectable enzyme activity near the site of injection (Ghodsi et al., 1998).

#### **1.4.3.2.2 Adeno-Associated Viral Techniques**

When newborn MPS VII mice were injected intravenously with recombinant AAV expressing  $\beta$ -glucuronidase, enzyme was detected in the liver, heart, lung, spleen, kidney, retina and brain (Daly et al., 1999). It is important to note that neurons, microglia and meninges showed dramatic improvement in cellular pathology. Like BMT and enzyme replacement, treatment in young animals appears to have a dramatic effect on the extent of treatment success. Daly et al. (1999) proposed that the improvement seen in the CNS was a result of the incompletely formed blood-brain barrier at the time of AAV injection.

### **1.4.3.2.3 Microencapsulation Techniques**

When mouse fibroblasts genetically altered to secrete  $\beta$ -glucuronidase were microencapsulated and implanted into the intraperitoneal cavity of MPS VII mice, a significant increase in enzyme activity was detected and a concurrent decrease in lysosomal inclusions was observed in the liver, kidney and spleen (Ross et al., 1999b). Further, when such microcapsules were implanted into the lateral ventricles of MPS VII mice, a decrease in lysosomal inclusions in cortical cells surrounding the implantation site was also observed with an increase in enzyme activity (Ross et al., 1999b). Additionally, the implanted mice showed a behavioral correction of circadian rhythm patterns suggesting that behavioral and cognitive deficits may be amenable to treatment and reversal in this disease (Ross et al., 1999b).

## 1.5 RATIONALE FOR CURRENT EXPERIMENTS

In 1999, our laboratory demonstrated the feasibility of using microencapsulated cells to deliver recombinant gene products to the CNS of rodents (Ross et al., 1999a). The microcapsules were delivered to the lateral ventricles, and human growth hormone was detected by ELISA and immunohistochemistry around the implantation site for up to 16 weeks. Further, this technique proved to be effective in delivering  $\beta$ -glucuronidase to MPS VII affected mice and decreasing the cerebral lysosomal storage (Ross et al., 1999b). We were interested in determining if this technology could also be used in the CNS of large animals, with the eventual goal of testing it in the MPS I canine model.

With the hope of maximizing delivery to as much of the brain as possible, we decided to implant human growth hormone secreting microcapsules into the ventricular system of the dog. While the lateral ventricles proved to be an effective implantation site in the mouse, such an invasive procedure was expected to be much more complicated in the large animal. We therefore decided to also examine a less invasive route of delivery, that is, implantation of the microcapsules to the spinal subarachnoid space via the cisterna magna. The feasibility of this route has been established in other experiments. For example, in an effort to deliver products to the CNS for the treatment of cancer, investigators examined the use of polymer encapsulated cells in the subarachnoid space of the sheep (Joseph et al., 1994). The technique proved to be valid and safe and clinical trials employing the polymer capsules within the lumbar spinal intrathecal space are now underway for the treatment of cancer pain and amyotrophic lateral sclerosis (Aebischer et al., 1994b; Aebischer et al., 1996a; Aebischer et al., 1996b).

The following experiments were designed to establish the techniques and delivery potential of intraventricular and spinal intrathecal microcapsule implantations in the central nervous system of the dog.

**Table 1-1** Sequential enzymatic degradation of heparan sulfate. Deficiencies of these enzymes result in the various MPS types. Adapted from McKusick and Neufeld, 1983.

<b>Enzyme</b>	<b>Disease Resulting from Enzyme Deficiency</b>
Iduronate sulfate	MPS II (Hunter)
$\alpha$ -L-Iduronidase	MPS I (Hurler, Scheie, Hurler-Scheie)
Heparan N-sulfatase	MPS III type A (Sanfilippo Type A)
Acetyl transferase	MPS III type C (Sanfilippo Type C)
$\alpha$ -N-Acetyl glucosaminidase	MPS III type B (Sanfilippo Type B)
$\beta$ -Glucuronidase	MPS VII (Sly)
N-Acetyl glucosamine 6-sulfatase	MPS III type D (Sanfilippo Type D)

**Table 1-2** Sequential enzymatic degradation of dermatan sulfate. Deficiencies of these enzymes result in the various MPS types. Adapted from McKusick and Neufeld, 1983 and Gieselmann, 1999.

<b>Enzyme</b>	<b>Disease Resulting from Enzyme Deficiency</b>
Iduronate sulfatase	MPS II (Hunter)
$\alpha$ -L-Iduronidase	MPS I (Hurler, Scheie, Hurler-Scheie)
N-Acetylgalactosamine 4-sulfatase	MPS VI (Maroteaux-Lamy syndrome)
$\beta$ -Hexosaminidase	Tay Sachs; Sandhoff
$\beta$ -Glucuronidase	MPS VII (Sly)

## **2.0 MATERIALS AND METHODS**

### **2.1. *In Vitro* Procedures**

#### **2.1.0 Cell lines**

MDCK (Madin Darby Canine Kidney) cells were used in all experiments. The untransfected MDCK cells were supplied by Dr. Frank Graham (McMaster University). All cells were maintained in  $\alpha$ -minimal essential medium ( $\alpha$ -MEM) supplemented with 10% fetal bovine serum (FBS; Gibco BRL Cat No. 10437-028) and 1% penicillin/streptomycin (P/S; Gibco BRL, Cat No. 15140-122). The cells were maintained in 10cm tissue culture dishes at 37°C in 5% CO<sub>2</sub> water jacket incubators.

For chapters 3 and 4, MDCK cells previously transfected with a pNMG3 plasmid containing the human growth hormone (hGH) gene with the mouse metallothionein-I promoter (Chang et al., 1990) were used. Cells were transfected as previously described by Peirone et al., 1998 using the phosphate-mediated DNA precipitation method (Graham and Van der Eb, 1973).

For chapter 5, MDCK cells previously transfected with the canine  $\alpha$ -L-iduronidase cDNA (cIDUA) were used. The cIDUA was the kind gift of Dr. ED Kakkis, and was inserted into a R1dn10b plasmid with MCK enhancer and CMV promoter by KE Robinson, using the phosphate-mediated DNA precipitation method (Graham and Van der Eb, 1973).

### 2.1.1 Cell Encapsulation

Cell encapsulation was performed under sterile conditions and solid alginate-poly-L-lysine-alginate (APA) microcapsules were used for all experiments. MDCK cells were trypsinized and harvested in cold cell culture  $\alpha$ -MEM media supplemented with 10% FBS and 1% P/S. The number of cells were counted with a Coulter Counter, Model Z1 (Coulter Electronics, Cat No. 9914556), then spun down at 12,000 rpm. After the media was removed, the cells were resuspended and washed in cold 0.9% physiological saline and spun down again. The saline was removed and the cells were resuspended in final small volume of 0.9% physiological saline (1/20 volume of alginate to be used) and 2% potassium alginate such that there were approximately  $2.0 \times 10^6$  cells per millilitre of alginate. This mixture was drawn into a 20cc syringe, placed into a Orion Sage syringe pump (model M362) and extruded through a one inch - 27 gauge blunt-end needle (Vita Needle) at a rate of 99.9ml/hr x 1/100. The microcapsules were collected in 50ml cold 1.1% CaCl solution and transferred to a 50ml conical tube for subsequent solution washes. The solution washing protocol was as follows: 1.1% CaCl<sub>2</sub>, 0.55% CaCl<sub>2</sub>, 0.28% CaCl<sub>2</sub>, 0.1% CHES (3 minutes), 1.1% CaCl<sub>2</sub>, .05% PLL (6 minutes), 0.1% CHES, 1.1% CaCl<sub>2</sub>, 0.9% physiological saline, 0.04% potassium alginate (4 minutes), three washes of 0.9% physiological saline, two washes of non-supplemented cell culture  $\alpha$ -MEM media. The capsules were then maintained in normal cell culture conditions in REGM (Clonetics, Cat No. 3190) cell culture media.

### **2.1.2 Pre-surgery Microcapsule Preparation**

Prior to implantation, microcapsules were washed with 250-500ml sterile physiological saline to ensure that all media was removed. The microcapsules were drawn into a 1 or 3cc syringe under sterile conditions and implanted into the CNS within 30 minutes.

### **2.1.3 *In Vitro* Secretion Analysis**

On day 0 and every seven days throughout the duration of the experiments, *in vitro* secretion analyses were undertaken. 0.25-0.5ml microcapsules were transferred to a 15ml conical tube and washed twice with sterile PBS to remove the media. Microcapsules were then transferred to a 35mm cell culture dish and 1.5-1.75ml cell culture  $\alpha$ -MEM supplemented media was added. A 100 $\mu$ l sample was taken immediately and designated "time = 0 h". The 100 $\mu$ l sample was replenished by cell culture media. Samples were obtained every 1-2 hours for the first six hours, and once again after 24 hours. Samples were stored at -20°C until they were needed for quantitative analysis.

### **2.1.4 Cell Number per Capsule**

In order to express the product secretion as the amount of product per million viable cells, the number of cells per capsule was required. After the 24 hour secretion time course, the capsule sample was collected into a 1.5ml eppendorph tube. Trypan blue (Gibco BRL, Cat No. 15250-061) was added to the microcapsules and left at 4°C

overnight. A 100 $\mu$ l sample was then obtained and the number of capsules in this sample was determined by hand. These microcapsules were collected and crushed and 15 $\mu$ l samples were loaded onto a hemocytometer for cell counting.

### **2.1.5 Cell Viability Analysis**

On day 0 and every seven days throughout the duration of the experiments, the viability of the cells within the capsules was examined with the following procedure. A small sample of microcapsules were placed on a glass slide and covered with a few drops of trypan blue. The capsules were subsequently crushed with a coverslip. The slide was then examined in ten different fields for the proportion of alive (clear) vs. dead (blue) cells. The average of the ten fields was expressed as percent viability.

## **2.2 *In Vivo* Procedures**

### **2.2.0 Animals**

The animals used in all experiments were dogs, aged 1-3 years. Specific breed and conditions will be outlined with each specific experiment. All clinical procedures and animal care were performed in accordance with CCAC guidelines, Animals for Research Act and received prior approval by the University Animal Care Committee.

### **2.2.1 Blood Collection**

Two millilitre blood samples were obtained from the dogs prior to surgery and every 3-5 days thereafter by the Central Animal Facility staff as per the standard operating procedure for blood specimen collection (cafsop752.1), McMaster University Central Animal Facility, Hamilton, Ontario. All samples were collected in heparanized tubes and were spun down at 14,000rpm. Plasma was collected and frozen at -70°C until required for quantitative analysis. On CSF sample days, a portion of the blood sample for some dogs was collected in a non-heparanized tube and sent to Vitatech for the determination of white blood cell content and differential.

### **2.2.2 Canine Anaesthesia**

All dogs were premedicated and anaesthetized by Central Animal Facility technicians either at McMaster University or the University of Toronto. The animals were premedicated with butorphanol, acepromazine and atropine. General anaesthesia was induced 15-20 minutes post-premedication and the dogs were maintained on isoflurane, in accordance with the standard operating procedure for canine anaesthesia (caf304.sop), McMaster University Central Animal Facility.

### **2.2.3 Cerebrospinal Fluid Collection**

Cerebrospinal fluid (CSF) samples were obtained from anaesthetized animals by the clinical veterinarian, Dr. K. Delaney at McMaster University or Dr. W. Williams at the University of Toronto. All dogs had the area above the cisterna magna and skull

shaved and scrubbed as per the standard operating procedure for surgical preparation of the animal (caf757.1.0), McMaster University Central Animal Facility. The dog was placed in lateral recumbence, and the head held parallel to the table with the neck at a 90° angle to the long axis of the spine. A 20-gauge -3½” spinal needle (Becton Dickinson) was slowly inserted into the cisterna magna, identified by the dorsal midline depression (Allen, 1991). Approximately two millilitres of fluid were collected. One millilitre of CSF was sent to Vitatech for the determination of white blood cell and microprotein content, for some animals. The other millilitre was stored at -70°C.

#### **2.2.4 Spinal Intrathecal Implantation**

After CSF retrieval, a 3cc syringe containing 0.5-2ml of microcapsules suspended in 0.5-1.5ml physiological saline was attached to the inserted spinal needle and the microcapsule solution was injected into the cisterna magna over a five minute period (figure 2-1A). After the injection was complete, five minutes were allowed for microcapsule diffusion and the prevention of back-flow before the needle was removed.

#### **2.2.5 Computed Tomography Scan**

The two animals receiving intraventricular implantations in chapter 4, as well as the MPS I mutant dog received computed tomography (CT) scans performed by Dr. C. Coblenz up to one month prior to surgery. The dogs were anesthetized as described in section 2.2.2. The animals were transported from the McMaster Central Animal Facility to the McMaster Hospital Radiology Department where they were laid in a dorsoventral

position with the head flat on the CT table. Coronal scans were obtained from the frontal cortex to the caudal portion of the cerebellum and stored in the computer system. The canines were then returned to the McMaster Central Animal Facility where they received post-operative care as described in section 2.2.7.

### **2.2.6 Intraventricular Implantation**

The intraventricular surgeries were performed by Dr. W.A. MacKay and A. Mendonca, from the University of Toronto. The animal's head was fixed in a canine stereotaxic frame, the surgeons made an incision and cleared away any surrounding tissue and muscle to expose the dog's skull. Using a dental burr, the surgeons drilled holes through the skull (From Bregma: Anterior-Posterior=20mm; Lateral=4mm). A stainless steel cannula (14 gauge) was lowered with a micromanipulator, over five minutes, through the brain tissue to the lateral ventricle (17-19mm from brain surface). In the later surgeries, a small rubber capillary tube filled with saline was attached to the end of the cannula (figure 2-1B). The saline level was monitored as the cannula was lowered, and a small movement was noted when the cannula was within the ventricular space, thus confirming the coordinates before the microcapsules were injected. A syringe containing the microcapsules suspended in physiological saline was attached to the cannula with a small rubber tube (20 gauge). 0.25-1ml microcapsules in 0.25-1ml physiological saline were injected into each ventricle over five minutes. After an additional five minutes were allowed for diffusion of the microcapsules within the ventricular space, the cannula was

slowly removed over five minutes. The procedure was repeated for implantation into the contralateral ventricle.

The holes in the skull were closed with sterile bone wax and the incision was sutured with 2-0 Dexon degradable sutures for under the skin and 2-0 Prolene sutures for the skin. The incision line was then sprayed with a topical anaesthetic.

### **2.2.7 Post-Surgical Care**

Post-operative care was carried out as per McMaster Central Animal Facility standard operating procedures (cafsop304.4.0 and cafsop307.4.0, 5.0). For the animals in described in chapter 3, the drug morphine was used for analgesia and was administered at 0.05mg/kg every 4-6 hours starting post-operatively. The dogs were checked every 15 minutes for the first two hours and then every three to four hours for the first 24 hours post-surgical. The post-operative checks included a temperature, pulse, respiration and brief neurological examination.

### **2.2.8 Neurological Examination**

Three to seven days post-operative, a neurological examination was performed on the dogs by the clinical veterinarian, Dr. K. Delaney at McMaster University or Dr. W. Williams at the University of Toronto. The procedures of a neurologic examination have been previously described (Oliver and Lorenz, 1983). Briefly, mental status was assessed by observation of the dogs' behaviour in its natural surroundings. Posture and gait were observed while the dogs walked towards and away from the examiners. Additionally,

different manipulations of the dogs' legs, such as a wheelbarrow position, were implemented to examine any subtle changes or weaknesses in muscle strength and reflexes. The cranial nerves, except olfactory, were examined by observation and palpation of the dogs' head, eyes, menace response, mouth and tongue.

### **2.2.9 Euthanasia**

After a post-operative period of two to eight weeks, the animals were euthanized by Central Animal Facility staff as outlined by McMaster Central Animal Facility standard operating procedure for euthanasia by barbituate overdose (cafsop756.4.0, 5.0) after the final blood and cerebrospinal fluid samples were taken. The brain and spinal cord were removed by the consulting pathologist (as per cafsop300). Brain and spinal cord tissue were portioned and either frozen immediately in 2-methylbutane (Sigma-Aldrich, 27,034-2) at -40°C and stored at -70°C, post-fixed in 4% paraformaldehyde (Sigma-Aldrich, P-6148), or post-fixed in 2% glutaraldehyde for five to seven days. Any microcapsules that could be recovered were placed in supplemented  $\alpha$ -MEM cell culture media.

## **2.3 QUANTITATIVE ANALYSIS**

### **2.3.0 Tissue Processing**

After euthanization, brain tissue that was frozen and stored at  $-70^{\circ}\text{C}$  was homogenized in the following manner. While the tissue was still frozen, sections of different regions of the brain were sliced off and weighed. The following brain regions were sampled: prefrontal, frontal, parietal, temporal and occipital cortices, caudate nucleus, thalamus, hippocampus, and where possible, the lateral ventricle lining, midbrain, medulla, cerebellum and spinal cord. Homogenization buffer was added (100  $\mu\text{l}$  per mg of tissue). The tissue pieces were homogenized by sonication on ice for 30-60 seconds and then centrifuged at 14,000rpm for 30 minutes. Supernatants were collected and stored at  $-70^{\circ}\text{C}$  until required for quantitative assays.

### **2.3.1 Human Growth Hormone ELISA**

Human growth hormone ELISA kits were obtained from United Biotech Inc. (UBI-Magiwell hGH Quantitative kit, HP-901) and used as per manufacturer's instructions. Briefly, 25 $\mu\text{l}$  of standards and diluted samples (plasma and brain tissue samples diluted 1/5, CSF samples diluted 1/10 and media samples diluted 1/20) were loaded into separate wells and 100 $\mu\text{l}$  of enzyme conjugate was added to each. Each standard and sample was repeated in triplicate. Incubation occurred at room temperature for 60 minutes after which the wells were rinsed with tap water five times. 100 $\mu\text{l}$  of Solution A and 100 $\mu\text{l}$  of Solution B were added to each well and incubated at room

temperature for 30 minutes. The reaction was stopped with 50 $\mu$ l of 1N H<sub>2</sub>SO<sub>4</sub> and absorbance was read on a Microwell microplate reader at 450nm.

### **2.3.2 Anti-Human Growth Hormone Antibody Assay**

With the purpose of providing a positive control for the anti-hGH antibody assay, two pound source mixed-breed dogs were previously injected three times subcutaneously by M. Peirone with 500 $\mu$ g recombinant human growth hormone, 1:1 in Freund's complete adjuvant, for a total 1ml injection, as described (Peirone et al., 1998). A frozen plasma aliquot from one of these dogs was serially diluted and used as the standard in the antibody titre assays.

96-well plates were coated with 100 $\mu$ l recombinant hGH per well (200ng; Humatrope, supplied by Eli Lilly and Company, Indianapolis, In.) in .1M sodium bicarbonate buffer (pH 9.6). The plates were washed between each step with PBS/T. Each well was blocked overnight with 5% skim milk in PBS/T ("blotto") followed by the loading of diluted samples (plasma and CSF diluted 1/300) into each well for one hour at 37°C. Each sample was repeated in triplicate. After removal of the samples, 100 $\mu$ l rabbit anti-dog IgG conjugated to alkaline phosphatase (Sigma, Cat No. A-0793) diluted 1:2000 was loaded onto the plate for one hour at 37°C. After rinsing the plates, alkaline phosphatase developing solution was allowed to react for 10-15 minutes and absorbance was measured using a Microwell microplate reader at 405nm.

### **2.3.3 $\alpha$ -L-Iduronidase Activity Assay**

During the hydrolysis of an artificial iduronidase substrate, 4-MU- $\alpha$ -L-iduronide (Calbiochem Cat # 474525), 4-methylumbelliferyl (4-MU), is released and can be measured fluorometrically (Hopwood et al., 1979). Based on this reaction, an assay for  $\alpha$ -L-iduronidase activity was developed and described (Rome et al., 1979; Hopwood et al., 1979). Briefly, 25 $\mu$ l diluted samples (all samples diluted  $\frac{1}{2}$ ) were incubated with 25 $\mu$ l substrate solution (50 $\mu$ M 4-MU- $\alpha$ -L-iduronide in 0.4M formate buffer, pH 3.5) in black Co-star 96 well plates in the dark for one hour at 37°C. The reaction was stopped with the addition of 100 $\mu$ l glycine/carbonate stopping buffer. Fluorescent units were measured with a fluorometer (CytoFluor II) at an excitation of 360/40 and emission of 460/40.

### **2.3.4 Anti- $\alpha$ -L-Iduronidase Antibody Assay**

Based on a procedure described by Chang et al. (1986), C. Ross in our laboratory developed an immunoprecipitation assay for the quantification of antibodies against the lysosomal enzyme,  $\beta$ -glucuronidase. The pH of the Tris-HCl buffer was changed from 8.0 to 7.2 so that the antibodies against  $\alpha$ -L-iduronidase could be detected. This assay is an indirect measure of the antibody titre. That is, the antibody titre is expressed by the change in enzyme activity as a result of immunoprecipitation by the antibody.

In order to provide an enzyme source for this assay, MDCK cells secreting  $\alpha$ -L-iduronidase were grown to 80% confluence in culture. The cells were trypsinized and

harvested in 5ml  $\alpha$ -MEM media +10%FBS + 1%P/S. The cells were then lysed by sonication and spun down at 12,000 rpm for ten minutes. The supernatant was collected and enzyme activity was assayed, as outlined in section 2.3.3. Only samples that produced greater than 2,000 fluorescent units were used for the antibody assay.

30 $\mu$ l 0.04M Tris-HCl buffer (pH 7.2), 50 $\mu$ l  $\alpha$ -L-iduronidase sample and 20 $\mu$ l ddH<sub>2</sub>O, plasma or CSF sample were combined in a 1.5ml eppendorph tube for one hour at room temperature on a gentle shaker. 30 $\mu$ l Pansorbin (Calbiochem Cat No. 507861) was added to the solution to pull down any antibody present. The solution was mixed for one hour at room temperature on a gentle shaker and then spun at 14,000rpm for three minutes. The supernatant from each sample was removed and assayed for  $\alpha$ -iduronidase activity as described in section 2.3.3.

### **2.3.5 Protein Assay**

To determine the protein levels in homogenized brain tissue, the Bio-Rad Protein Assay kit was used, as per manufacturer's instructions for the standard procedure for microtitre plates. Bovine serum albumin (BSA) was serially diluted and used as protein standards. Briefly, 10 $\mu$ l of each standard and diluted sample solution (diluted 1/300) were loaded into separate wells and 200 $\mu$ l of diluted dye reagent was added to each well. Samples were incubated at room temperature for 15-20 minutes and absorbance was measured at 595nm on a Microwell microplate reader.

## **2.4 PATHOLOGY**

### **2.4.0 Tissue Processing and Embedding**

During euthanization, portions of tissue were placed in 4% paraformaldehyde or 2% glutaraldehyde (pH 7.4) for post-fixing at 4°C for 5-7 days. Tissue that was post-fixed in 4% paraformaldehyde was trimmed and embedded in paraffin blocks. The tissue processing and paraffin embedding was carried out by the Histology Department, McMaster University Hospital, Hamilton, Ontario, as follows: 70% ethanol for 2 hours, 80% ethanol for 30 min, 2 washes in 100% ethanol for 90 min each, 2 washes in 100% ethanol for 90 min each, 2 washes in xylene for 85 min each, and 3 washes in paraffin for 1 hour each. The paraffin-infiltrated tissue was then embedded in paraffin blocks and stored at room temperature until required for sectioning.

The resin embedding protocol is as follows: one millimetre by one millimetre blocks of 2% glutaraldehyde-fixed tissue were washed in 0.2M sodium cacodylate buffer (pH 7.4) two times for 5 minutes each. The tissue pieces were then transferred to 1% osmium tetroxide in 0.1M sodium cacodylate (pH 7.4) for one hour. The tissue was dehydrated through series of five and ten minute washes of increasing alcohol solutions (50%, 70%, 90%, 100%) followed by two five minute washes in 100% propylene oxide. Brain tissue was then infiltrated with increasing concentrations of Spurr's Resin (firm) solutions for 30 minutes each (50:50, 25:75 propylene oxide: Spurr's Resin). Finally, the tissue was incubated in 100% Spurr's Resin for twice for 60 minutes each. All washes took place at room temperature.

The processed tissue pieces were individually placed into plastic molds, embedded in 100% Spurr's Resin and left in an oven (65°C) to polymerize overnight.

### **2.4.1 Tissue Staining**

After the tissue was paraffin embedded, the blocks were cut at 8µm on an American Optical No. 817 paraffin microtome with disposable metal blades. The sections were warmed on a 45-50°C distilled water bath and mounted on APTEX-treated (Sigma, Cat No. A-3648) slides.

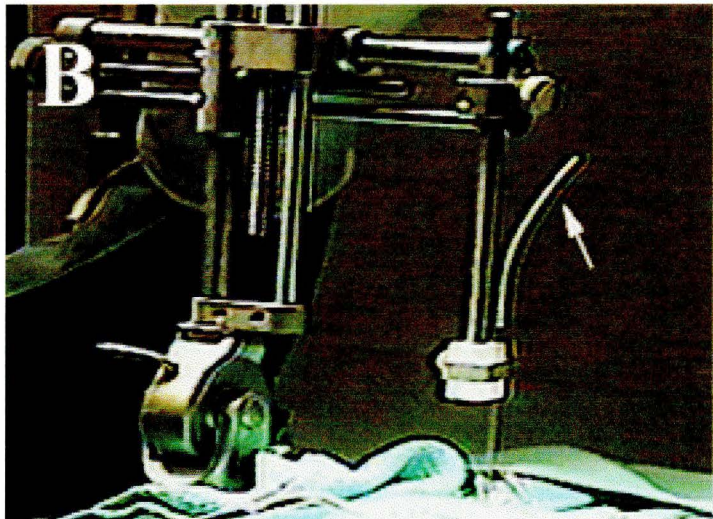
In preparation for staining, the dried sections were de-paraffinized overnight in xylene and re-hydrated through a series of decreasing alcohol solutions (100%, 95%, 70%, 50%, 25%). Sections were then stained with either a cresyl violet stain (Sigma, Cat No. C-1791), a standard hematoxylin (Mayer's hematoxylin solution; Sigma, Cat No. MHS-16) and eosin (Sigma, Cat No. HT110-2-16) stain, or a periodic acid schiff (PAS) stain (AJP Scientific Inc./Maynard Scientific Co.). After staining, the tissue sections were dehydrated through a decreasing alcohol series, placed into xylene for ten minutes and coverslipped using Permount (Fisher Scientific, Cat No. SP15-500).

Resin embedded tissue was sectioned at 5µm on a Reichert OmU2 ultramicrotome with glass knives. The tissue was stained immediately in heated Toluidine Blue solution (Marivac, Cat No. CT009-0) and rinsed two times with distilled water. Sections were then placed on slides, left to dry, and were then coverslipped using Permount.

## 2.4.2 Immunohistochemistry

The presence of hGH (chapters 3 and 4) and glial fibrillary acidic protein (GFAP; all experiments), were detected in brain tissue by immunohistochemistry. Mounted tissue sections were de-paraffinized overnight in xylene and re-hydrated through a series of decreasing alcohol solutions. The tissue was prepared for immunohistochemistry by incubation for 30 minutes in a serum block solution consisting of 5% horse serum and 0.3% Triton-X-100 (Biorad, Cat No. 161-0407) in 0.1M sodium phosphate buffer. The primary monoclonal antibody (hGH – Sigma, Cat No. G-8523, 1:1000; GFAP – Boehringer Mannheim Biochemica, Cat No. 814369, 5 $\mu$ g/ml) was placed on the tissue for 16 hours. Sections were then washed three times in phosphate buffer followed by addition of the secondary antibody (mouse IgG; Vector Laboratories, Vectastain Kit PK-4002) for one hour. Antibody detection was carried out using an avidin-biotin peroxidase complex (Vector Laboratories, Vectastain Kit PK-4002). The antigen was visualized with 80mg 3,3' diaminobenzidine (Sigma, Cat No. D-5637) per 100ml 0.1M phosphate buffer and reacted with hydrogen peroxide.

**Figure 2-1** Surgical methods. (A) Spinal intrathecal surgery. A syringe filled with microcapsules suspended in physiological saline (arrow) is attached to the inserted spinal needle. (B) Intraventricular surgery. Part of the stereotaxic apparatus is shown with a rubber capillary tube (arrow) attached to the intraventricularly placed cannula.



### **3.0 DELIVERY OF HUMAN GROWTH HORMONE-SECRETING MICROCAPSULES TO THE CENTRAL NERVOUS SYSTEM OF DOGS**

#### **3.1 RATIONALE**

Implantation of microcapsules secreting human growth hormone (hGH) into the lateral ventricles of mice results in diffusion of the hormone to the surrounding brain tissue (Ross et al., 1999). The purpose of this experiment was to scale up the delivery of microcapsule technology for application in the large animal brain. The following study was designed to establish the techniques and delivery potential of intraventricular and spinal intrathecal microcapsule implantations in the central nervous system of naïve dogs.

#### **3.2 MATERIALS AND METHODS**

##### **3.2.1 Animals**

Three dogs were used in this experiment, aged 12-24 months. Two dogs were male plott hounds, both 24kg, obtained from the University of Guelph. The third animal was a female beagle, 12kg. All procedures in this experiment were carried out at the University of Toronto, Toronto, Ontario.

##### **3.2.2 CNS Treatment**

All dogs received microcapsules containing MDCK cells secreting human growth hormone, as described in section 2.1.0. One plott hound, Duffy, received a spinal intrathecal implantation of 2ml microcapsules, while the other plott hound, Dino,

received an intraventricular implantation of 1ml microcapsules into each lateral ventricle (2ml total microcapsules). These two surgeries were performed on the same day, with the same batch of microcapsules. During the surgeries, the capsules were noted to be “fuzzy” and upon subsequent microscopic examination, they were determined to be compromised. That is, approximately 50-60% of the capsules appeared broken and fragmented with loss of the outer coat.

At a later time, the beagle, Dana, received 0.25ml microcapsules in 0.25ml physiological saline per lateral ventricle (total 0.5ml microcapsules). Only Dana’s intraventricular surgery employed the rubber capillary tube adjustment outlined in section 2.2.6.

### **3.2.3 Analyses**

For each dog, there was a post-operative clinical assessment, post-mortem analysis of gross findings at euthanization, quantitative analysis of the human growth hormone and antibody content in the plasma, CSF and brain tissue, and histological and immunohistological examination of the brain. Further, encapsulated cell viability and secretion assessments were carried out on microcapsules maintained *in vitro* and on retrieved capsules, when possible.

## **3.3 RESULTS**

### **3.3.1 Post-operative Clinical Assessment**

All animals recovered from surgery without complication. They remained healthy until euthanization on day 14.

### **3.3.2 Post-mortem Analyses**

Duffy's brain was removed and appeared normal upon post-mortem examination. After the removal of Dino's brain, the cannula tracks could be observed in the parietal/occipital cortex area. During brain cutting, an approximately 5mm x 5mm hole was observed in the left hemisphere representing the capsule implantation site. This hole was observed 3-5mm below the lateral ventricle, close to the anterior portion of the hippocampus. No microcapsules could be retrieved from either dog. The spinal cords were not obtained.

Upon removal of Dana's brain, cannula tracks could not be observed on the dorsal surface of the brain. During the brain cutting, capsules were found free, mostly located within the left lateral ventricle. Some of these microcapsules were retrieved for cell viability analysis. An aggregation of capsules, approximately 4-6mm in length, was also noted along the midline of the corpus callosum, 2-3mm above the lateral ventricles (figure 3-1).

### 3.3.3 Microcapsule Cell Viability and Secretion Analysis

Cell viability and human growth hormone secretion rates from the microcapsules maintained *in vitro* are summarized in table 3-1. Cell viability from the capsules retrieved from Dana's brain are also included in the table, however, secretion rates could not be assessed, since only 5-10 microcapsules could be obtained.

### 3.3.4 Quantitative Analysis

Significant levels of human growth hormone delivery were observed in the CSF of Duffy and Dino on day 7, and in Dana on days 7 and 14 as compared to day 0 values. Duffy showed the highest growth hormone delivery levels with 72.22 ng hGH/ml,  $p < 0.01$ , on day 7, followed by Dana (21.11 ng hGH/ml,  $p < 0.01$ ) and then Dino (20.98 ng hGH/ml,  $p < 0.05$ ). On day 14, 2.33 ng hGH/ml could still be detected in Dana's CSF ( $p < 0.01$ ). In the plasma, human growth hormone could not be detected in any dog. These data are illustrated in figure 3-2.

Significant levels of growth hormone delivery were observed only in Dino's brain in the thalamus, near the implantation site (0.02ng hGH/mg protein,  $p < .01$ ). The lack of hormone delivery to the various brain regions of each dog are illustrated in figure 3-3.

Within the two week survival period, only Duffy developed antibodies against the human growth hormone in the CSF (7.47x increase on day 7,  $p < 0.01$ ; 741.57x increase on day 14,  $p < 0.01$ ). Significant antibody levels were also detectable in Duffy's plasma on days 10 and 14 (39.4x increase on day 10,  $p < 0.01$ ; 37.7x increase on day 14,  $p < 0.01$ ).

Antibody titres could also be detected in Dana's plasma on day 14 (52.15x increase,  $p < 0.01$ ). These data are illustrated in figure 3-4.

White blood cell (WBC) content in the CSF was only measured in Dana. The WBC normal reference range is  $0-2.0 \times 10^6/L$  (Allen et al., 1991). Dana's WBC level increased dramatically from  $2.0 \times 10^6/L$  on day 0 to  $2.8 \times 10^7/L$  on day 7 and  $8.9 \times 10^7/L$  on day 14. Microprotein levels remained within normal range ( $0.1-0.3g/L$ ; Allen et al., 1991).

### **3.3.5 Pathology**

Duffy's brain appeared normal upon microscopic examination. There was no evidence of treatment histologically or immunohistologically as far caudal as the cerebellum. The spinal cord was not obtained, and could therefore not be examined.

Dino's brain appeared normal in all brain regions except the areas surrounding the right lateral ventricle and thalamus. The blood vessels lining the lateral ventricle and the immediate vicinity were cuffed with lymphocytes (figure 3-5B). There was also some minimal loss of the ependymal lining organization. The inflammatory reaction appeared to be more developed in the thalamus where capsule debris and hGH-immunopositive MDCK cells could be visualized (figure 3-6B). The blood vessels in this region were also cuffed with lymphocytes. The capsule debris was surrounded by inflammatory infiltrate, including lymphocytes, macrophages and multinucleated giant cells (figure 3-5C). There was a massive loss of neural organization, as demonstrated by both the H&E and Nissl stains.

GFAP immunostaining demonstrated mild gliosis around the ventricle lining and a more severe reaction at the microcapsule implantation site. The astrocytes appeared hypertrophied, but glial scarring was not yet apparent (figure 3-6D).

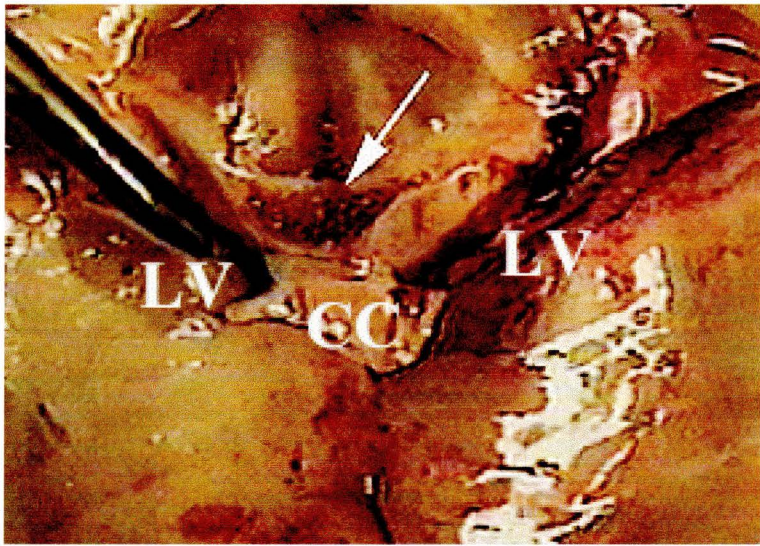
The blood vessels surrounding the lateral ventricles in Dana's brain were also cuffed with many lymphocytes (figure 3-7B, D). Massive inflammatory infiltration was observed at the ventral portion of the lateral ventricle, near the caudate nucleus (3-7E). This infiltration consisted of lymphocytes, epithelial macrophages, and multinucleated giant cells. The organization of ependymal lining was lost, particularly in the more infiltrated regions. No hGH could be detected with immunohistochemical staining. GFAP immunostaining demonstrated an astrogliosis reaction in the area of inflammation (figure 3-7G).

The inflammatory reaction decreased at the posterior sections of the lateral ventricle, demonstrating only cuffed blood vessels. The corpus callosum did not harbour any microcapsule debris and showed a mild inflammatory reaction with a few cuffed blood vessels. The occipital cortex, medulla, cerebellum and spinal cord all appeared normal.

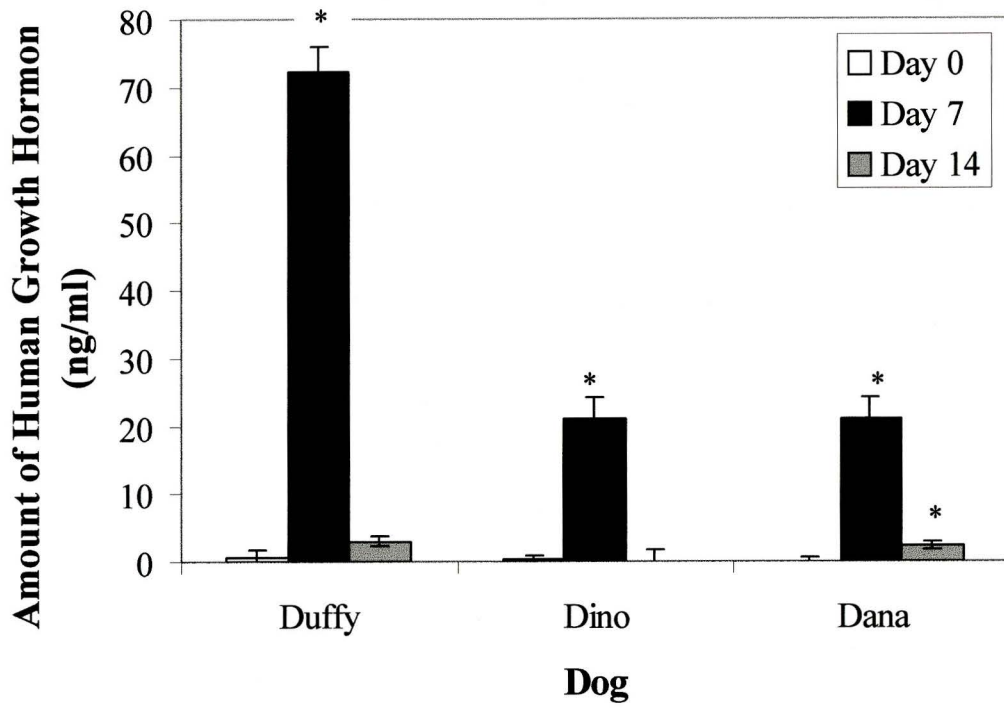
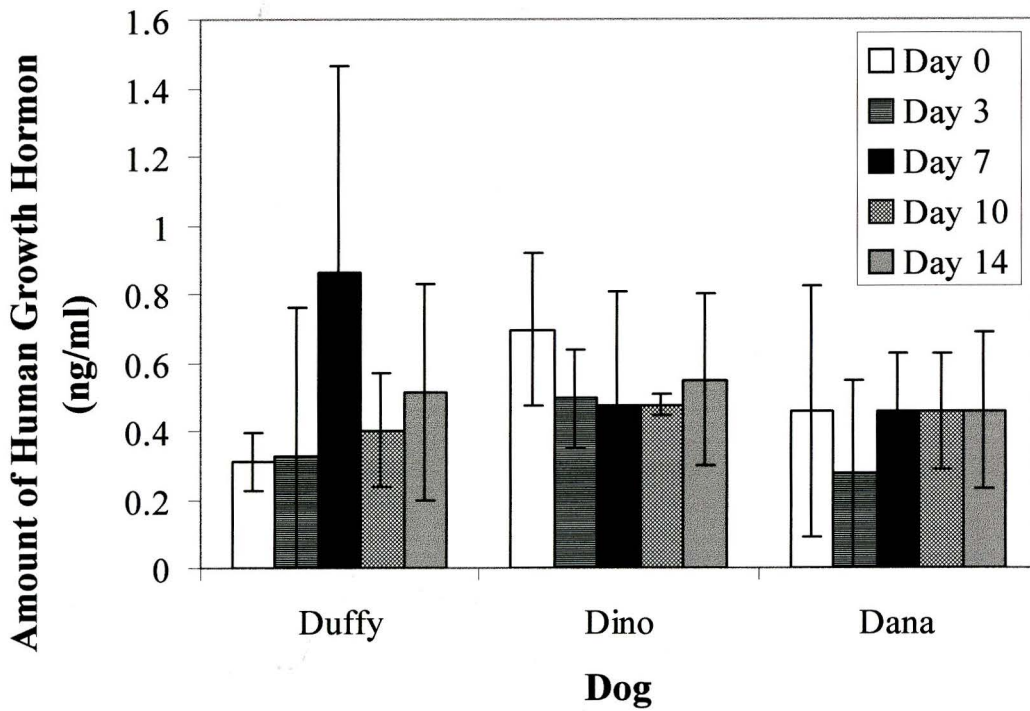
**Table 3-1** Encapsulated cell viability and human growth hormone secretion assessments from microcapsules maintained *in vitro* throughout the post-operative survival period. The cell viability from microcapsules retrieved from Dana during post-mortem examination is also included. Secretion values are the average of duplicate samples  $\pm$  average deviation.

<b>Microcapsule Batch</b>	<b>Day Number</b>	<b>% Viability <math>\pm</math> SD</b>	<b>Secretion (ng hGH/million live cells/hr)</b>
<b>Dino/Duffy – Maintained <i>in vitro</i></b>	0	89.9 $\pm$ 7.6	69.486 $\pm$ 9.168
	7	69.9 $\pm$ 18.0	43.532 $\pm$ 0.081
	14	67.6 $\pm$ 4.0	88.369 $\pm$ 7.105
<b>Dana – Maintained <i>in vitro</i></b>	0	70.3 $\pm$ 6.9	130.04 $\pm$ 3.920
	7	69.7 $\pm$ 17.2	N/A
	14	64.3 $\pm$ 11.8	29.312 $\pm$ 0.310
<b>Dana – Retrieved</b>	14	64.3 $\pm$ 11.5	N/A

**Figure 3-1** Photo taken of coronal brain section during Dana's post-mortem examination. Arrow indicates free microcapsules discovered on the dorsal portion of the corpus callosum. CC- corpus callosum; LV- lateral ventricle.

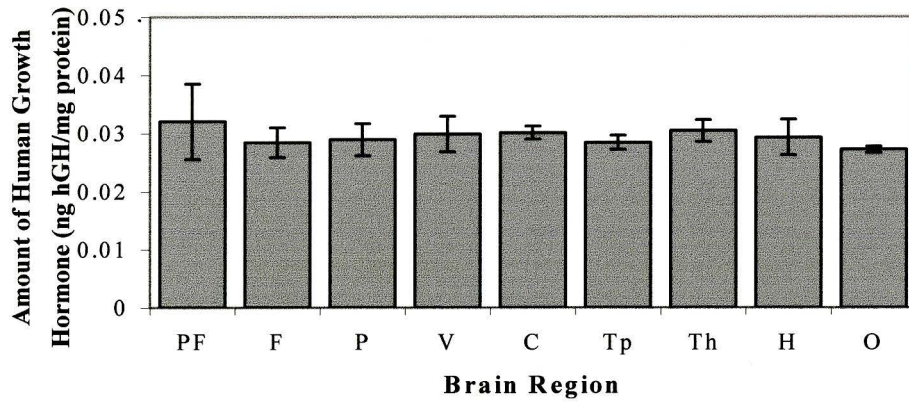
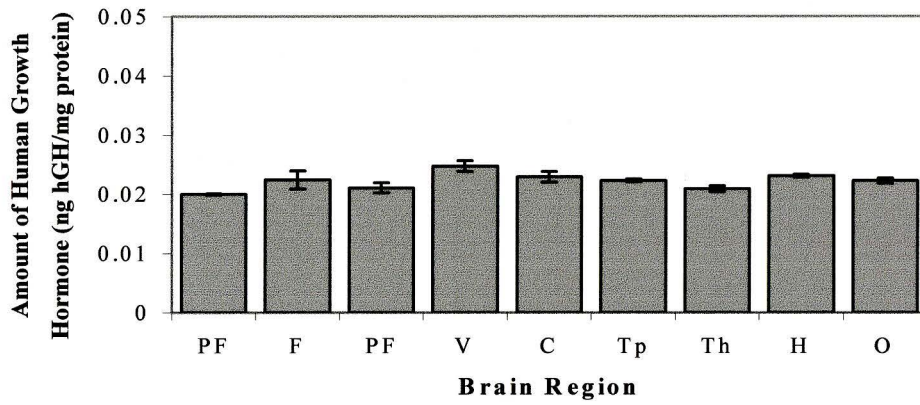
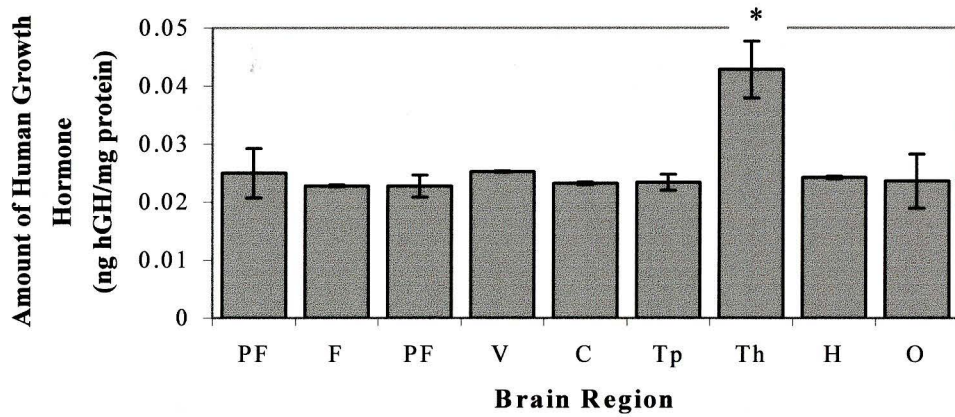
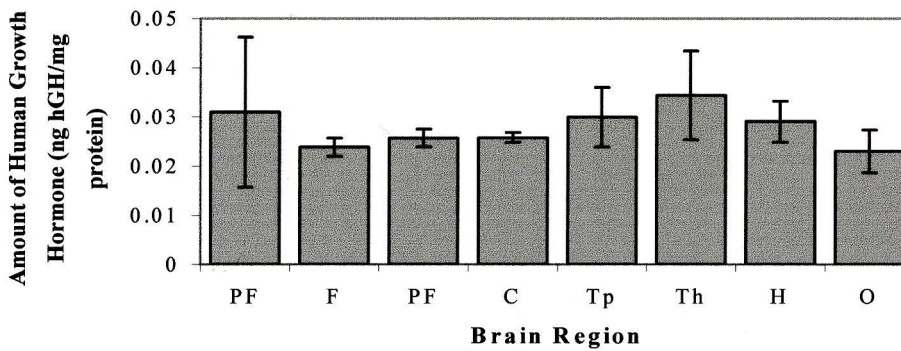


**Figure 3-2** Delivery of human growth hormone to the cerebrospinal fluid (A) and plasma (B). Data are the average of triplicate hGH ELISA values  $\pm$  SD. In the CSF, all three dogs showed significant hormone levels on day 7 ( $p < .01$  for Duffy and Dana;  $p < .05$  for Dino) while only Dana showed significant levels on day 14 ( $p < .01$ ). Significant delivery levels were not observed in the plasma.

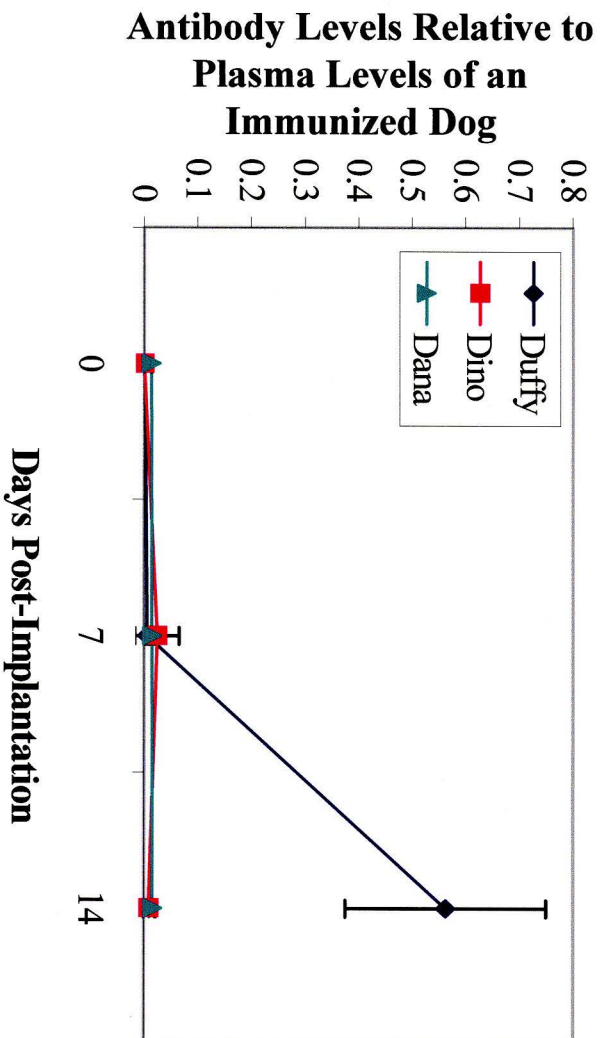
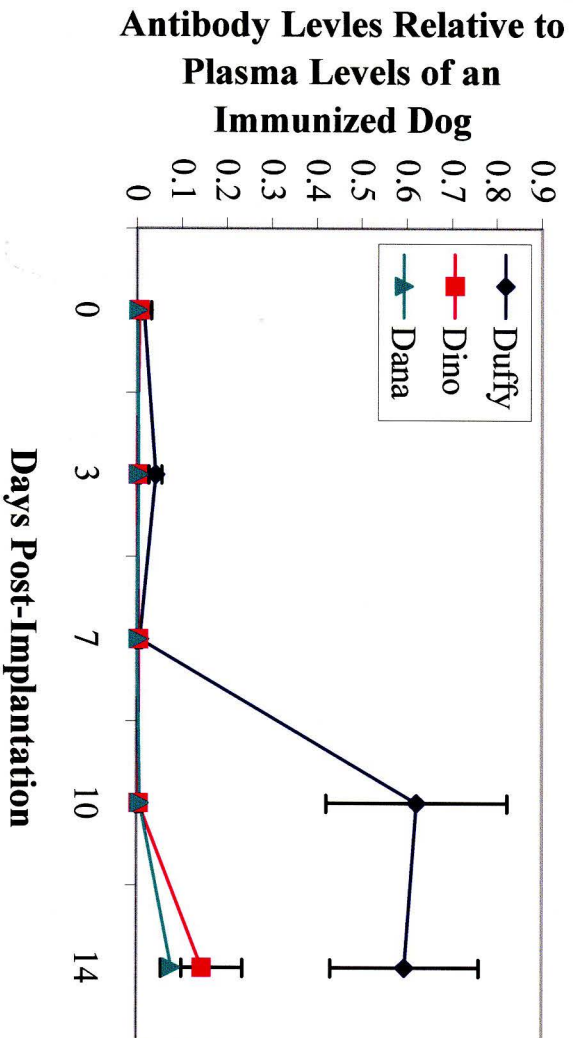
**A****B**

**Figure 3-3** Delivery of human growth hormone to various brain regions. The thalamus, lateral ventricles, caudate nucleus and hippocampus are the brain regions anatomically closest to lateral ventricle implantations. Data are the mean of hGH ELISA values/protein measurements  $\pm$  SD. Significant hormone levels were observed only in Dino's thalamus,  $p < .01$ , on the border of the microcapsule implantation site. (A) Tissue dog control, (B) Duffy, (C) Dino, (D) Dana.

**PF**-Prefrontal cortex; **F**-Frontal cortex; **P**-Parietal Cortex; **V**-Lateral ventricle lining; **C**-Caudate nucleus; **Th**-Thalamus; **Tp**-Temporal cortex; **H**-Hippocampus; **4<sup>th</sup>**- Fourth ventricle lining **O**-Occipital cortex

**A****B****C****D**

**Figure 3-4** Detection of antibody against human growth hormone in the cerebrospinal fluid (A) and plasma (B). Antibody titre is expressed as a value relative to antibody levels in the plasma of an immunized dog (where immunized dog value = 1). Data are the average of triplicate samples  $\pm$  SD. In the CSF, significant antibody titre increases from day 0 were observed in Duffy on day 14 ( $p < .01$ ). In the plasma, only Duffy and Dana showed significant antibody titre increases from day 0,  $p < .01$ .

**A****B**

**Figure 3-5** Histological examination of Dino's brain tissue. (A) H&E staining of control brain demonstrating blood vessels (arrows) and normal tissue elements. (B) H&E staining of lining of the lateral ventricle (LV). White arrow indicates blood vessel cuffed with lymphocytes; black arrow indicates microcapsule debris within the ventricular cavity. (C) H&E staining of capsule debris at implantation site and surrounding inflamed tissue. White arrow denotes microcapsule material. Inflammatory infiltrate includes lymphocytes, macrophages and multinucleated giant cells.

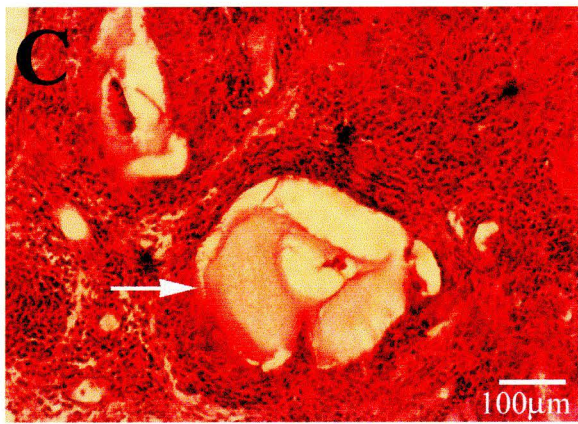
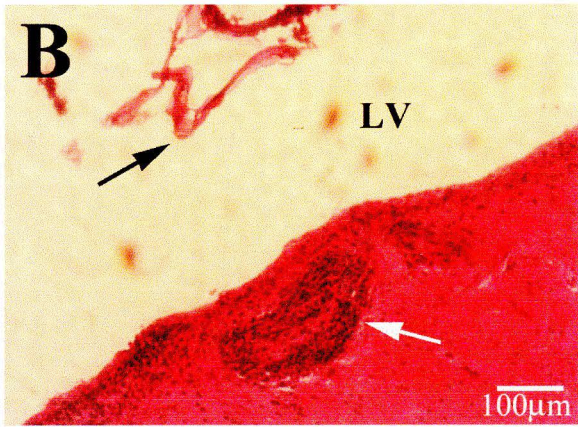
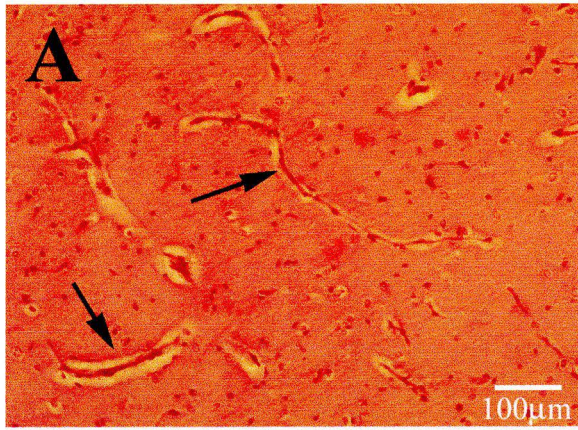


**Figure 3-6** Immunohistochemistry samples from Dino's brain tissue. (A) Negative control for immunohistochemistry against human growth hormone. (B) Human growth hormone positive cells (brown) counterstained with a cresyl violet Nissl stain. Arrows highlight some of the many hGH-positive MDCK cells released from the compromised capsules into the brain parenchyma. (C) Normal astrocytes (arrows) as demonstrated with GFAP immunohistochemistry. Note the thin cell bodies and fibrous processes. (D) GFAP immunostaining demonstrating reactive astrocytes surrounding the site of inflammation (arrows). Note the swollen cell bodies and more prominent processes.

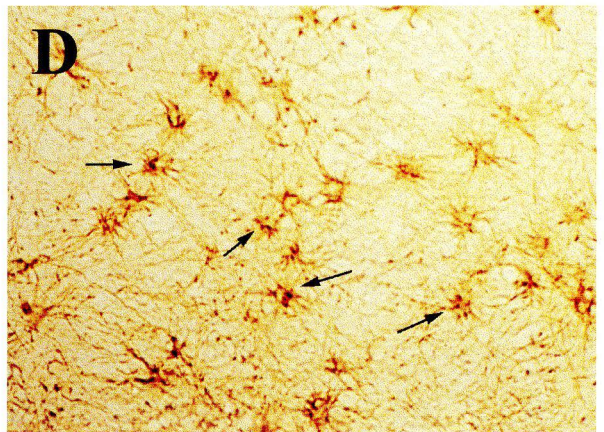
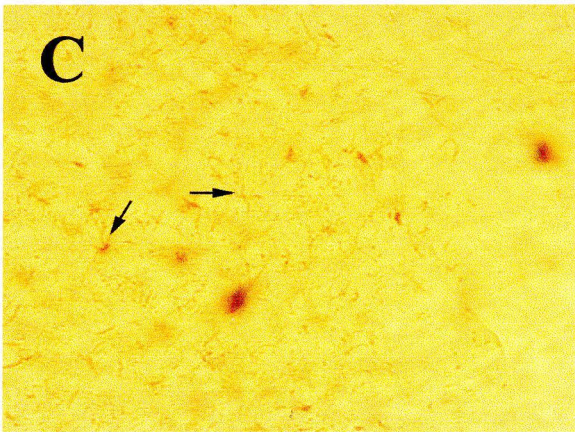
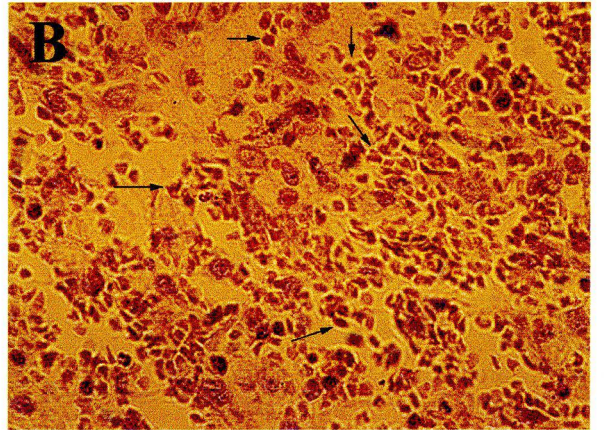
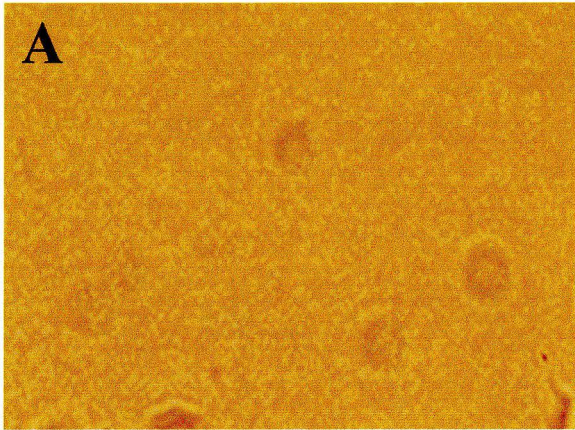
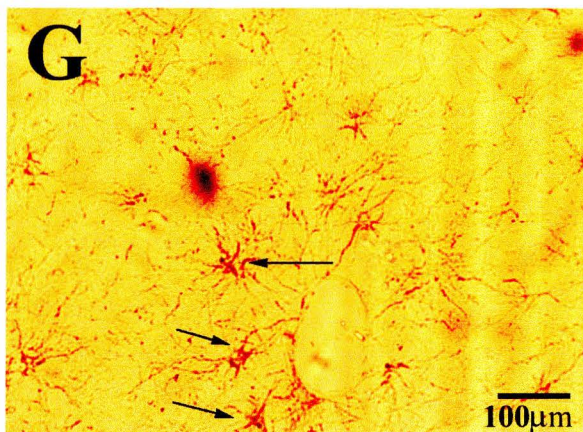
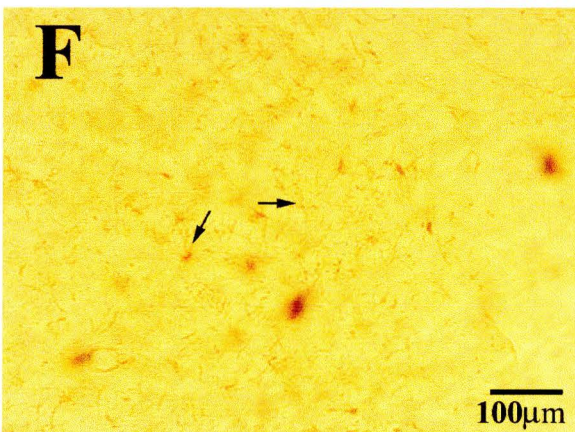
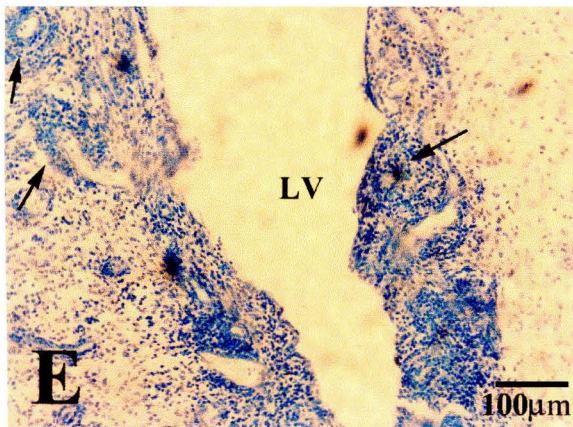
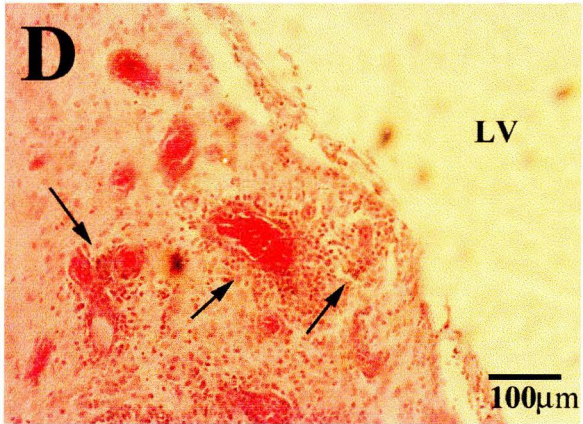
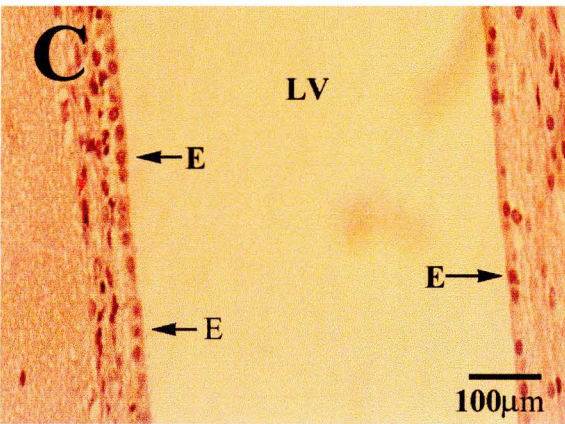
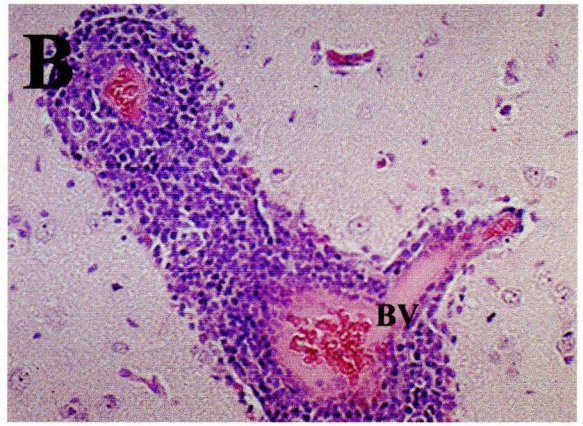
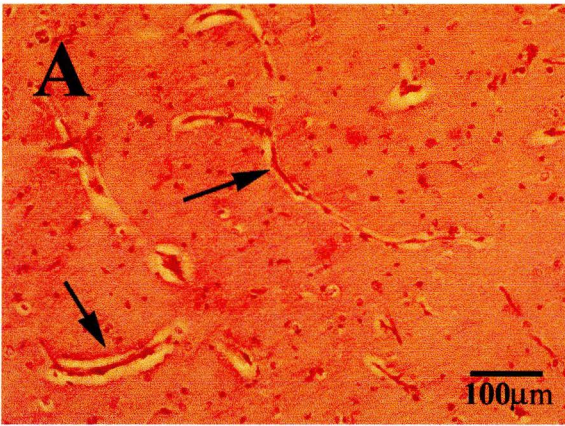


**Figure 3-7** Histological examination of Dana's brain tissue. (A) H&E staining of control brain. Arrows highlight normal blood vessels. (B) H&E staining of a blood vessel near the lateral ventricles in Dana's brain. Note the extensive cuffing of the blood vessels by lymphocytes. (C) H&E staining of normal ependymal lining of the lateral ventricle (LV). Arrows with E highlight ependymal cells. (D) H&E staining of lining of the lateral ventricle (LV) with many blood vessels cuffed with lymphocytes (arrows). Also note the loss of ependymal organization. (E) Nissl stain of the lateral ventricle lining demonstrating the extensive inflammatory infiltrate and loss of ependymal organization. (F) Normal astrocytes (arrows) as demonstrated with GFAP immunohistochemistry. Note the thin cell bodies and fibrous processes. (G) GFAP immunostaining of reactive astrocytes (arrows) near the lateral ventricles in Dana's brain.



## **4.0 DELIVERY OF MICROCAPSULES WITH VARYING CONTENTS TO THE CENTRAL NERVOUS SYSTEM OF PREVIOUSLY TREATED DOGS**

### **4.1 RATIONALE**

With the unexpected immune reaction observed in the canine CNS after the microcapsule treatment described in chapter 3, we felt it was necessary to determine what specific factor was inducing the foreign body reaction. The three major candidates appeared to be the microcapsule material, the encapsulated cells or the secreted product, human growth hormone. The following experiment was designed to investigate the potential contribution of each of the immunogenic candidates to the development of the foreign body reaction.

The animals used in this experiment had been previously treated with microcapsules secreting human growth hormone either into the intraperitoneal cavity or subcutaneously. Data from this chapter must therefore be interpreted with caution due to confounding factors from the sensitization of the dogs to human growth hormone and foreign cells. In spite of these limitations, the ethical considerations and the prohibitive cost of dogs were the basis of our decision to ensure maximal use of the large experimental animals. These dogs were sufficient for achieving the objectives of determining the immunogen, improving the microcapsule quality to eliminate the factors contributed by compromised capsules as well as improvement of both surgical techniques.

## **4.2 MATERIALS AND METHODS**

### **4.2.1 Animals**

The six animals used in this experiment were female beagles, aged 19-23 months. All of the dogs had been previously implanted with microcapsules during another experiment in our laboratory six to ten months prior to this study. The dogs received the previous implantation either intraperitoneally or subcutaneously, with the microcapsules containing either MDCK cells or canine fetal myoblast (CFM) cells, both secreting human growth hormone.

### **4.2.2 Central Nervous System Treatment**

The animals were divided into two groups, those receiving a spinal intrathecal implantation of microcapsules, and those receiving an intraventricular implantation. The groups were further divided by the content of the microcapsules - empty, untransfected MDCK cells, or transfected MDCK cells secreting human growth hormone. Four of the six animals also received intraperitoneal and subcutaneous implantations of empty capsules as a part of another student's experiment. See table 4-1 for a summary of previous and current treatments.

#### **4.2.2.1 Spinal Intrathecal Implantation**

Four dogs received a spinal intrathecal implantation of microcapsules, as outlined in section 2.2.4.

The first dog (Polly) received 2ml microcapsules, but quickly developed severe clinical complications (to be described below), apparently the partial result of the impinging volume upon the spinal cord. Blood samples were obtained on days 0 (pre-surgery), 3 and 8 (pre-euthanization) while CSF samples were obtained on days 0 and 8. Due to the development of meningitis-like symptoms, this dog was euthanized early, at eight days post-operative.

In an attempt to alleviate the development of clinical symptoms, the remaining three dogs received a smaller microcapsule volume, 0.5ml, suspended in 0.5ml physiological saline. Blood samples were obtained on days 0 (pre-surgery), 3, 7, 10, and 14 (pre-euthanization). CSF samples were obtained on days 0 (pre-surgery), 7, and 14 (pre-euthanization). Neurological examinations were carried out prior to the spinal tap on day 7. The animals were euthanized 14 days post-operative.

#### **4.2.2.2 Intraventricular Implantation**

Two dogs received intraventricular implantations as described in section 2.2.6. In an attempt to increase the likelihood of successful intraventricular targeting, the capillary tube adjustment described in section 2.2.6 was implemented for both of these animals and both dogs received CT scans 10-20 days prior to the microcapsule implantations, as described in section 2.2.5 (figure 4-1).

The surgeries were performed at McMaster University, Central Animal Facility. Each dog received a total of 0.5ml of microcapsules (0.25ml microcapsules suspended in 0.25ml physiological saline into each hemisphere).

### **4.2.3 Analyses**

For each dog, there was a post-operative clinical assessment, including a neurological examination and post-mortem analysis of gross findings at euthanization, quantitative analysis of the human growth hormone and antibody content in the plasma, CSF and brain tissue, and histological and immunohistological examination of the brain and spinal cord tissue. Further, encapsulated cell viability and secretion assessments were carried out on microcapsules maintained *in vitro* and on retrieved capsules, when possible.

## **4.3 RESULTS**

### **4.3.1 Clinical Evaluation**

All dogs that received a total of 0.5ml microcapsules, whether into the spinal intrathecal space or intraventricularly, were normal upon clinical and neurological assessment. All dogs were alert and active for the 14 post-operative days. Posture and gait were normal - dogs were able to hop and wheelbarrow upon manipulation of the limbs. Proprioceptive reactions, muscle strength and reflexes and cranial nerve evaluations were normal.

The dog that received 2ml of microcapsules into the spinal intrathecal space, Polly, showed severe twitching, shivering and pain immediately after surgery. She appeared to be very sensitive to touch or movement of the neck area. Steroid and analgesic treatment alleviated the pain, and the dog improved dramatically over the following days. Upon neurological examination, a head tilt towards the right and abnormal gait were observed. Further, right leg semi-ataxia was demonstrated by right front paw slowed proprioception and difficulty wheelbarrowing and hopping on the right side. Six days post-operative, the animal was found demonstrating meningitis-like symptoms, bent over and shivering with a fever of 42.5°C. The subsequent administration of morphine and antibiotics appeared to decrease the pain, but the animal remained in poor condition. The spinal tap on day 7 was cancelled, and the decision was made to euthanize this animal on day 8 post-operative.

## **4.3.2 Post-Mortem Analyses**

### **4.3.2.1 Post-Mortem Analyses - Spinal Intrathecal Implantations**

*Spot:* Upon removal of the brain and spinal cord, the empty microcapsules appeared to have migrated from the cisterna magna and had aggregated at the ventral medulla. Microcapsules were discovered along the skull surface, and there was no evidence of edema or any inflammatory reaction.

*Jazz:* Upon removal of the brain and spinal cord, the microcapsules containing non-transfected MDCK cells were found embedded underneath the pia and subarachnoid

mater along the brainstem. Some microcapsules were also found at the optic chiasm, but none were observed along the skull surface. A few microcapsules were retrieved for cell viability analysis. The spinal cord showed redness and evidence of edema.

*Squirt:* Upon removal of the brain and spinal cord, microcapsules containing MDCK cells secreting human growth hormone were found to be embedded within the tissue and meninges surrounding the spinal cord and brainstem. Some microcapsules were retrieved for cell viability analysis. The meninges appeared red and swollen, with evidence of inflammation (cloudy/opaque).

*Polly:* Upon removal of the brain and spinal cord, microcapsules containing MDCK cells secreting human growth hormone were found ventrally along the spinal cord (as far as C4), brainstem and scattered as far anterior as the pituitary stalk. Some capsules were retrieved for cell viability assessment. The microcapsules were embedded within the leptomeninges which appeared markedly red, edematous and congested.

#### **4.3.2.2 Post-Mortem Analyses – Intraventricular Implantations**

*Jewel:* Upon removal of the brain and spinal cord, the cannula tracks from the surgical procedure were observed on the surface of the brain in the parietal cortex. The microcapsules containing non-transfected MDCK cells were free and non-adherent, located within the lateral, third and fourth ventricles, the cerebral aqueduct, and in the space between the occipital lobes and the cerebellum, indicative of movement throughout

the ventricular system (figure 4-2). Some microcapsules were retrieved for cell viability analysis. The dura mater was noted to be slightly haemorrhagic, while the choroid plexus in the left lateral ventricle as well as the anterior portions of the spinal cord appeared red.

*Smudge:* Upon removal of the brain and spinal cord, the cannula tracks were once again observed on the brain surface, but were more caudal than those noted in Jewel. The microcapsules containing MDCK cells secreting human growth hormone were found in the fourth ventricle and in the space between the occipital cortex and cerebellum (figure 4-3B). In the right hemisphere, an aggregation of capsules was discovered below the lateral ventricle, creating a hole in the thalamus (figure 4-3A). Some microcapsules were retrieved for cell viability and secretion analysis (figure 4-4).

### **4.3.3 Microcapsule Cell Viability and Secretion Analyses**

Table 4-2 summarizes the findings of cell viability and secretion assessments for the encapsulated cells maintained *in vitro* throughout the duration of the experiment, as well as those retrieved from the CNS during post-mortem examination, where possible. Cell viability decreased with time. The capsules retrieved from Squirt and Smudge showed cell viabilities that were comparable to those maintained *in vitro*. The microcapsules retrieved from Jazz, Polly and Jewel, however, showed cell viabilities that were significantly lower than those maintained *in vitro*.

Although secretion assessments could not be obtained from the small volume (5-10 microcapsules) retrieved from the animals, some of the capsules from Jewel were broken open and cells were re-grown *in vitro*. This manipulation had also been carried out on microcapsules maintained *in vitro* for the duration of the experiment. The cells from the retrieved microcapsules secreted significantly more human growth hormone than the cells from the *in vitro* microcapsules ( $p < .01$ ).

#### 4.3.4 Quantitative Analyses

Using an ELISA for human growth hormone detection, hGH could not be detected in the plasma or brain tissue of any of the dogs. Analysis of the CSF resulted in growth hormone detection only in Smudge's fluid on day 7 (34.25 ng/ml,  $p < .001$ ). These data are illustrated in figures 4-5 and 4-6.

Antibody to human growth hormone was detected in the CSF and plasma of most of the dogs. In the CSF, Squirt, Polly, Jewel and Smudge showed 144.4 fold,  $p < .001$  (day 14), 17.90 fold,  $p < .01$  (day 8), 11.63 fold,  $p < .001$  (day 14) and 1.91 fold,  $p < .01$  (day 14) increases from day 0 values, respectively. In the plasma, the antibody titre increased from day 0 values in Squirt on days 10 (95.23 fold,  $p < .01$ ) and 14 (99.58 fold,  $p < .001$ ), Polly on day 8 (5.0 fold,  $p < .01$ ), and Smudge on days 10 (13.70 fold,  $p < .001$ ) and 14 (13.61 fold,  $p < .001$ ). These results are illustrated in figure 4-7.

The white blood cell (WBC) content in the CSF of dogs normally ranges from 0- $2.0 \times 10^6$ /L while microprotein levels range from 0.1-0.3g/L (Allen et al., 1991). These

parameters were not examined in Spot or Polly, but were increased in the other four animals after treatment as summarized in table 4-3.

### **4.3.5 Pathology**

#### **4.3.5.1 Pathology – Spinal Intrathecal Implantations**

*Spot:* Minimal changes were observed in the brain and spinal cord tissue (figures 4-9A, C, 4-11A). H&E staining demonstrated occasional lymphocytes and macrophages around blood vessels in the thalamus, midbrain, cerebellum and medulla. Microcapsule debris was observed around the spinal cord, surrounded by a thin fibrous capsule (figure 4-8A, 4-10A). Mild localized chronic meningitis and foreign body reaction was noted, but the capsule material in the CSF can be considered to be essentially biologically inert (figure 4-8A, 4-10A).

*Jazz:* A severe inflammatory reaction was observed in the brain, spinal cord and leptomeninges of this dog, against the cell-containing microcapsules. H&E staining exposed diffuse to patchy infiltration around the vascular system by lymphocytes, plasma cells and macrophages. This inflammatory reaction was observed in the striatum, thalamus, midbrain, pons and cerebellum. Microcapsule debris was noted, containing some necrotic cells. The microcapsule material, particularly in the pons and cervical and thoracic spinal cord regions, was the centre of extensive inflammatory activity, as indicated by the presence of epithelioid macrophages, eosinophils and multinucleated giant cells (figure 4-8B). Nissl staining demonstrated the loss of cellular organization, as

well as cellular necrosis (figure 4-8D). GFAP immunostaining demonstrated an astrogliosis reaction around the area of inflammation (figure 4-8F).

*Squirt:* A severe inflammatory reaction was also observed in this animal in the brain, spinal cord and leptomeninges (figure 4-9B). H&E staining revealed a diffuse to severe inflammatory reaction in the frontal cortex, striatum, thalamus, midbrain, cerebellar peduncles and obex, with increasing severity towards the midbrain and medulla (figure 4-9D). The infiltrate included macrophages, eosinophils, lymphocytes, and plasma cells, and was often aggregated around blood vessels or microcapsular material. Again, some microcapsules contained clumps of necrotic cells. GFAP immunostaining demonstrated an astroglial response to the foreign material (figure 4-9F).

*Polly:* This animal demonstrated the most severe inflammatory reaction, affecting the brain, spinal cord and leptomeninges (figure 4-10D). With H&E staining, diffuse inflammatory infiltrate was observed as far anterior as the basal ganglia. Severity of the inflammation increased from the thalamus towards the midbrain, with the most severe reaction localized to the medulla and cerebellum. Most of the infiltrate was in the area of the leptomeninges and included macrophages, lymphocytes, eosinophils, plasma cells and multinucleated giant cells. The choroid plexus also showed diffuse infiltration as well as edema. The eighth cranial nerve was also showed severe inflammation.

Small blood vessels showed hypertrophy in the basal meninges. Further, large vacuoles and neuronal degeneration were observed throughout the caudal portion of the brain and spinal cord, as visualized with the Nissl stain in figure 4-10F.

Microcapsule material, surrounded by inflammatory infiltrate (figure 4-10B), was discovered in the fourth ventricle as well as the central canal of the spinal cord. The central canal of the C1 section was mostly obliterated by a massive inflammatory reaction, including lymphocytes foamy macrophages, epithelial macrophages, plasma cells and eosinophils. The other portions of the spinal cord showed inflammatory infiltration of the meninges. GFAP immunohistochemistry revealed severe astrogliosis (figure 4-10H) with the development of the glial scar.

Immunostaining for human growth hormone was negative for all dogs.

#### **4.3.5.2 Pathology – Intraventricular Implantations**

*Jewel:* Severe and widespread granulomatous inflammation was observed throughout the brain and leptomeninges (figure 4-11D, E). The choroid plexi in the lateral and fourth ventricles were edematous and were mildly infiltrated by macrophages (figure 4-11B). Some microcapsule material was located in the lateral ventricle, surrounded by a thin eosinophilic band, while the material found in the fourth ventricle was surrounded by a more intense inflammatory reaction with the encapsulated cells appearing necrotic. The lateral ventricle and the cerebral aqueduct appeared dilated and contained inflammatory infiltrate, including macrophages and giant cells. A large haemorrhage extended from the corpus callosum to the third ventricle, apparently a result of the injection. The

haemorrhage and nearby microcapsular material was surrounded by intense localized inflammation mediated by epithelioid macrophages and multinucleated giant cells (figure 4-11E,F). Blood vessels and leptomeninges also showed severe inflammatory infiltration. Again, astrogliosis around the site of inflammation could be visualized with GFAP immunostaining (figure 4-12).

*Smudge:* H&E staining of the brain and spinal cord tissue showed evidence of a severe inflammatory reaction. Small blood vessels around the lateral ventricle were associated with lymphocytes, while the choroid plexus within the lateral and fourth ventricles was edematous and contained mild, patchy infiltration. The fourth ventricle contained microcapsule fragments. The leptomeninges were also affected by the inflammatory reaction, with the severity increasing with more caudal sections. The spinal cord showed mild infiltration by macrophages in the meninges, and the central canal appeared dilated with macrophages surrounding the microcapsular material (figure 4-13B).

In the right hemisphere, approximately 3mm below the lateral ventricle, the capsule implantation site was visualized within the thalamus. This site was surrounded by epithelioid macrophages and multinucleated giant cells (figure 4-13C). Further, there was evidence of necrotic cells, swollen axons and microgliosis. GFAP immunostaining also revealed extensive astrogliosis around the site of implantation (figure 4-13E).

**Table 4-1** Summary of previous and current microcapsule implantations.

<b>Dog</b>	<b>Age (months)</b>	<b>Previous Peripheral Microcapsule Implantation</b>	<b>Concurrent Peripheral Microcapsule Implantation (Empty Capsules)</b>	<b>Central Nervous System Microcapsule Treatment</b>
<b>Spot</b>	21	Intraperitoneal; hGH-CFM cells	N/A	Spinal intrathecal; 0.5ml Empty capsules
<b>Jazz</b>	21	Subcutaneous; hGH-CFM cells	50ml PLL intraperitoneal; 15ml PLL subcutaneous	Spinal intrathecal; 0.5ml Non-transfected MDCK cells
<b>Squirt</b>	22	Subcutaneous; hGH-CFM cells	50ml PLA intraperitoneal; 15ml PLA subcutaneous	Spinal Intrathecal; 0.5ml hGH-MDCK cells
<b>Polly</b>	19	Subcutaneous; hGH-MDCK cells	N/A	Spinal intrathecal; 2ml hGH-MDCK cells
<b>Jewel</b>	23	Intraperitoneal; hGH-MDCK cells	50ml PLL intraperitoneal; 15ml PLL subcutaneous	Intraventricular; 0.5ml Non-transfected MDCK cells
<b>Smudge</b>	23	Intraperitoneal; hGH-CFM cells	50ml PLA intraperitoneal; 15ml subcutaneous	Intraventricular; 0.5ml hGH-MDCK cells

**Table 4-2** Encapsulated cell viability and secretion assessments from microcapsules maintained *in vitro* throughout the survival period or retrieved during post-mortem examination. P values compare retrieved viability to *in vitro* day 14 viability. All secretion values are the average of duplicate samples expressed in ng hGH/million live cells/hour  $\pm$  average deviation.

Microcapsules	Day Number (Post-operative)	% Viability $\pm$ SD	Secretion $\pm$ Ave Deviation
Spot	--	--	--
<b>Jazz – Maintained In Vitro</b>	0	89.4 $\pm$ 5.3	--
	7	--	--
	14	81.5 $\pm$ 11.9	--
<b>Retrieved (5-10 capsules)</b>	14	65.4 $\pm$ 11.1 (p<.05)	--
<b>Squirt – Maintained In Vitro</b>	0	58.8 $\pm$ 11.4	52.408 $\pm$ 0.431
	7	57.26 $\pm$ 9.2	54.981 $\pm$ 4.296
	14	55.06 $\pm$ 5.1	21.975 $\pm$ 0.150
<b>Retrieved (5-10 capsules)</b>	14	56.76 $\pm$ 16.7	--
<b>Polly – Maintained In Vitro</b>	0	65.4 $\pm$ 9.2	52.947 $\pm$ 2.986
	8	89.1 $\pm$ 5.2	21.537 $\pm$ 0.571
<b>Retrieved (5-10 capsules)</b>	8	70.6 $\pm$ 12.0 (p<.01)	--
<b>Jewel – Maintained In Vitro</b>	0	81.2 $\pm$ 9.8	--
	7	72.5 $\pm$ 14.1	--
	14	69.1 $\pm$ 9.1	--
<b>Retrieved (5-10 capsules)</b>	14	58.3 $\pm$ 11.3 (p<.05)	--
<b>Smudge – Maintained In Vitro</b>	0	79.8 $\pm$ 9.4	40.717 $\pm$ 0.624
	7	76.1 $\pm$ 5.0	18.411 $\pm$ 0.043
	14	67.2 $\pm$ 9.4	14.710 $\pm$ 0.425*
<b>Retrieved (5-10 capsules)</b>	14	59.7 $\pm$ 12.3	19.839 $\pm$ 0.263* (p<0.01 as compared to cells broken out of <i>in vitro</i> capsules)

\*Encapsulated cells were broken out of capsules and grown *in vitro* for one month before secretion assay.

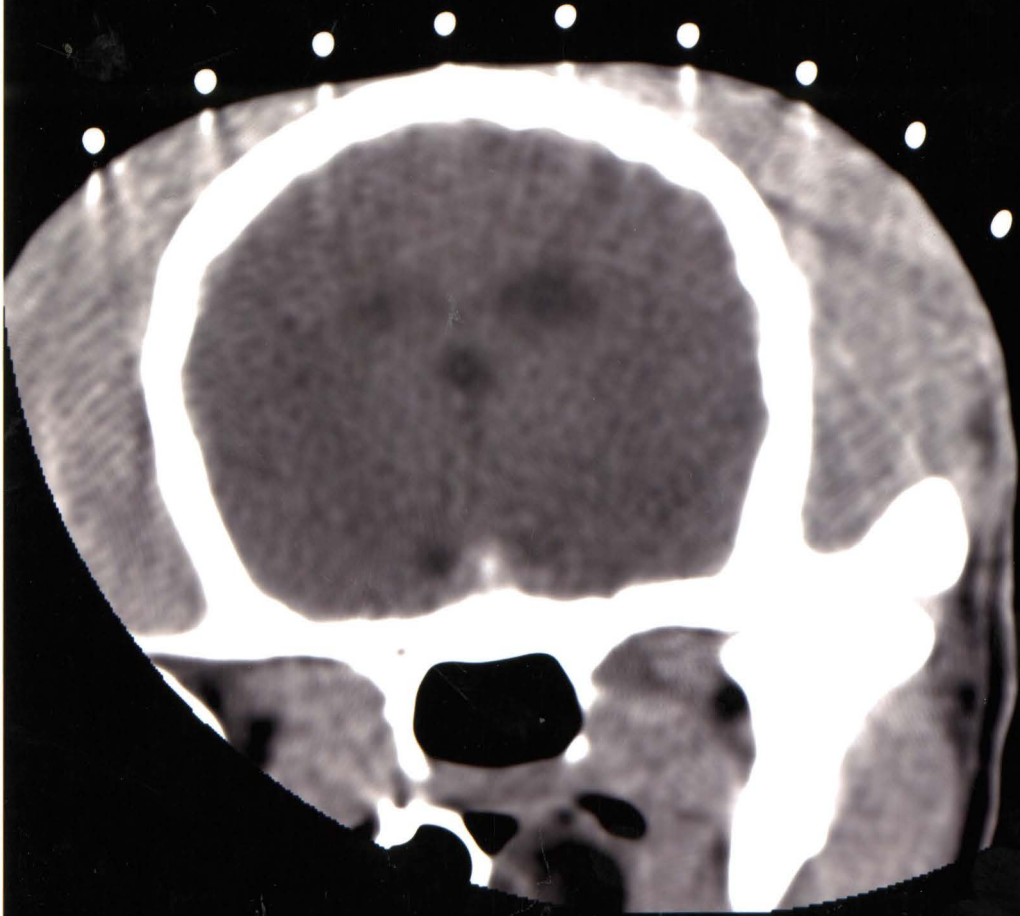
**Table 4-3** White blood cell (WBC) and microprotein content increases in the CSF of 4 dogs. Day 0 values were all within normal range - normal WBC range is  $0-2.0 \times 10^6/L$ ; normal microprotein range is  $0.1-0.3g/L$  (Allen et al., 1991).

<b>Dog</b>	<b>WBC Content</b>	<b>Microprotein Content</b>
Jazz	$2.5 \times 10^8/L$ on day 7 $5.69 \times 10^8/L$ on day 14	$0.48g/L$ on day 14
Squirt	$2.78 \times 10^9/L$ on day 7 $3.00 \times 10^8/L$ on day 14	$0.57g/L$ on day 7 $0.68g/L$ on day 14
Jewel	$2.92 \times 10^8/L$ on day 7 $3.70 \times 10^8/L$ on day 14	$0.62g/L$ on day 14
Smudge	$1.0 \times 10^7$ on day 7 $1.09 \times 10^8$ on day 14	no increase

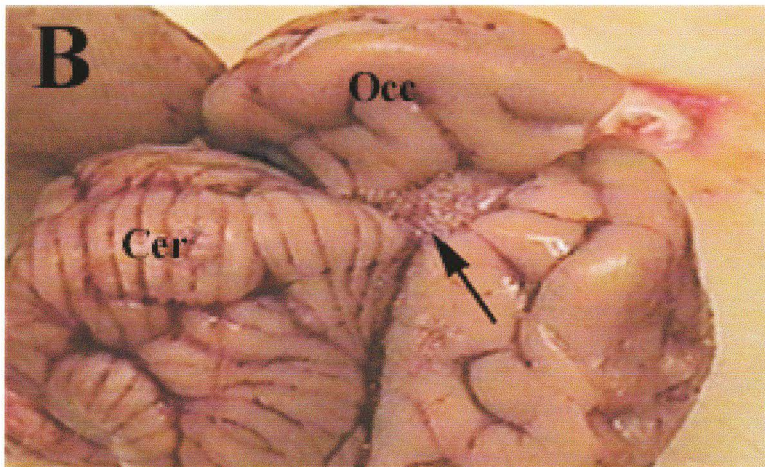
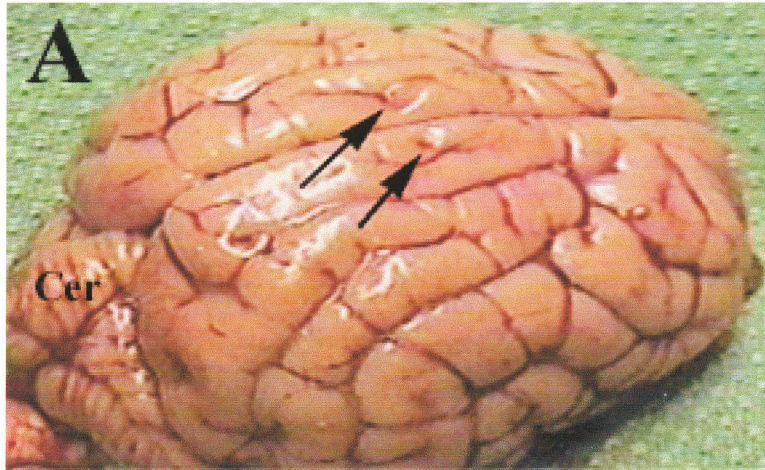
**Figure 4-1** Representative CT scan from Jewel at the level of the lateral ventricles.

S000  
e7530  
04Nov1998

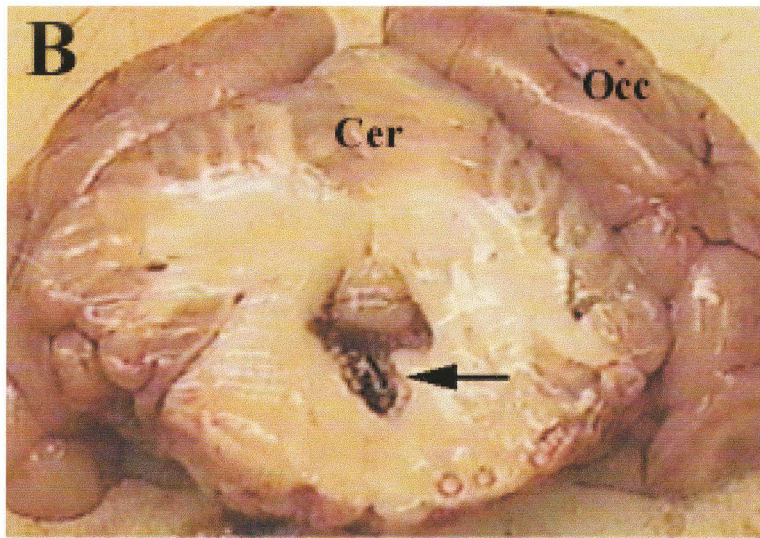
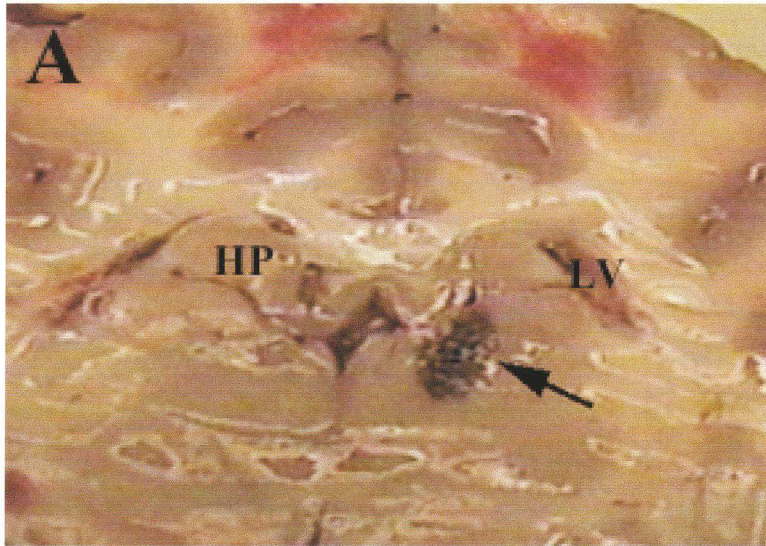
McMaster Univer  
Medical Centr



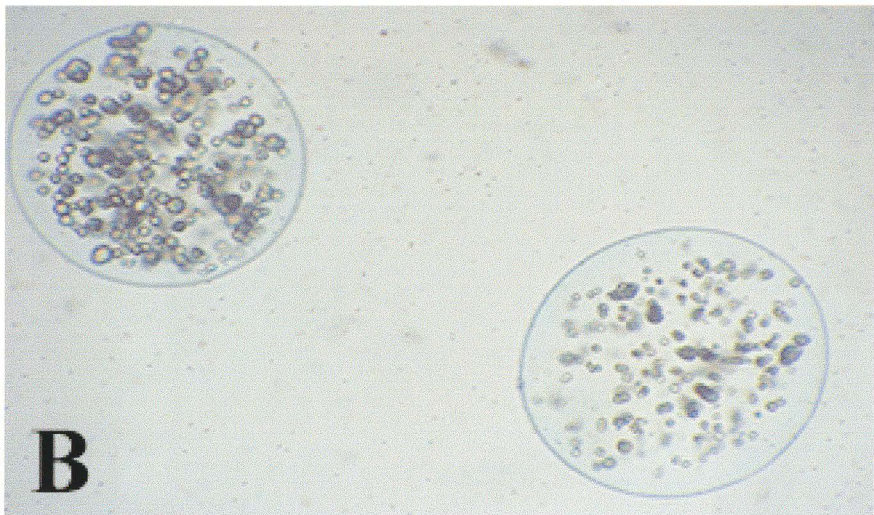
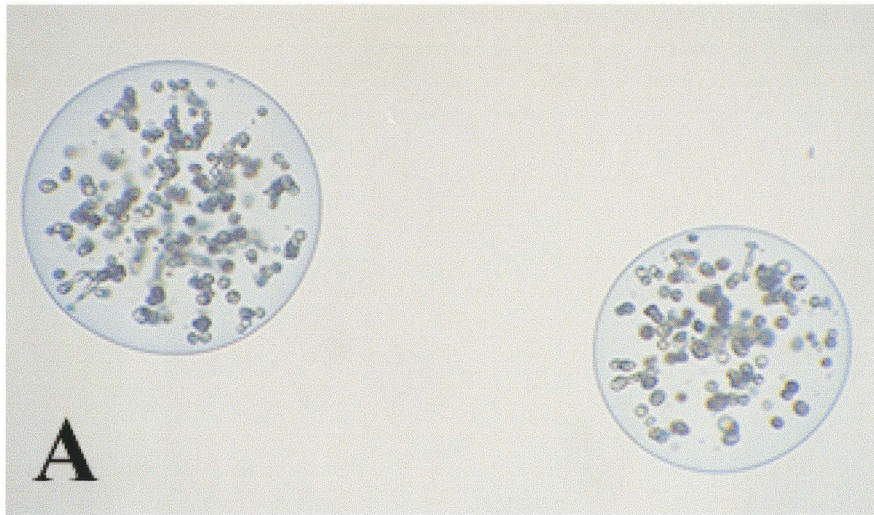
**Figure 4-2** Photos from Jewel's post-mortem examination. (A) Whole brain. Arrows indicate the cannula tracks remaining from the intraventricular surgery procedure. **Cer-**cerebellum. (B) Free microcapsules (as indicated by the arrow) discovered between the cerebellum (**cer**) and occipital cortex (**occ**).



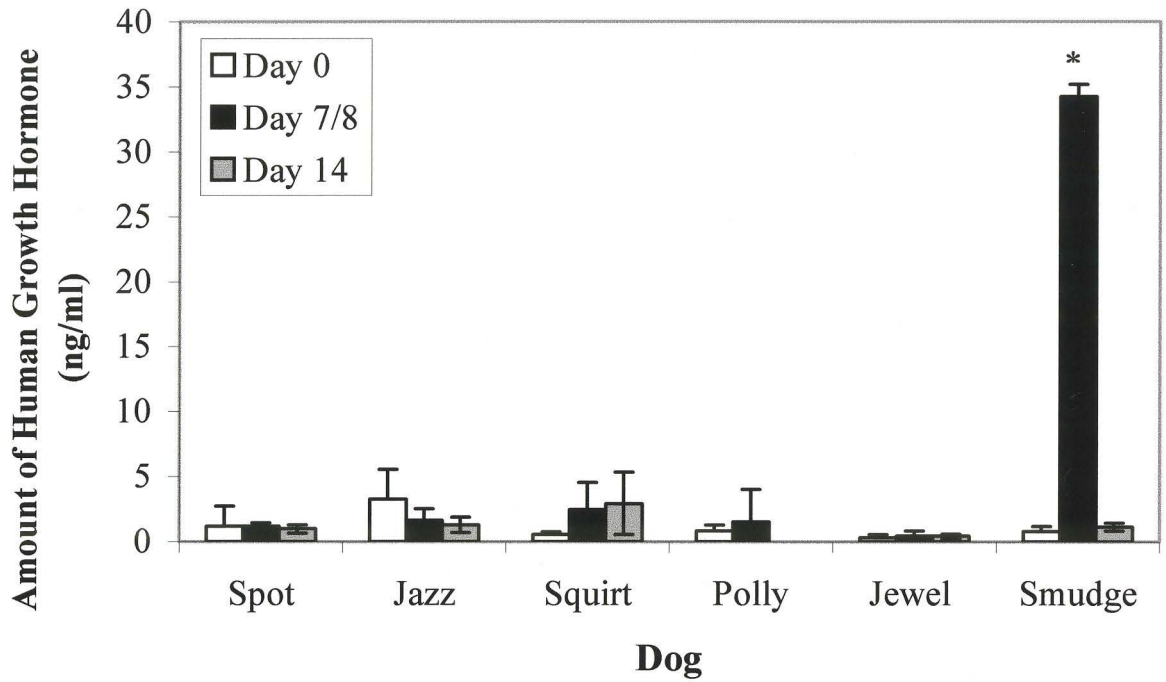
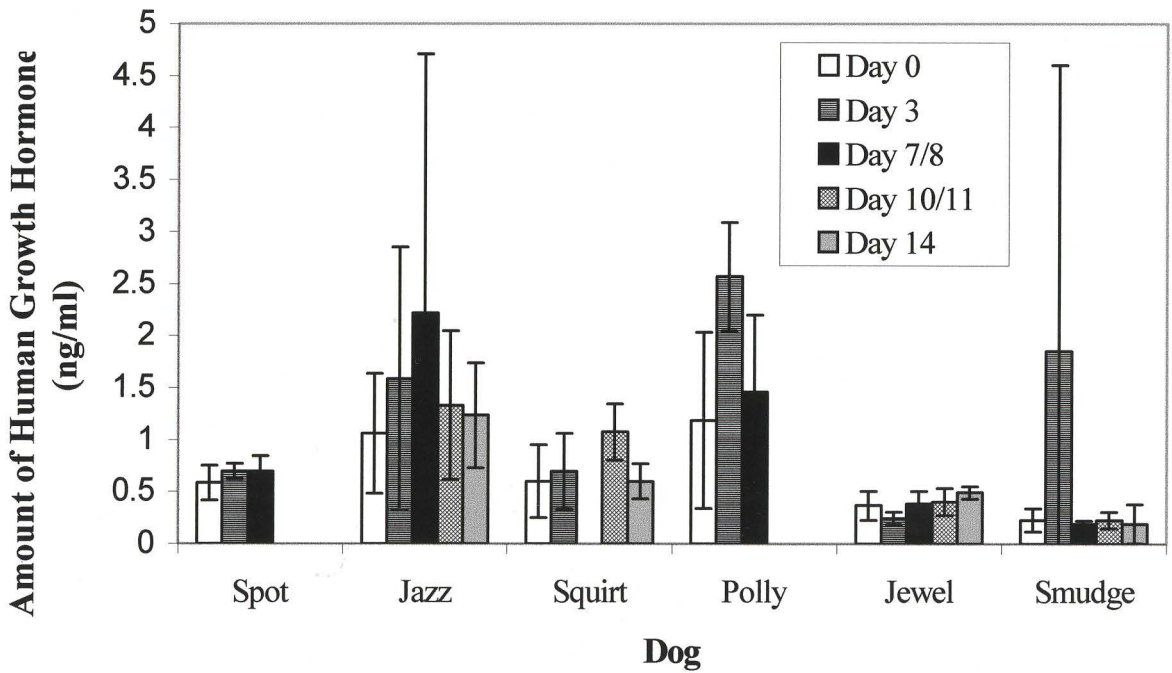
**Figure 4-3** Photos taken during Smudge's post-mortem examination. (A) Coronal brain section demonstrating the intrathalamic microcapsule implantation site (arrow). **HP**-hippocampus; **LV**- lateral ventricle. (B) Free microcapsules (arrow) located in the fourth ventricle. **Cer**- cerebellum; **Occ**- occipital cortex.



**Figure 4-4** (A) Microcapsules containing MDCK cells maintained *in vitro* for two weeks. (B) Microcapsules containing MDCK cells retrieved at post-mortem from Smudge.

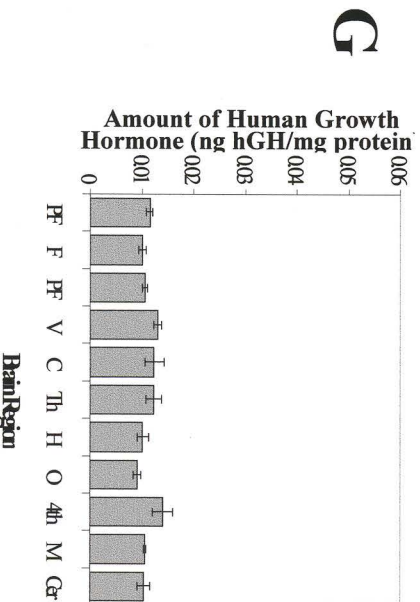
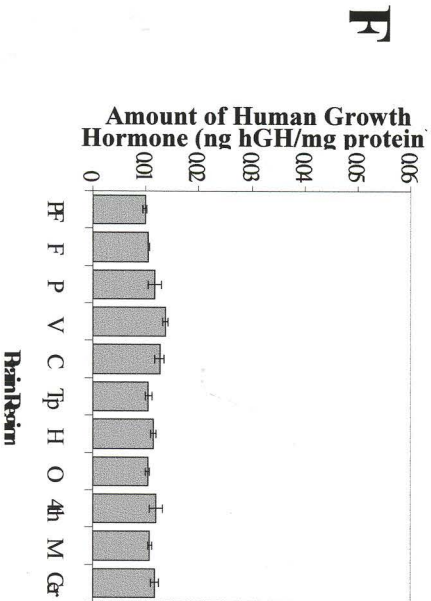
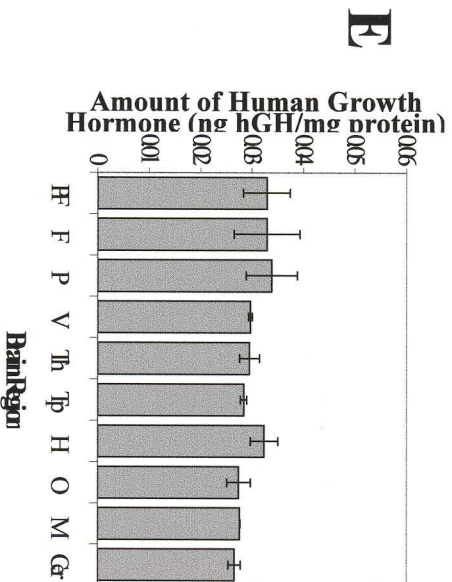
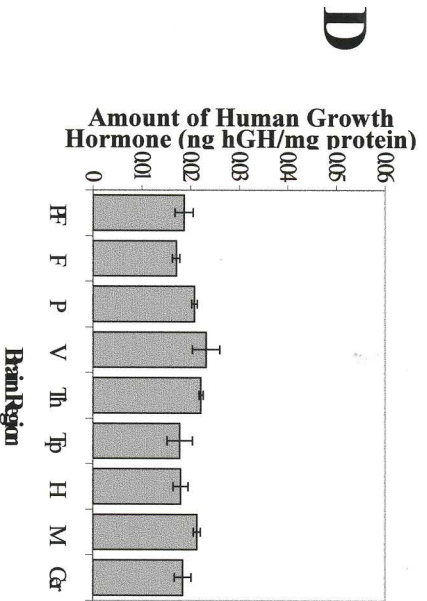
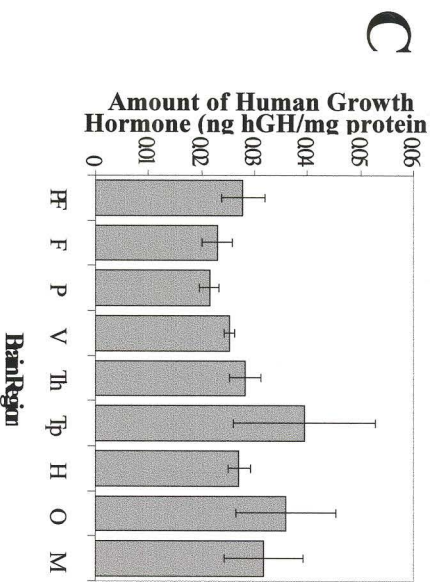
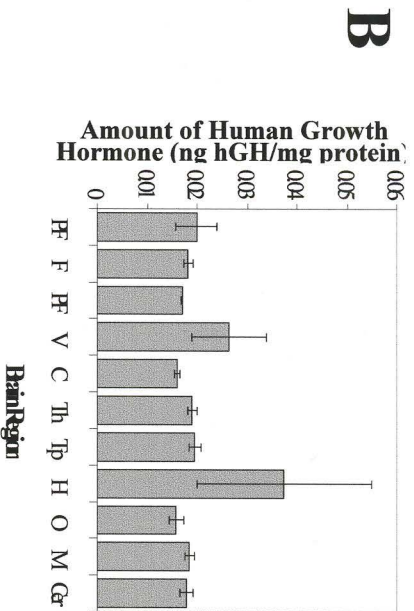
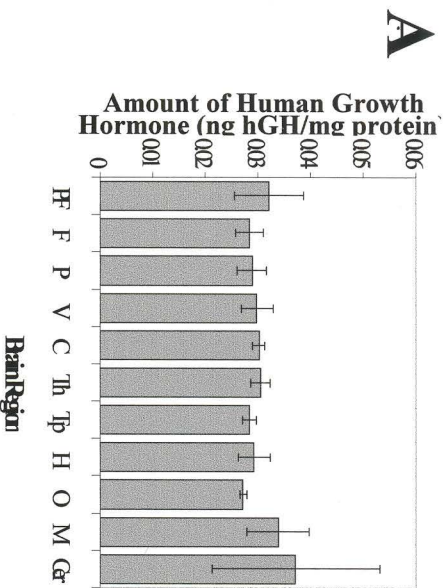


**Figure 4-5** Delivery of human growth hormone to the cerebrospinal fluid (A) and plasma (B). Data are the mean of triplicate hGH ELISA samples  $\pm$  SD. Significant levels were observed only in Smudge's CSF on day 7,  $p < .001$ .

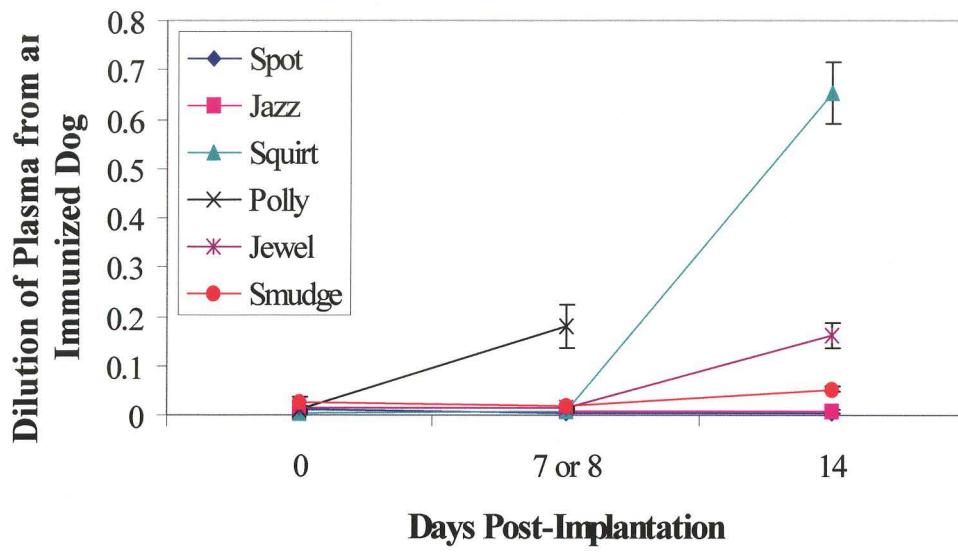
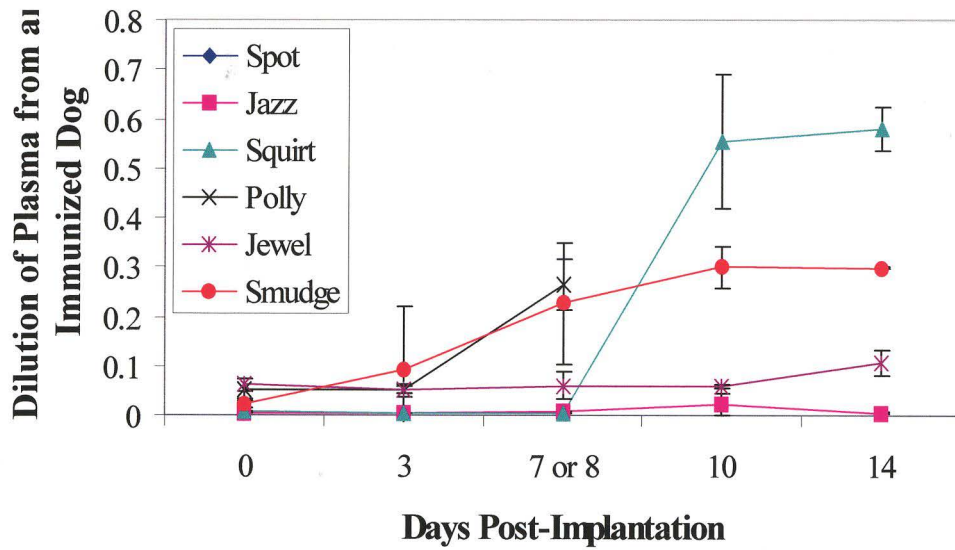
**A****B**

**Figure 4-6** Detection of human growth hormone in various brain regions. Data are the mean of triplicate samples of hGH ELISA values/protein measurements  $\pm$  SD. No significant delivery levels were observed. (A) Tissue dog control, (B) Spot, (C) Jazz, (D) Squirt, (E) Polly, (F) Jewel, (G) Smudge. For Spot, Jazz, Squirt and Polly, regions close to the implantation site include cerebellum and occipital cortex. For Jewel and Smudge, areas close to the implantation site include the lateral ventricle lining, caudate nucleus, thalamus and hippocampus.

**PF**-Prefrontal cortex; **F**-Frontal cortex; **P**-Parietal Cortex; **V**-Lateral ventricle lining; **C**-Caudate nucleus; **Th**-Thalamus; **Tp**-Temporal cortex; **H**-Hippocampus; **4<sup>th</sup>**- Fourth ventricle lining **O**-Occipital cortex; **M**-Medulla; **Cer**-Cerebellum.



**Figure 4-7** Levels of antibody against human growth hormone detected in the cerebrospinal fluid (A) and plasma (B). Antibody titre is expressed as a value relative to antibody levels in the plasma of an immunized dog (where immunized dog value = 1). Values shown are the mean of triplicate samples  $\pm$  SD. Significant antibody titre increases from day 0 in the CSF were observed in Squirt,  $p < .001$ , Polly,  $p < .01$ , Jewel,  $p < .001$ , and Smudge,  $p < .01$ . In the plasma, significant antibody titre increases from day 0 were observed in Squirt on day 10,  $p < .01$  and day 14,  $p < .001$ , Polly on day 8,  $p < .01$ , and Smudge on days 10 and 14,  $p < .001$ .

**A****B**

**Figure 4-8** Histological sections demonstrating pathology from Jazz. (A) Section from Spot (H&E) demonstrating non-immunogenic empty microcapsule material located beneath the meninges. **C**-microcapsule debris; **N**-nerves; **M**-meninges. (B) Microcapsule debris in the area of the Jazz's pons with surrounding inflammation including a multinucleated giant cell. **C**-microcapsule debris; **MG**-multinucleated giant cell. (C) Cresyl violet nissl stain of control tissue. (D) Cresyl violet nissl stain in Jazz surrounding microcapsule debris highlighting the loss of cellular organization. (E) Normal astrocytes (arrows) as demonstrated with GFAP immunohistochemistry. Note the thin cell bodies and fibrous processes. (F) GFAP immunostaining demonstrating reactive astrocytes (arrows) surrounding the area of inflammation.

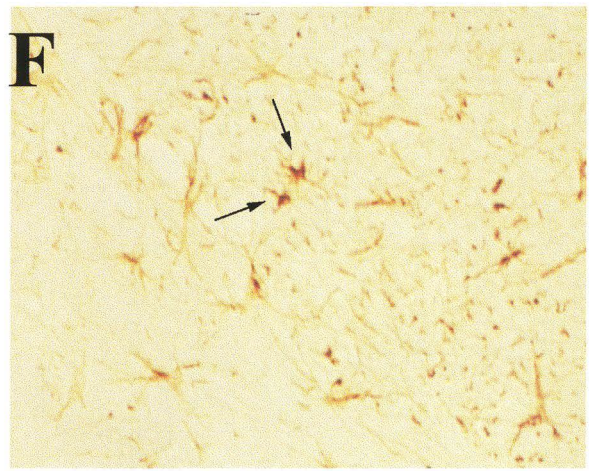
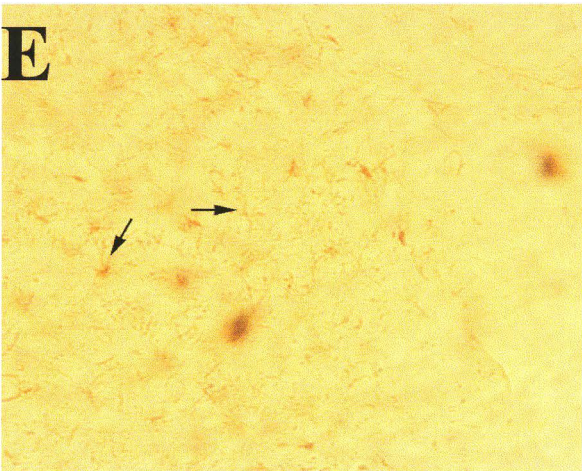
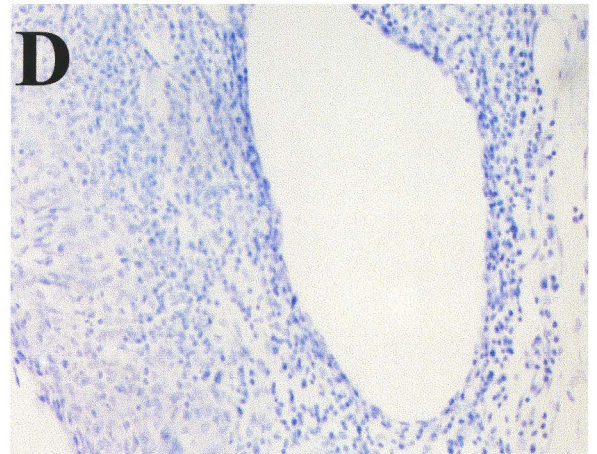
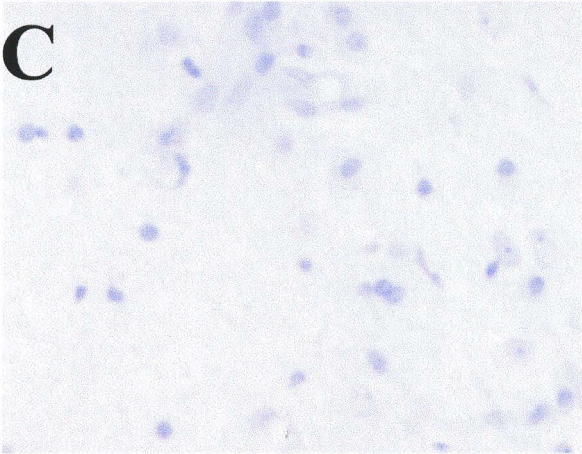
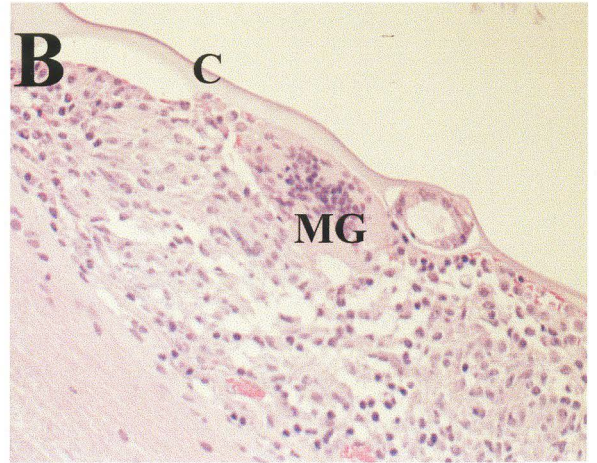
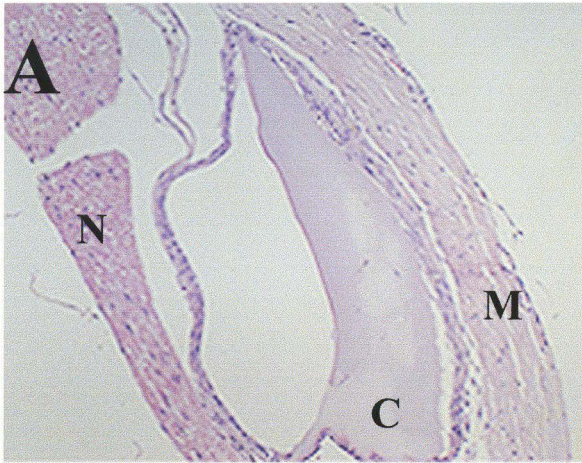


**Figure 4-9** Histological sections demonstrating pathology from Squirt. (A) H&E staining of normal meninges (arrow). Note how the tissue is fibrous with few distinguishable cells. (B) H&E staining of Squirt's inflamed meninges (arrow) on the surface of the spinal cord. (C) H&E staining of normal ependymal lining of the lateral ventricle (LV). Arrows with the **E** highlight ependymal cells. (D) Inflamed lateral ventricle (LV) lining. Arrow highlights the loss of ependymal organization. (E) Normal astrocytes (arrows) as demonstrated with GFAP immunohistochemistry. Note the thin cell bodies and fibrous processes. (F) GFAP immunostaining demonstrating reactive astrocytes surrounding a site of inflammation.

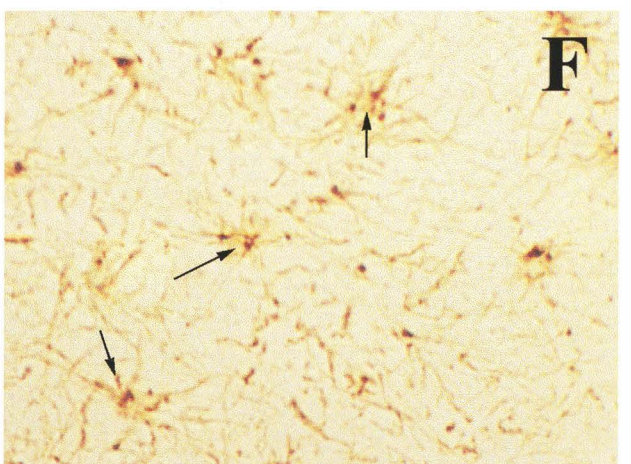
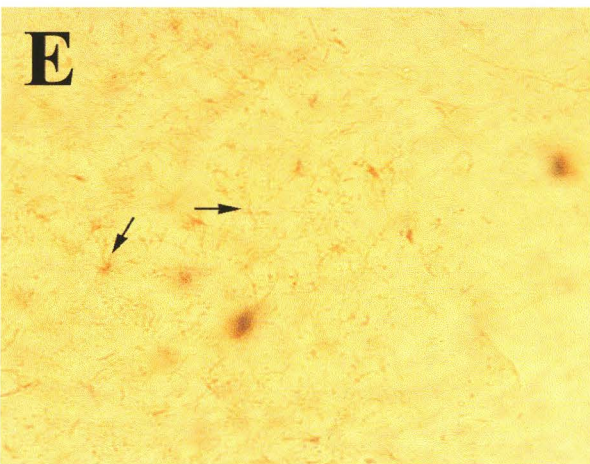
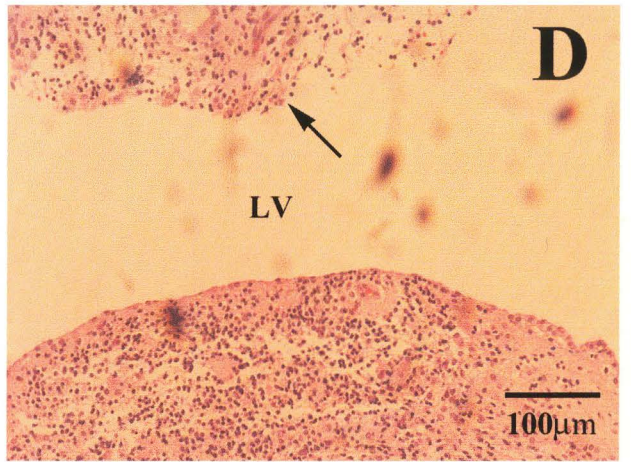
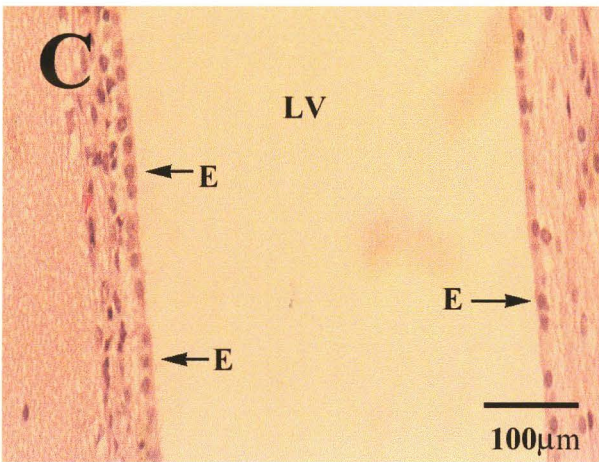
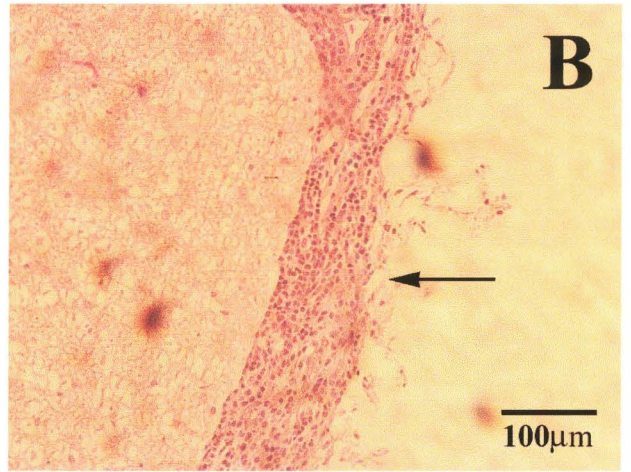
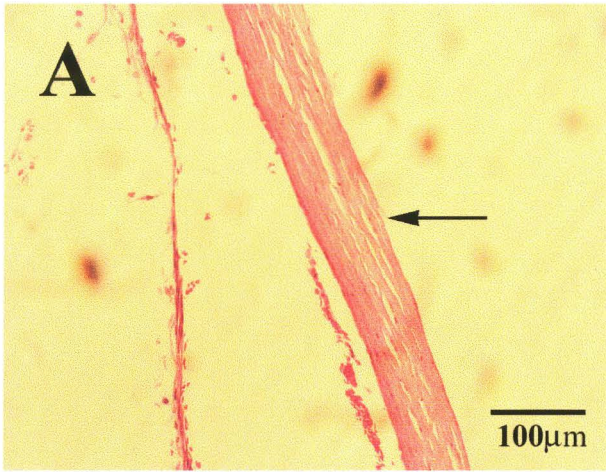


**Figure 4-10** Histological sections demonstrating pathology from Polly. (A) Section from Spot (H&E) demonstrating a non-immunogenic empty microcapsule located below the meninges. **C**-capsular debris **N**-nerves **M**-meninges. (B) Microcapsule debris in Polly's brain parenchyma with surrounding inflammation (arrow). **C**-capsular debris. (C) H&E staining of normal meninges (arrow and **M**). Note how the tissue is fibrous with few distinguishable cells. (D) Inflamed meninges surrounding Polly's spinal cord. **M**-meninges. (E) Normal cresyl violet nissl staining demonstrating a healthy neuron with a clearly defined nucleus (arrow) and nucleolus. Nissl substance is maintained within the cytoplasm. (F) Degenerating neurons from Polly's spinal cord (cervical section). Note the lack of cellular definition and the scattered nissl substance distribution. (G) Normal astrocytes (arrows) as demonstrated with GFAP immunohistochemistry. Note the thin cell bodies and fibrous processes. (H) GFAP immunostaining demonstrating reactive astrocytes surrounding the site of inflammation in Polly's spinal cord (cervical).

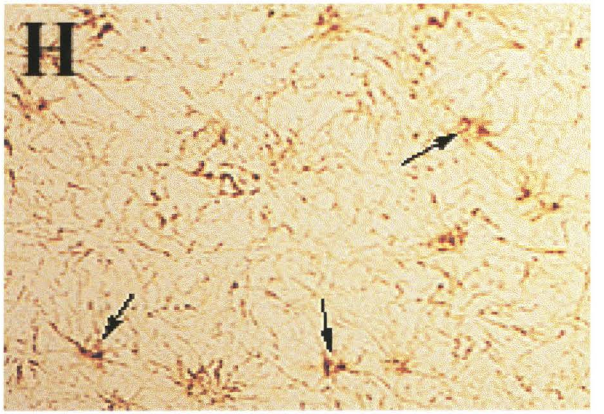
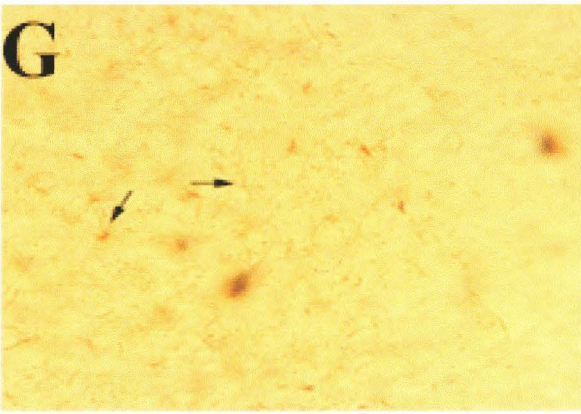
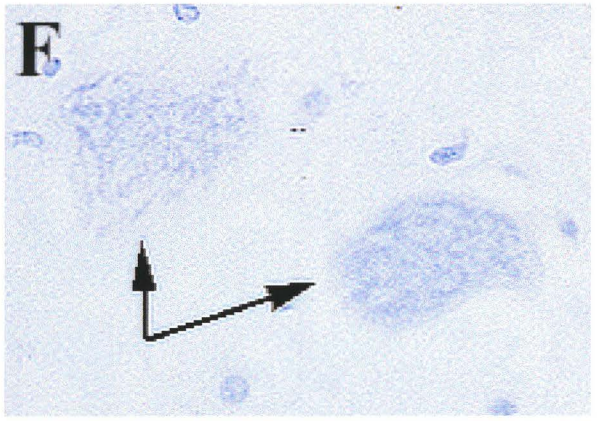
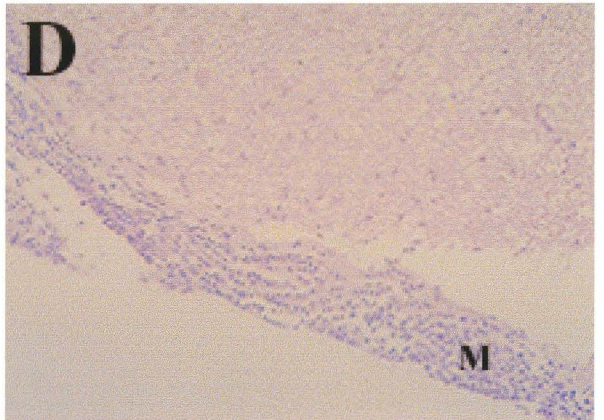
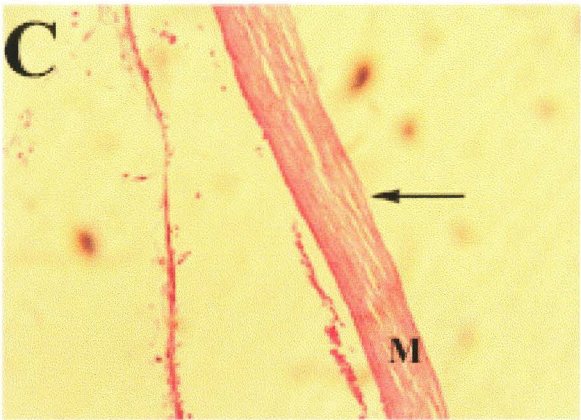
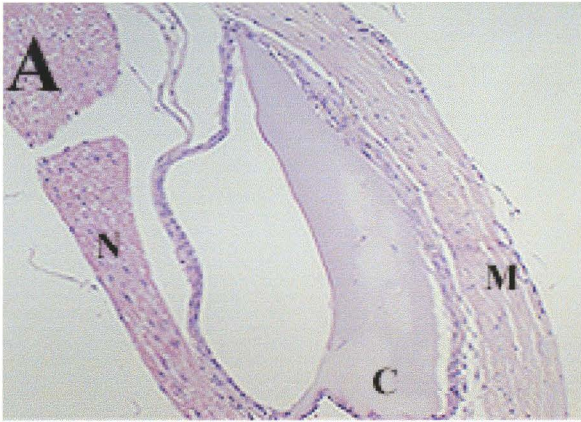


**Figure 4-11** Histological sections demonstrating the pathology observed in Jewel. (A) H&E staining of normal choroid plexus from Spot located within the lateral ventricle. **CP**-choroid plexus; **LV**-lateral ventricle. (B) Edematous choroid plexus (**CP**) from Jewel located within the 4<sup>th</sup> ventricle (**4<sup>th</sup>V**). (C) H&E staining of normal meninges (arrow). Note how the tissue is fibrous with few distinguishable cells. (D) Jewel's inflamed meninges (**M**). (E) Microcapsule debris in Jewel's brain tissue near an area of haemorrhage (enclosed by square). **C**-capsular debris; **MG**-multinucleated giant cell. (F) Enlargement of hemorrhagic area in Jewel's brain with an adjacent blood vessel cuffed with lymphocytes. **H**-haemorrhage; **BV**-blood vessel.

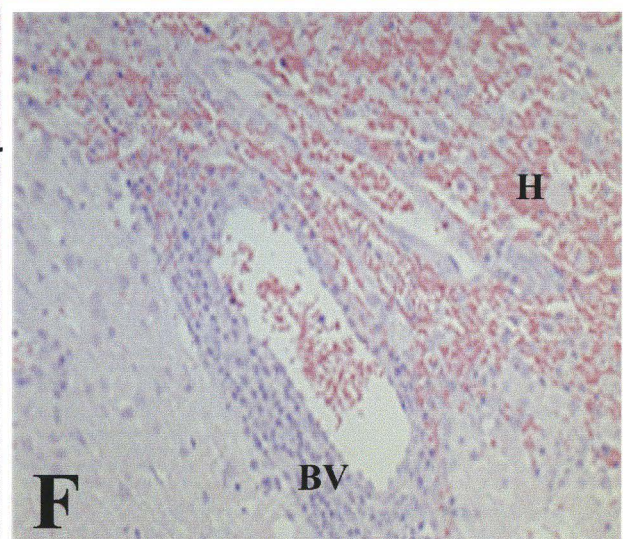
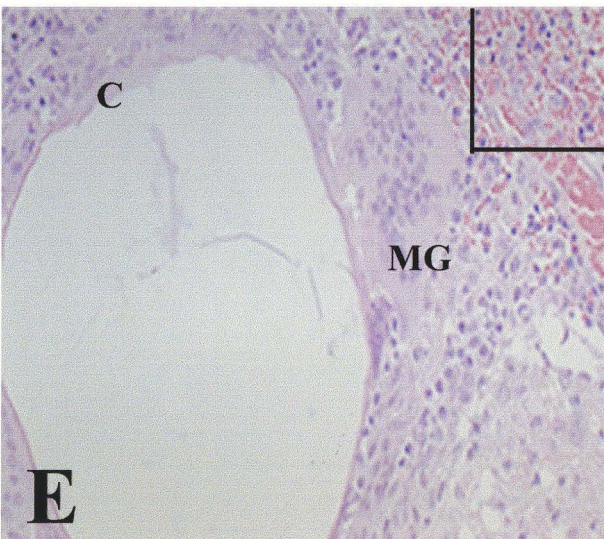
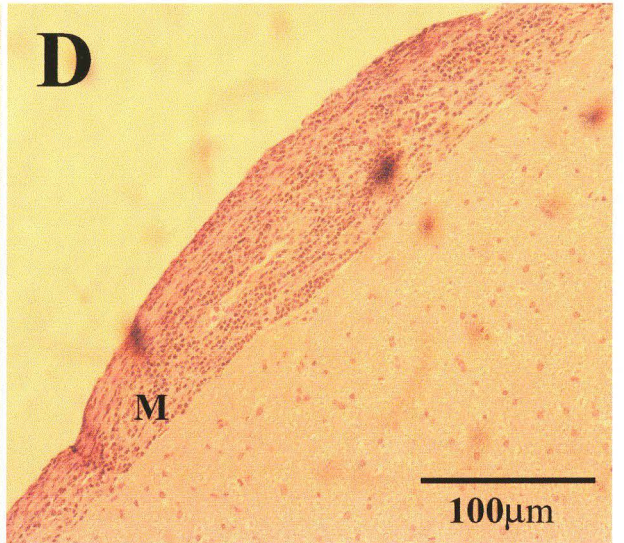
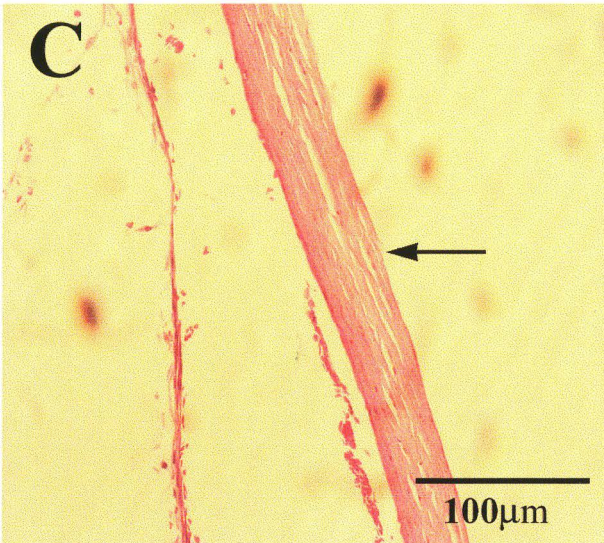
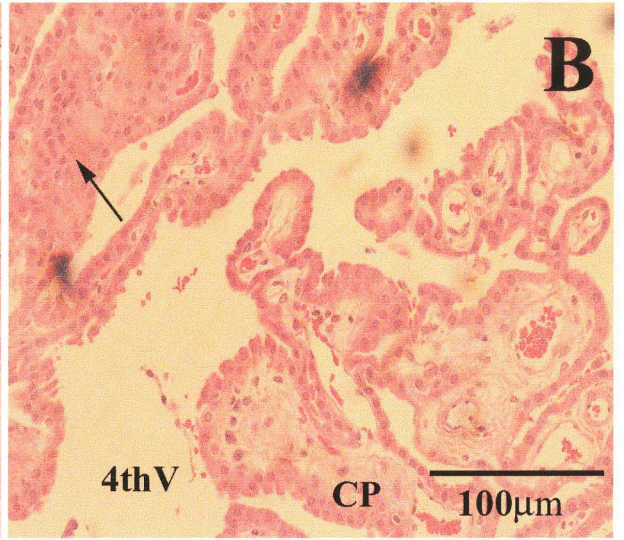
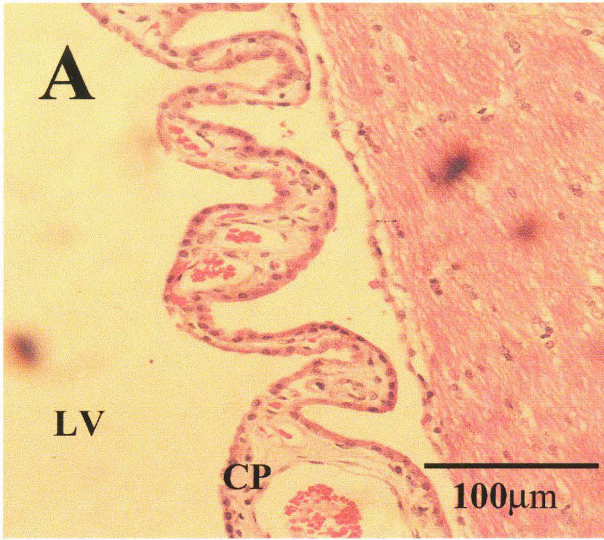


**Figure 4-12** Immunohistochemistry against GFAP for Jewel (A) Normal astrocytes (arrows) as demonstrated with GFAP immunohistochemistry. Note the thin cell bodies and fibrous processes. (B) GFAP immunostaining in Jewel's brain tissue demonstrating reactive astrocytes (arrows) surrounding the site of inflammation.

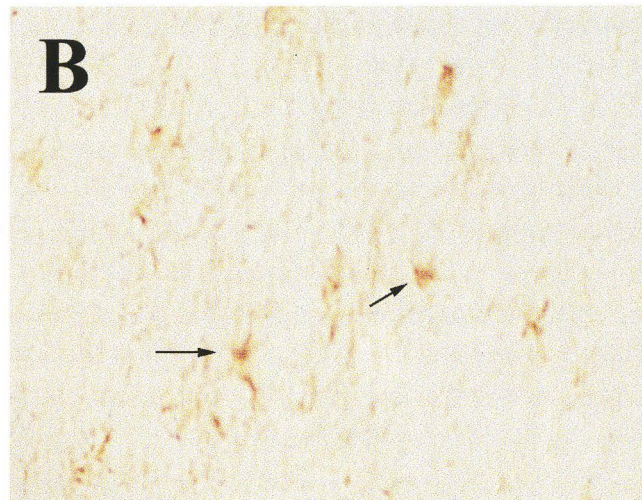
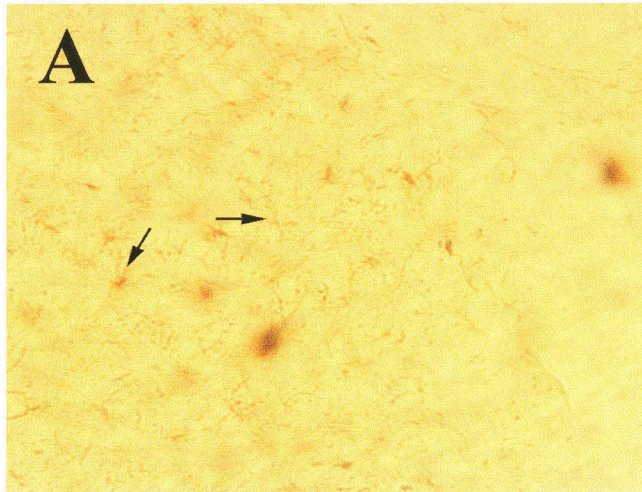
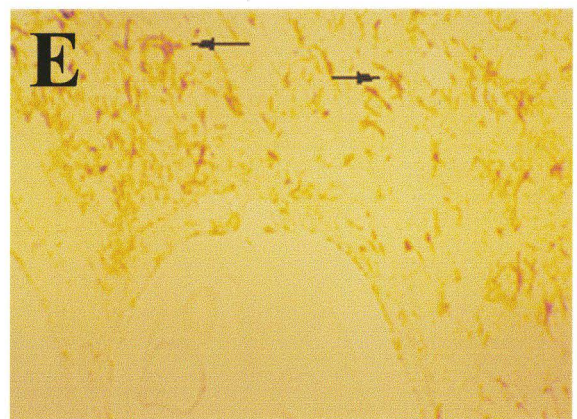
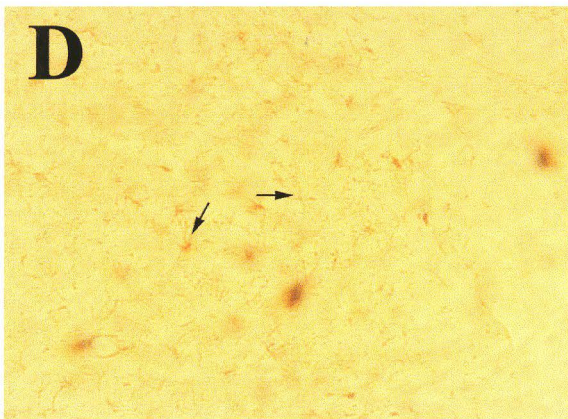
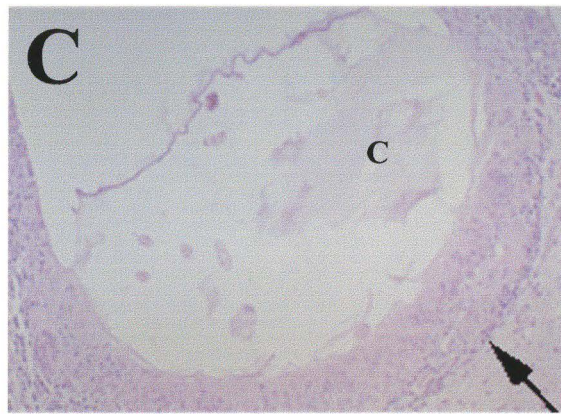
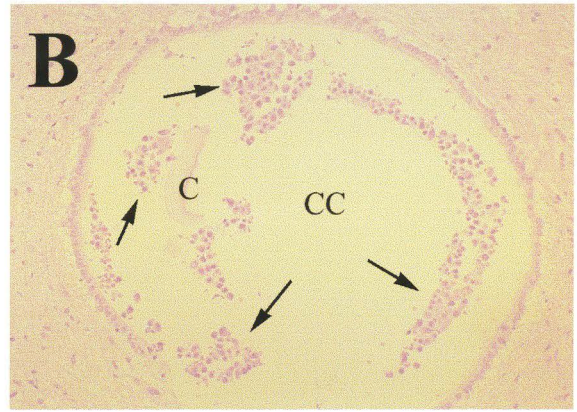
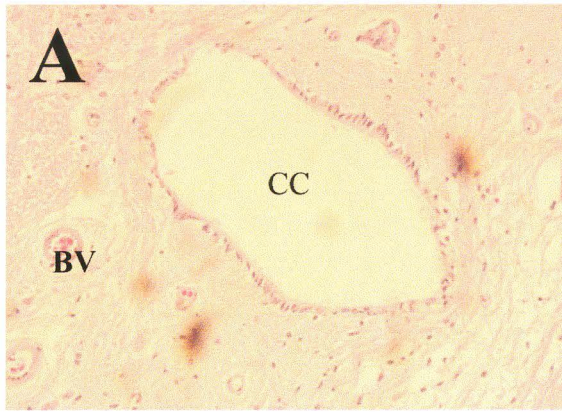


**Figure 4-13** Histological sections demonstrating the pathology observed in Smudge. (A) Normal central canal of the spinal cord (CC). Note the organized ependymal lining and empty canal space. (B) Central canal in Smudge (CC). Note the capsular debris (C) and inflammatory cells (arrows). (C) Microcapsule debris (C) in Smudge's thalamus with surrounding inflammation (arrow). (D) Normal astrocytes (arrows as demonstrated with GFAP immunohistochemistry). Note the thin cell bodies and fibrous processes. (E) Same area as seen in panel C demonstrating the surrounding astrogliosis (GFAP immunohistochemistry). Note the larger cell bodies (arrows) and more prominent processes.



## **5.0 DELIVERY OF $\alpha$ -L-IDURONIDASE-SECRETING MICROCAPSULES TO THE BRAIN OF A DOG WITH MUCOPOLYSACCHARIDOSIS TYPE I**

### **5.1 RATIONALE**

With the recent success in treating MPS VII mice intraventricularly with microencapsulated cells secreting  $\beta$ -glucuronidase and thereby decreasing the amount of lysosomal accumulations (Ross et al., 199b), we were interested to test the microcapsule technology on a large animal model. The following experiment is the first attempt at treating the brain of an MPS I dog with microcapsules secreting  $\alpha$ -L-iduronidase.

### **5.2 MATERIALS AND METHODS**

#### **5.2.1 Animals**

Three male Plott hounds bred at the University of Guelph, Guelph, Ontario were used in this experiment, aged 2-3 years, 25-28kg in weight. Quincy was an MPS I mutant dog, Buick a heterozygote carrier of the MPS I trait, and Angus a normal littermate, as determined by genotyping by Dr. S. Kruth from the University of Guelph. All animals were housed at the University of Toronto and underwent behavioural testing there.

Distinguishing clinical features of the MPS I dog included stunted growth, abnormal limb joints, corneal clouding, and many extra tissue folds on the tongue (figure 5-1). Quincy had been previously infused with autologous bone marrow genetically modified to express high levels of functional  $\alpha$ -L-iduronidase, as described by Lutzko et

al. (dog M3; 1999). Briefly, the marrow harvest was exposed to retroviral vectors *in vitro* and the transduced long-term marrow cultures were infused with evidence of engraftment.  $\alpha$ -L-iduronidase activity was undetectable and low levels of humoral and cellular immune responses to  $\alpha$ -L-iduronidase were evident in spite of posttransplant cyclosporine A treatment.

### **5.2.2 Intraventricular Implantation**

All three animals received intraventricular implantations of microcapsules containing MDCK cells secreting canine  $\alpha$ -L-iduronidase (cIDUA). All surgeries were performed by Dr. W.A. MacKay and A. Medonca. Angus and Buick each received 1ml microcapsules into each hemisphere, for a total of 2ml. Quincy received 0.25ml in 0.25ml physiological saline into each hemisphere, for a total of 0.5ml microcapsules. Quincy was the only dog in this experiment to have CT scans (prior to surgery and euthanization; figures 5-2, 5-3) and to have the capillary tube adjustment included in his surgery. All procedures were carried out on Angus and Buick at the University of Toronto, while Quincy's CT scans, surgeries and euthanization were performed at McMaster University. Angus and Buick were euthanized 56 days post-surgery while Quincy was euthanized on day 21.

### **5.2.3 Analyses**

All dogs underwent behavioural testing prior to and following surgery at the University of Toronto as H. Callahan's project. For each dog, there was a post-operative

clinical assessment, post-mortem examination at the time of euthanization, quantitative analysis of cIDUA activity and antibody content in the CSF, plasma and brain tissue, and histological and immunohistological examination of the brain (and spinal cord tissue for Quincy).

## **5.3 RESULTS**

### **5.3.1 Clinical Evaluation**

*Angus:* Angus recovered from the anesthetic with sensitivity in the hind legs, presumed to be the result of the pre-surgical spinal tap. This sensitivity gradually disappeared over the following three days. The remaining survival period was unremarkable.

*Buick:* Buick recovered from the anaesthetic without any complications. Neurologic examination was normal.

*Quincy:* Quincy demonstrated classical MPS I symptoms, both before and after the CNS surgery. Upon recovery from the anaesthetic, Quincy demonstrated left facial sensory and motor paralysis. These symptoms persisted for the duration of the three week post-operative survival period. The spinal tap on day 7 was unsuccessful, and Quincy was found to be depressed on day 8. The depression, marked by decreased food intake and lack of response to behavioural testing, improved over the following week. In the first two weeks post-operative, Quincy lost 2kg in weight and developed anemia.

### 5.3.2 Post-mortem Evaluation

*Angus:* Upon removal of the brain, cannula tracks were visualized in the frontal cortex. The right lateral ventricle contained many microcapsules, some of which were retrieved for encapsulated cell viability analysis. In the left hemisphere, a hole, approximately 3 mm x 5 mm containing the microcapsules was observed approximately 5mm above the lateral ventricle.

*Buick:* Upon removal of the brain, cannula tracks were observed in the anterior portion of the parietal cortex. 3mm x 5mm holes were observed in both hemispheres approximately 5-8mm dorsal to the lateral ventricles. Some microcapsules were retrieved for encapsulated cell viability analysis.

*Quincy:* Upon removal of the brain, the meninges appeared clouded along the dorsal and ventral surfaces of the brain, particularly around the pituitary gland. A fresh haemorrhage was noted surrounding the brainstem, apparently the result of a spinal tap procedure. The leptomeninges also appeared haemorrhagic at the ventral portions of the C1 and C2 levels of the spinal cord. This haemorrhagic reaction appeared dark in colour, thus signifying that it was not fresh, but also likely to be the result of one of the preceding spinal taps.

Free microcapsules were not apparent during the brain cutting procedure and therefore none could be retrieved. However, a small focus of necrosis (~1mm x ~3mm) was noted approximately 5mm below the right lateral ventricle (figure 5-4).

Upon removal of the spinal cord, it was noted that the vertebral joints between C4-C5 and C5-C6 were large and soft, indicating that the vertebral disks were apparently protruding into and may have been compressing the spinal cord. This abnormality is in line with the MPS I disease process, and its associated joint abnormalities (Shull et al., 1982; Tandon et al., 1996).

### **5.3.3 Microcapsule Cell Viability and Secretion Analyses**

At the time of implantation, encapsulated cells *in vitro* showed 0.08-0.31 nmol  $\alpha$ -L-iduronidase activity/million cells/hour with viabilities of 56-71%. Later *in vitro* secretion assessments could not be made due to instability of the enzyme during the freezing process (see Appendix B). However, upon retrieval, encapsulated cells showed 61% viability from Angus (vs 68% *in vitro*) and 51% viability from Buick (vs 55% *in vitro*).

### 5.3.4 Quantitative Analyses

Levels of enzyme activity in the plasma and CSF could not be determined. See Appendix B.

$\alpha$ -L-iduronidase enzyme activity was detected in various brain regions as demonstrated in figure 5-4. The average enzyme activity in the tissue dog control brain was 0.001 units enzyme per mg protein (where 1 unit enzyme = 1nmol enzyme hydrolyzed per hour)  $\pm$  0.0005. The average enzyme activity in Angus was 0.00053 units enzyme per mg protein  $\pm$  0.0002 and 0.00046  $\pm$  0.00005 in Buick. Quincy's average enzyme activity was 0.00026 units enzyme per mg protein  $\pm$  0.00016. The outer portion of Quincy's hippocampus demonstrated significant ( $p < .01$ ) enzyme activity as compared to the mean activity.

In figure 5-5, the antibody titre detected in the CSF and plasma were expressed as the units of  $\alpha$ -L-iduronidase immunoprecipitated per millilitre where one unit is equal to one nmol enzyme hydrolyzed per hour. Only Quincy developed antibodies towards  $\alpha$ -L-iduronidase and these were detected in both the CSF (days 14 and 21,  $p < 0.001$ ) and plasma (days 7-21,  $p < 0.001$ ).

### 5.3.5 Pathology

*Angus and Buick:* H&E staining demonstrated chronic inflammatory reactions in the regions dorsal to the dilated lateral ventricles, at the sites of capsule implantation. Inflammatory infiltrate, consisting of predominantly lymphocytes, macrophages and

multinucleated giant cells, was aggregated around what appears to have been microcapsule debris (figure 5-7B,C). The capsule material was completely obliterated and was replaced by granulomas (figure 5-7D). Fibroblastic scarring was observed surrounding the implantation sites and GFAP immunostaining revealed a well-developed glial scar (figure 5-7E). The Nissl stain also demonstrated the loss of cellular organization, as well as vacuolation and generalized cell death.

*Quincy:* At the microcapsule implantation site, a classic severe granulomatous inflammatory reaction was observed (figure 5-8B). The inflammatory infiltrate included lymphocytes, macrophages, multinucleated giant cells, including Langerhans-type, and plasma cells. Meningitis, swollen axons and vascular edema were apparent. GFAP immunostaining revealed reactive astrocytes surrounding the site of inflammation (figure 5-8D). A small piece of microcapsule debris was observed in the cerebral aqueduct, also surrounded by inflammatory exudate.

PAS staining demonstrated cytoplasmic accumulation of PAS+ granules, interpreted as stored glycosaminoglycans (GAGs). This MPS I pathology was observed throughout the brain, with the most abundant accumulation in large cells such as the pyramidal cells of the neocortex, hippocampal neurons, the purkinje cells of the cerebellum, the olivary nucleus of the brainstem and in the grey matter of the spinal cord (figures 5-9 and 5-10). Neurons were laden with the cytoplasmic accumulation, resulting in the nucleus adapting a peripheral location. Some neurons in the hippocampus and cerebellum appeared dark, shrunken and picnotic, an indication of neuronal necrosis.

PAS+ cells were observed in close proximity to the capsule implantation site, suggesting that the  $\alpha$ -L-iduronidase treatment was not effective in clearing the neuronal pathology. Cytoplasmic inclusions were also demonstrated with Toluidine blue staining (figure 5-11).

**Figure 5-1** The MPS I dog, Quincy. Note the abnormal limb joints (white arrow), extra folds on the tongue (black arrow) and cloudy eyes.



**Figure 5-2** CT scan of Quincy's brain at the level of the lateral ventricles pre-surgery.

Ventricles appear normal in size and shape.

SOLUNCY  
eD06  
09Feb1999

McMaster Univer  
Medical Centr

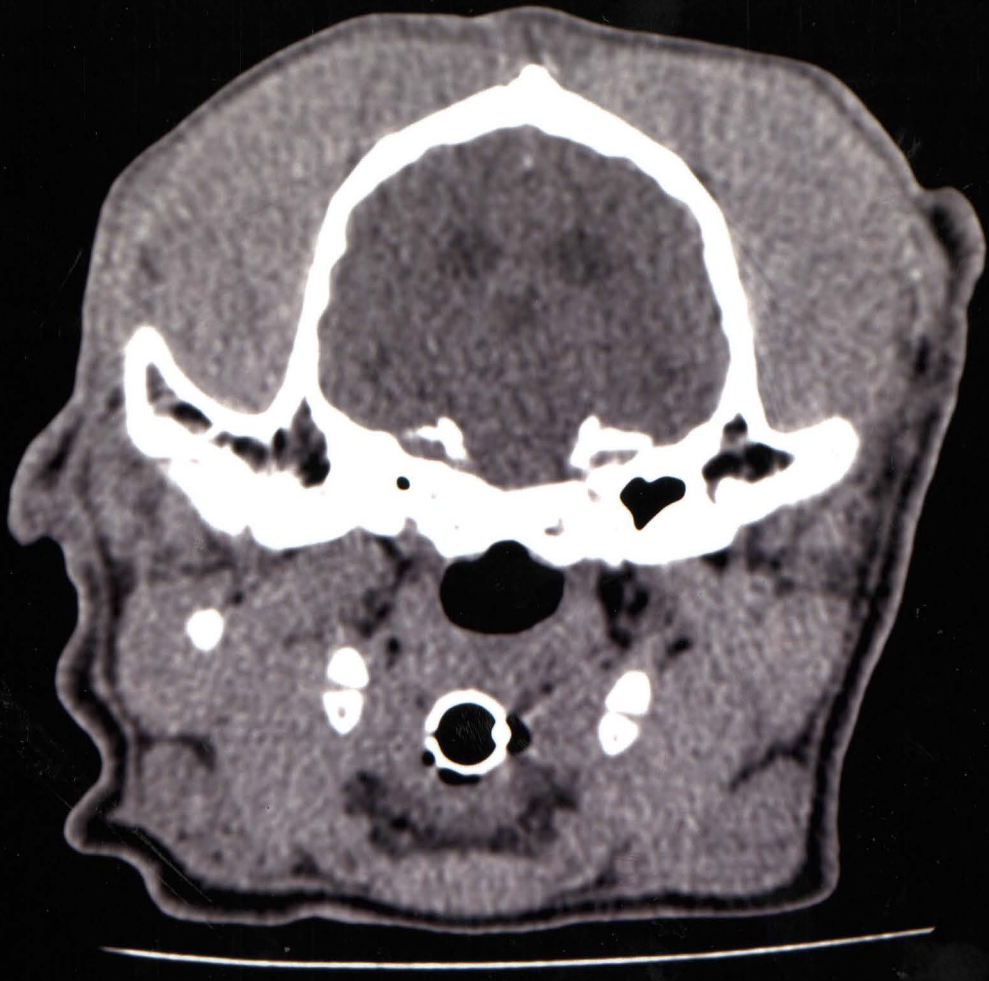


**Figure 5-3** CT scan of Quincy's brain at the level of the lateral ventricles post-surgery.

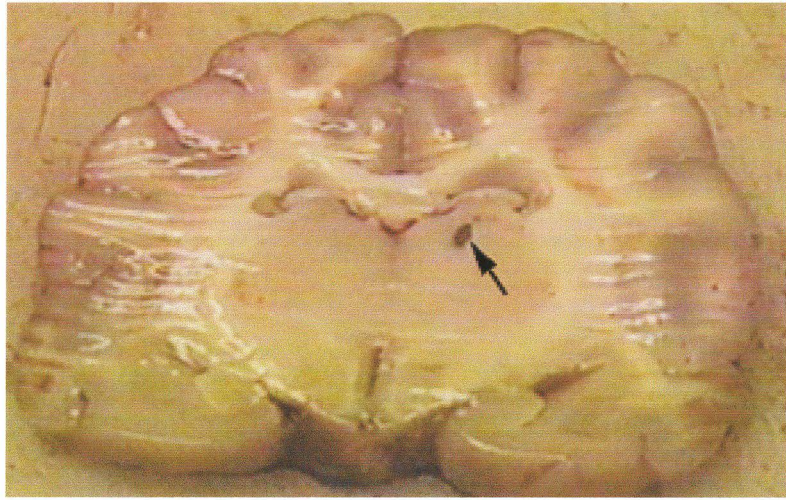
Ventricles appear normal in size and shape.

SDC QUINCY  
e1111  
31 Mar 1999

McMaster Univer  
Medical Centr

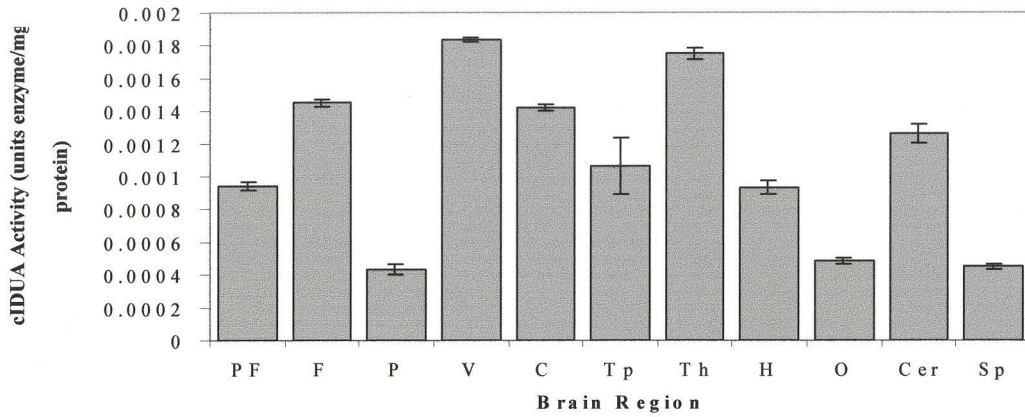
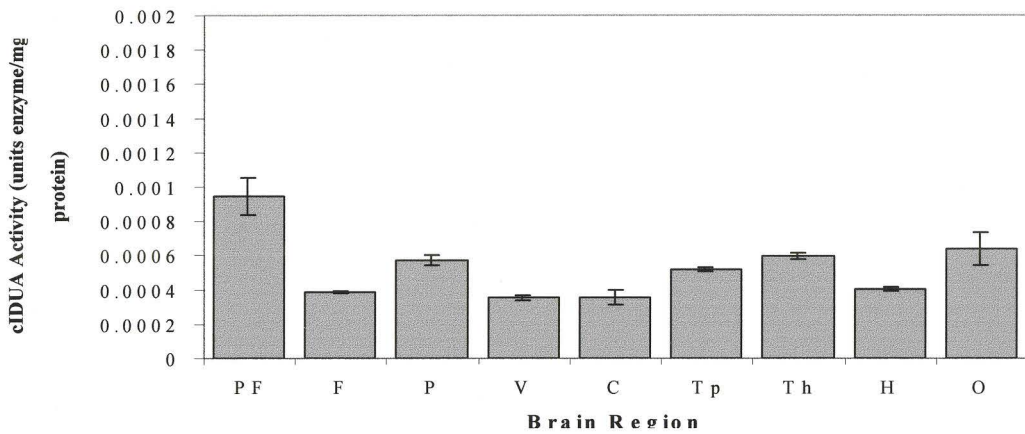
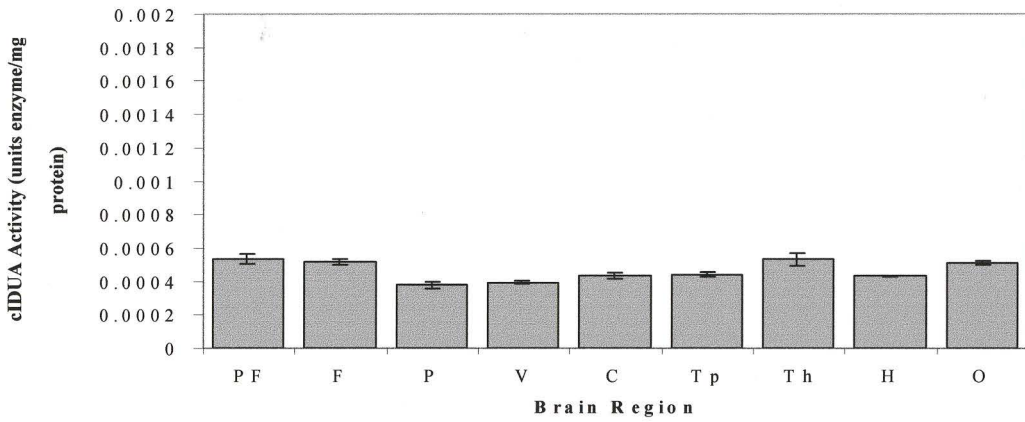
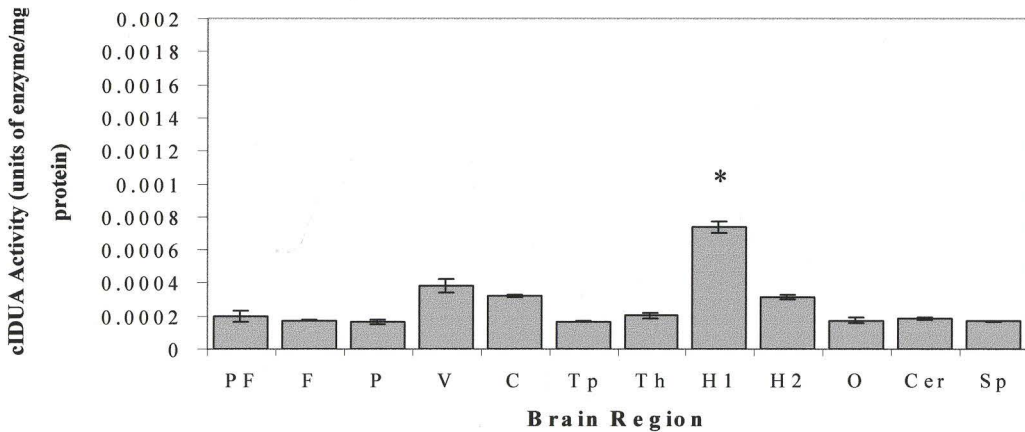


**Figure 5-4** Post-mortem coronal section from Quincy's brain. Arrow indicates the intrathalamic focus of necrosis/microcapsule injection site.

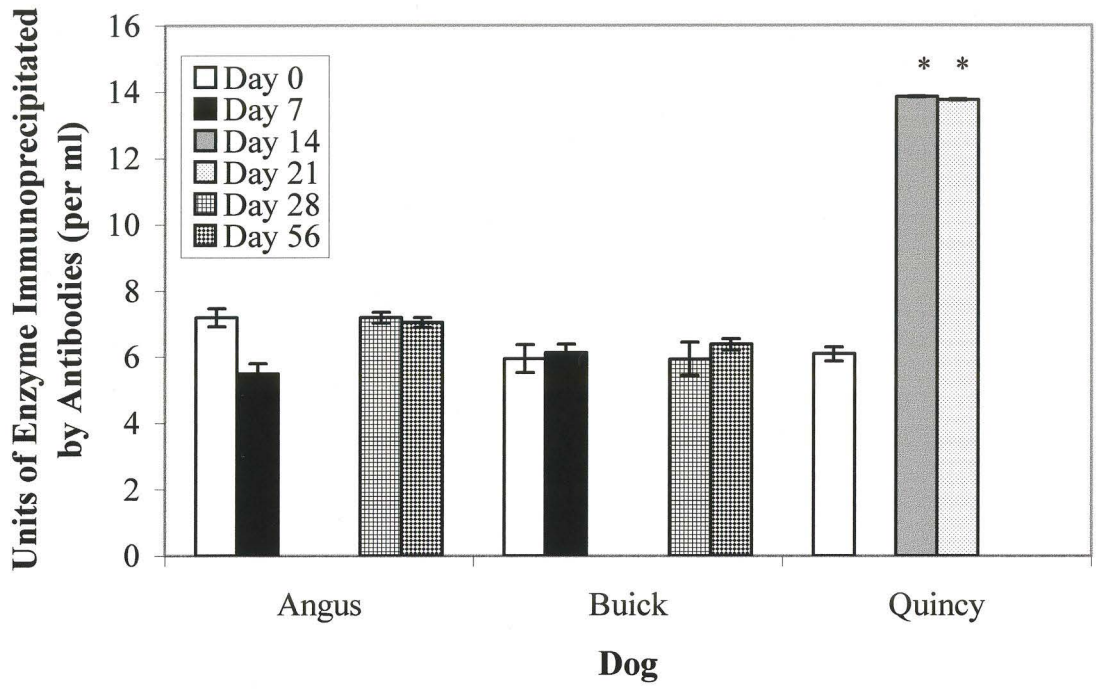
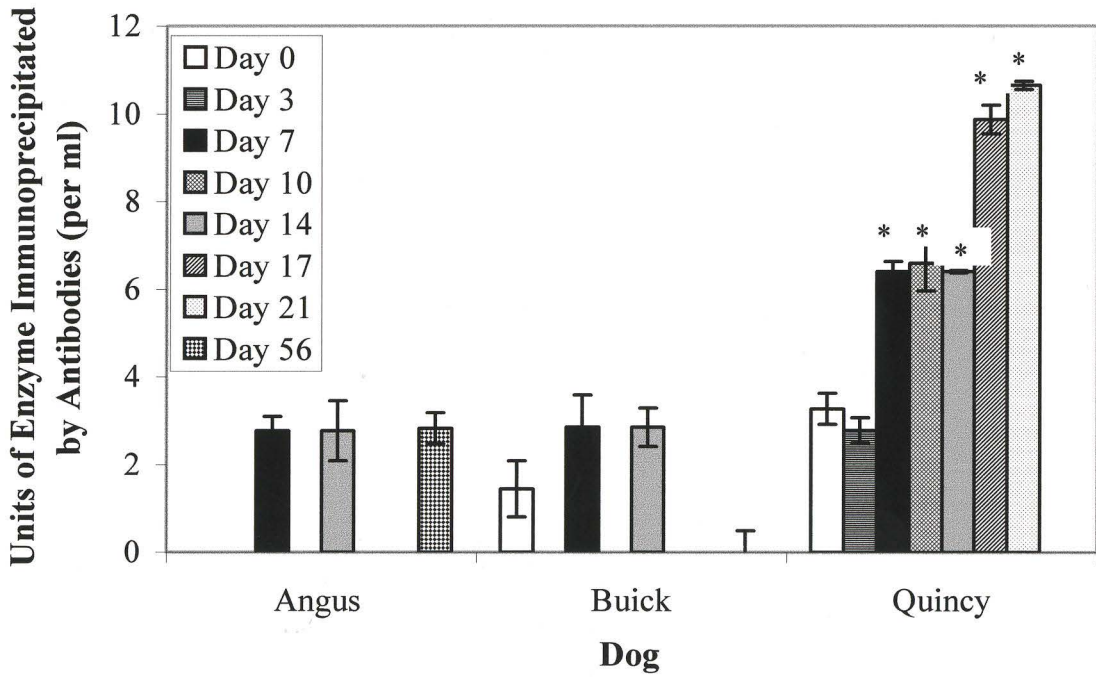


**Figure 5-5**  $\alpha$ -L-iduronidase activity detected in various brain regions. Data are the mean of triplicate samples of the  $\alpha$ -L-iduronidase activity assay/protein measurements  $\pm$ SD. One enzyme unit corresponds to 1nmol  $\alpha$ -L-iduronidase hydrolyzed/hour. (A) Tissue dog control, mean activity level is 0.001 enzyme units/mg protein  $\pm$  .0005 (B) Angus, mean activity level is 0.00053 enzyme units/mg protein  $\pm$  0.0002 (C) Buick, mean activity level is 0.00046 enzyme units/mg protein  $\pm$  0.00005 (D) Quincy, mean activity level is 0.00026 enzyme units/mg  $\pm$  0.00016. H1 refers to the exterior portion of the hippocampus (lining the lateral ventricle) and H2 refers to the interior portion. H1 shows significant  $\alpha$ -L-iduronidase activity, as compared to Quincy's mean brain activity ( $p < .001$ ).

**PF**-Prefrontal cortex; **F**-Frontal cortex; **P**-Parietal cortex; **V**-Lateral ventricle; **C**-Caudate nucleus; **Tp**-Temporal Cortex; **Th**-Thalamus; **H**-Hippocampus; **O**-Occipital cortex; **Cer**-Cerebellum; **Sp**-Spinal cord.

**A****B****C****D**

**Figure 5-6** Levels of antibody against  $\alpha$ -L-iduronidase detected in the cerebrospinal fluid (A) and plasma (B). Antibody titre is expressed as the units of enzyme precipitated by antibodies, where one unit of enzyme corresponds to one nmol  $\alpha$ -L-iduronidase activity/hour. No significant antibody titres were found in Angus or Buick. Quincy showed significant antibody levels in the CSF on days 14 and 21 ( $p < 0.001$ ) and in the plasma on days 7 to 21 ( $p < 0.001$ ).

**A****B**

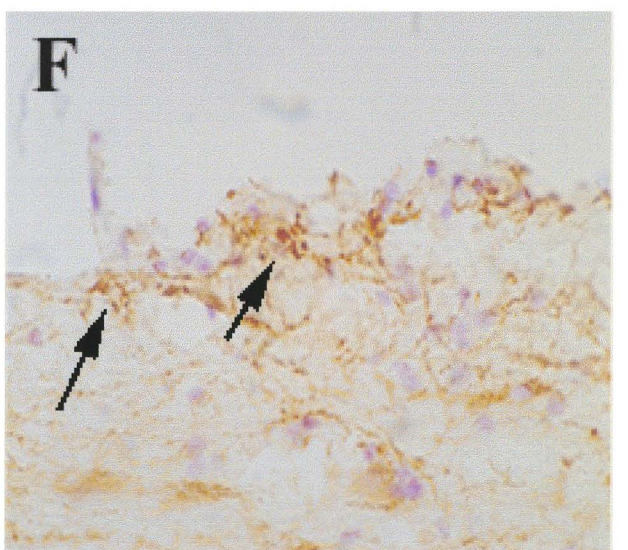
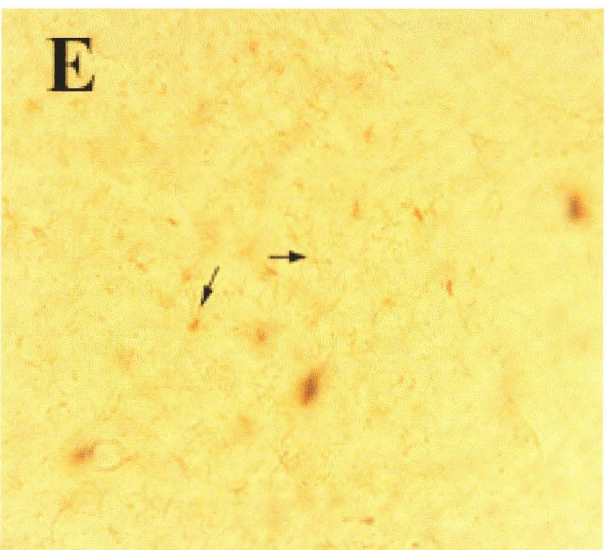
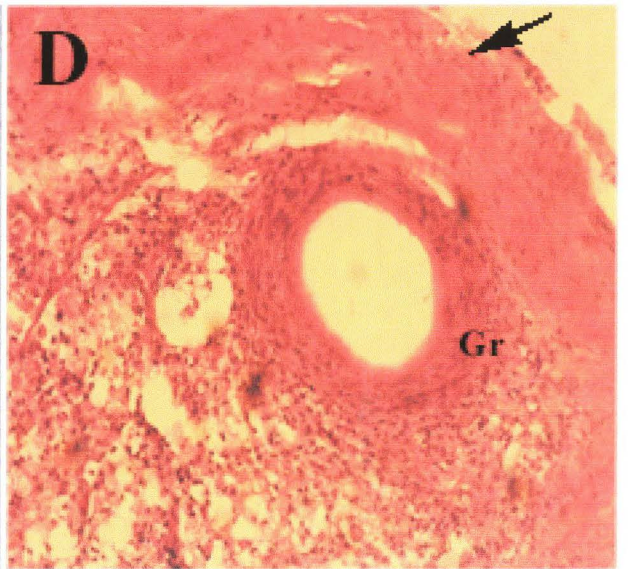
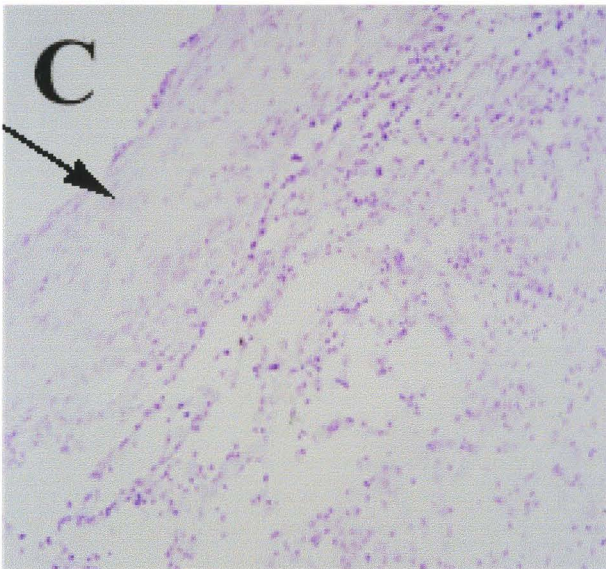
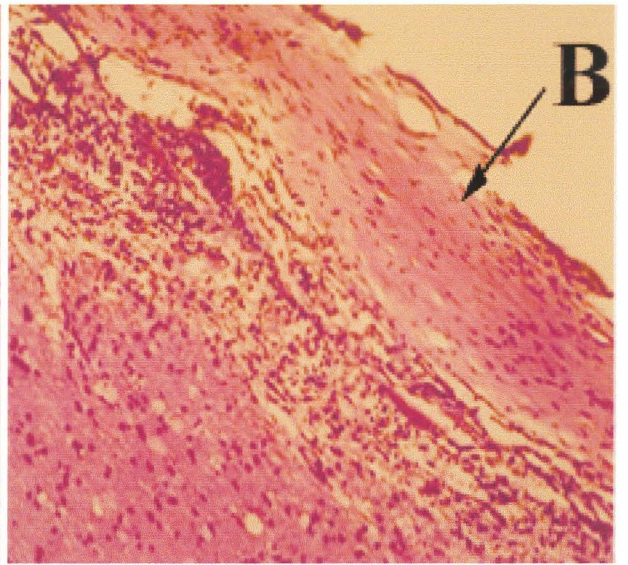
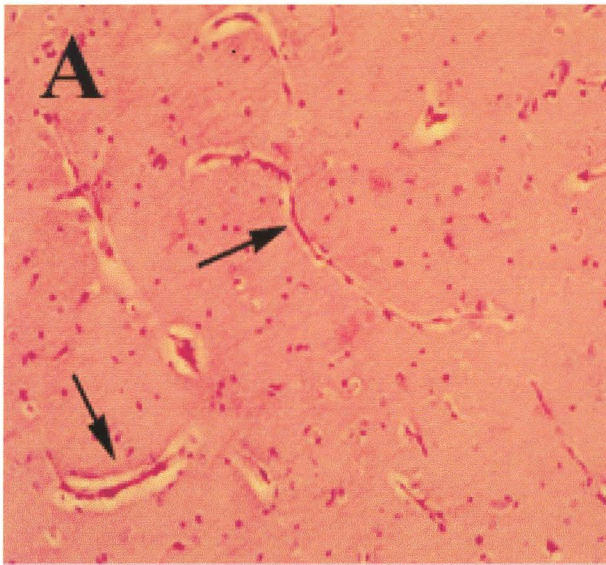


**Figure 5-8** Histological sections demonstrating the pathology observed in Quincy as a result of the microcapsule implantation. (A) H&E staining of control brain demonstrating blood vessels (arrows) and normal tissue elements. (B) H&E staining of Quincy's brain at the intrathalamic implantation site. Arrow depicts microcapsule material. Blood vessels (**BV**) and the implant site are surrounded by inflammatory cells. (C) Normal astrocytes (arrows) as demonstrated with GFAP immunohistochemistry. Note the thin cell bodies and fibrous processes. (D) GFAP immunostaining demonstrating reactive astrocytes surrounding the site of inflammation.

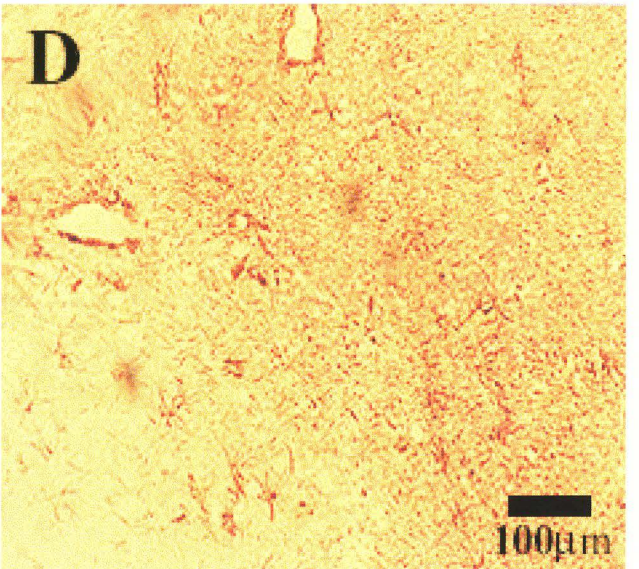
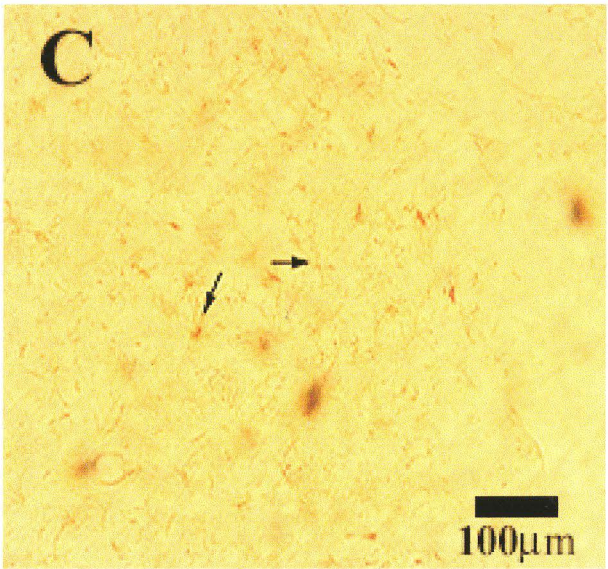
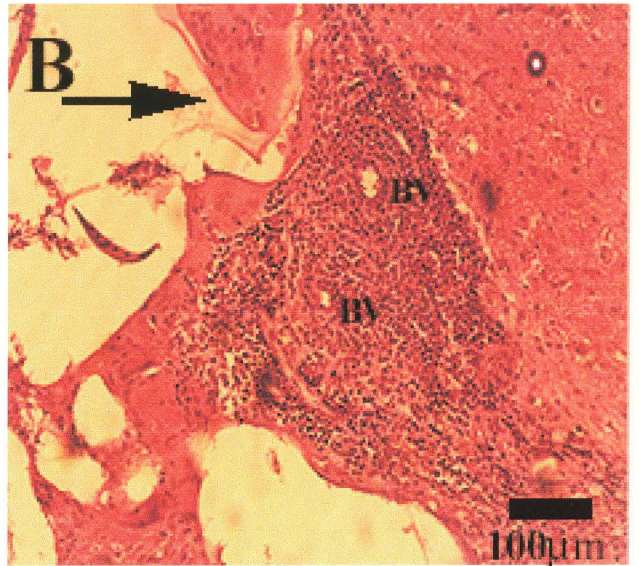
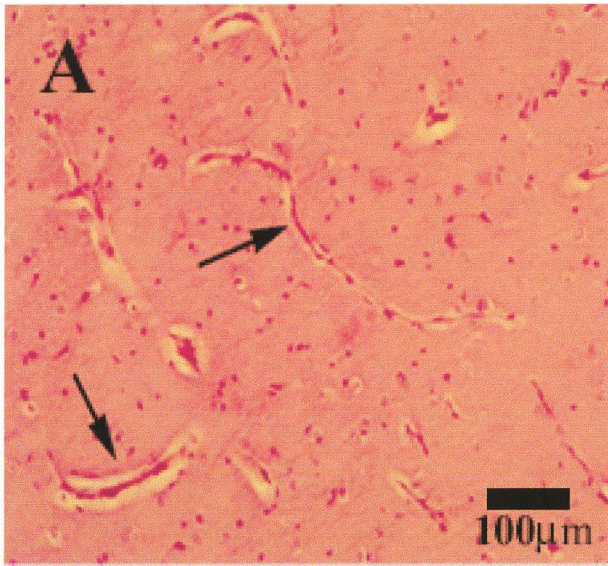


**Figure 5-9** PAS counterstained with hematoxylin demonstrating a normal cerebellar Purkinje cell (A) and a glycogen-laden, PAS<sup>+</sup> (pink) cerebellar Purkinje cell observed in Quincy's brain (B). Also note the peripherally located nucleus of the affected cell (arrow).

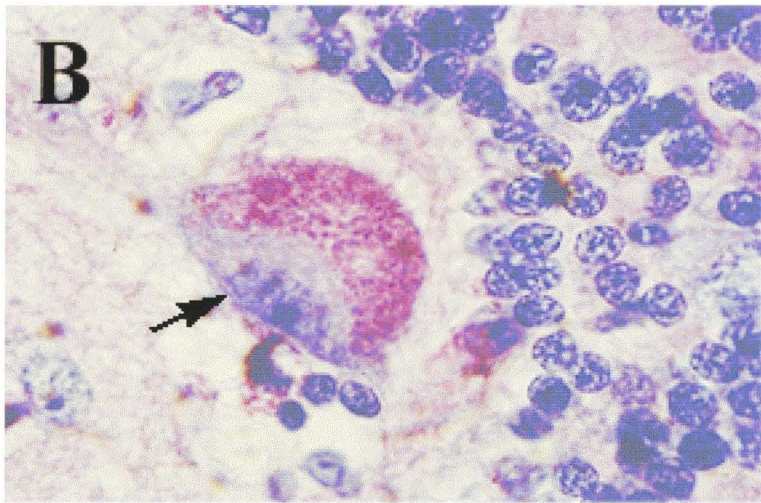
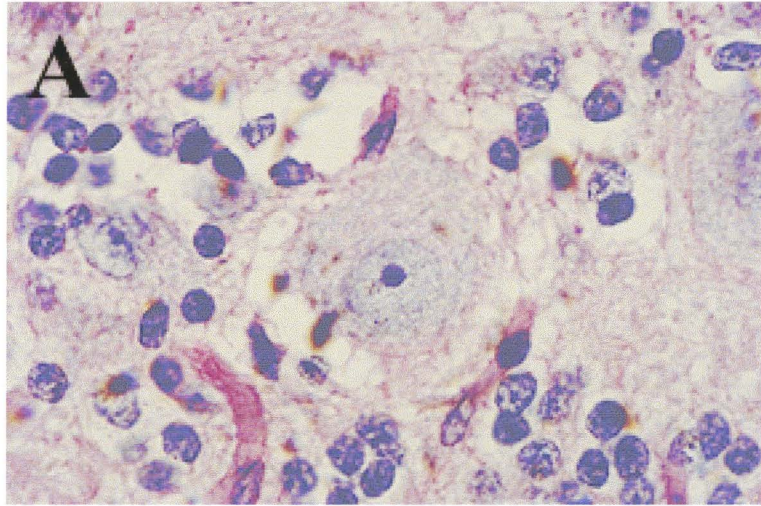


**Figure 5-10** Neurons from Quincy's olivary nucleus. (A) H&E. (B) PAS counterstained with hematoxylin. Arrow denotes the PAS<sup>+</sup> granules.

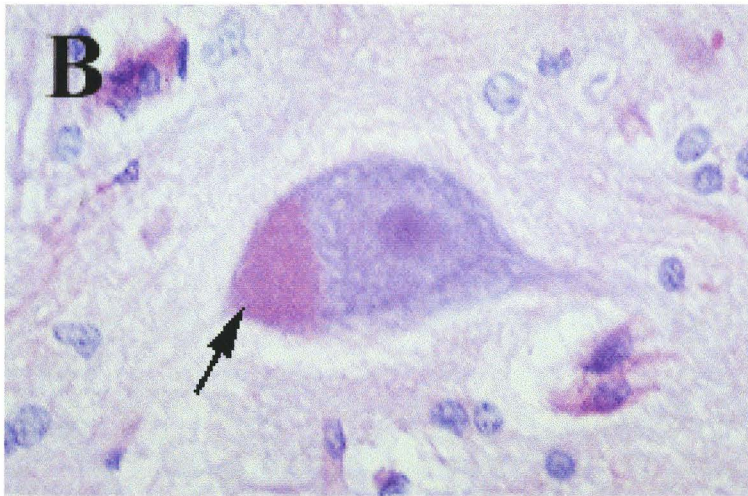
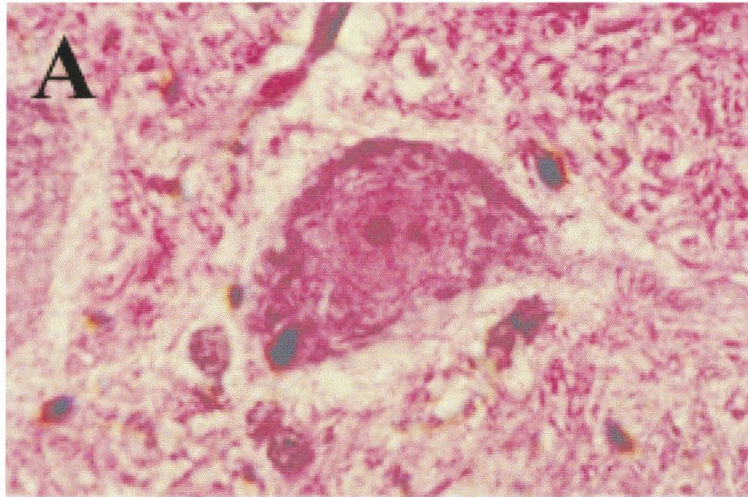
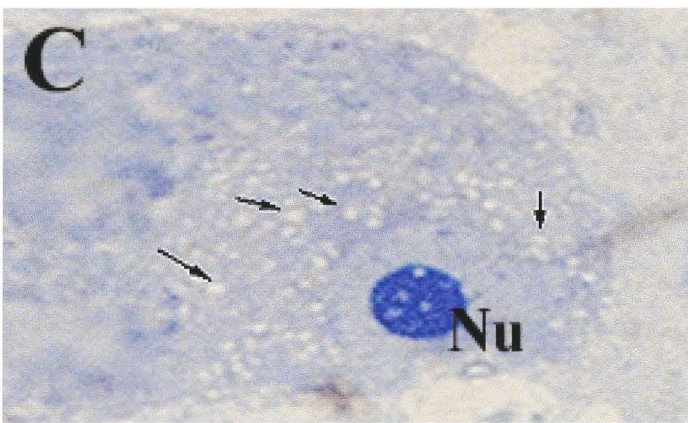
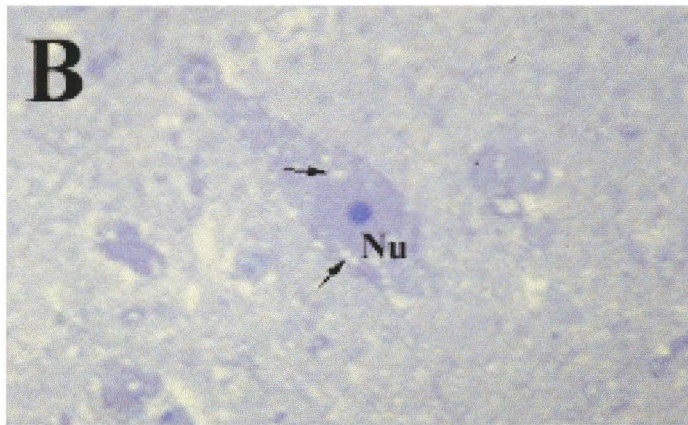
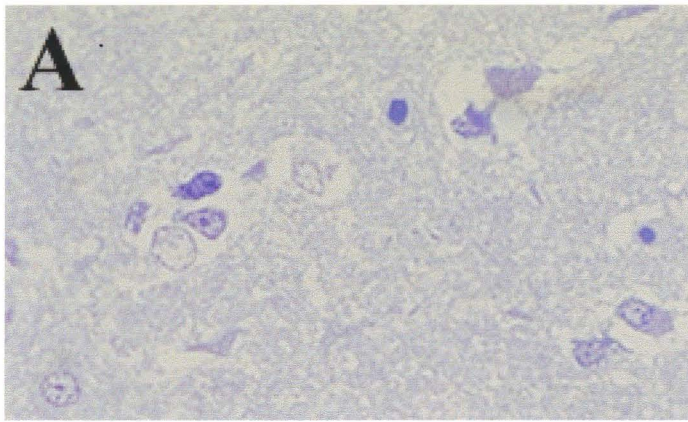


**Figure 5-11** Toluidine blue staining. (A) Control brain – prefrontal cortex (B) and (C) Neurons from Quincy’s prefrontal cortex. Arrows highlight the intracellular vacuolization. Note the peripherally located nucleus (**Nu**) in (C).



## 6.0 DISCUSSION

The experiments presented here demonstrate the challenges and obstacles that need to be overcome to effectively scale up therapies from rodent experiments to large animals. While implantation of microcapsules into the lateral ventricles of mice achieves the delivery of transgene products to surrounding brain tissue (Ross et al., 1999a, 1999b), the results of this thesis indicate that the procedure and host response is more complicated and thus less effective in the dog.

The most obvious factor accounting for the differences between the murine and canine results is the difference in brain and CSF volume between the two animals and the consequent diffusion difficulties (Zlokovic and Apuzzo, 1997b). Clearly, any product delivered to the dog has a much larger distance to diffuse than in the mouse brain. In an attempt to account for this, the volume of microcapsules was increased in these experiments, from 5 $\mu$ l in the mouse to 500-2000 $\mu$ l in the dog. It is possible that this volume of microcapsules was still insufficient for the delivery of a therapeutically relevant amount of product to the brain. While implantation of a greater number of microcapsules may be attempted, there are risks associated with injecting large volumes in the finite space of the ventricular system. This volume limitation in the CNS is highlighted by the clinical problems observed in Polly as a result of the large amount of capsules impinging upon the spinal cord. The specific spinal cord problems are alleviated with intraventricular surgeries, however, implantation into this site with a large volume produces the risk that the ventricular system may become blocked by microcapsules resulting in hydrocephalus and other intracerebral complications.

## 6.1 Microcapsule Implantation Techniques

Two CNS implantation techniques were examined in the experiments presented, intraventricular and spinal intrathecal injections.

Intraventricular surgery is a common route of product delivery to rodents (Emerich et al., 1996; Winn et al., 1996). The procedure in large animals, such as dogs, is much more invasive and less precise due to the vast differences in brain size and shape among “higher” animals. The imprecise nature of the surgery is exemplified here by the difficulties in accurately targeting the lateral ventricles. The CT scans was helpful in determining the depth of our target site, however, once the animal’s head was adjusted in the stereotaxic apparatus, coordinates from the scan could not be directly applied to the newly angled head. The saline filled capillary tube was useful for targeting only the first ventricle because once the ventricular lining was punctured with the first injection, the CSF pressure was not high enough for the capillary tube to be useful for localizing the second ventricle. This procedure, therefore, may be more accurate for unilateral injections. One hundred percent accuracy in targeting brain regions in the dog might only be attained with real-time visualization techniques analogous to those used for human neurosurgery.

Spinal intrathecal implantations were investigated here for the purpose of avoiding the drawbacks of intraventricular surgery. The procedure is a simple one and much less invasive than the brain surgery. Further, implantation is always accurate since the preceding removal of CSF is a confirmation of the subarachnoid placement. Disadvantages of this method include the risk of puncturing the spinal cord with the

needle, causing haemorrhage if the needle is improperly placed during the spinal tap and impinging on the spinal cord if the volume of capsules is too large.

## 6.2 Product Delivery

In the cases where microcapsules could be retrieved from the animals, the encapsulated cell viabilities were comparable to those maintained *in vitro* for Dana, Squirt, Smudge, Angus and Buick, suggesting that the CNS may provide the environment necessary for maintenance of encapsulated cells. However, the capsules retrieved from Jazz, Polly and Jewel showed encapsulated cell viabilities significantly lower than those maintained *in vitro*. When cells were broken out of retrieved capsules and tested for secretion in chapter 4, the secretion rate was greater than that obtained from the cells broken out of capsules maintained *in vitro*. Since the cells were able to secrete human growth hormone, this suggests that the cells retained their transgene expression while *in vivo* if they were not trapped by inflammatory mediators.

In chapter 3 (naïve dogs), hGH was detected in the CSF of all dogs only on day 7 post-operative. In Dino and Duffy, the capsules were compromised as a result of an improper CHES protocol. The decline in hGH levels on day 14 in these two dogs might therefore be explained by host rejection of the unprotected implant. Antibodies to hGH were detected in Duffy and also may account for the decline of hormone in his CSF. In all cases, an inflammatory immune response was revealed upon histological examination and this may have played a role in disrupting product delivery (see below).

In chapter 4 (previously treated dogs), hGH was detected only in Smudge's CSF on day 7 while antibodies to hGH could be detected in all dogs receiving hormone-secreting microcapsules. While this may be interpreted as intraventricular delivery being more effective than spinal intrathecal delivery, caution must be taken in interpreting these results due to the previous treatment variables, specifically the sensitization to hGH and foreign cells. The severe inflammatory responses seen here are likely to have had a negative effect on the delivery potential of the microcapsules (Winn et al., 1996) and one cannot rule out the possibility that differences in the dogs' immune responses prevented accurate comparison of the delivery routes.

In chapter 5,  $\alpha$ -L-iduronidase activity levels could not be detected in the CSF or plasma due to freezing-thawing procedures (see Appendix B). While enzyme activity was detectable in the brain tissue, the MPS I dog levels remained significantly lower than control in all brain regions. The increase in activity observed in the outer portion of the hippocampus may be a result of the microcapsule treatment, but could also be accounted for by regional differences within this structure. Fresh frozen untreated mutant brain tissue is necessary to make a conclusion regarding these possibilities.

The gross observations of the microcapsules being embedded in the tissue, as well as the histological findings of necrotic cells within the attacked capsules suggests that the immune response may have interrupted the microcapsule delivery of the transgene product. In addition to directly attacking many of the cells, the reaction in the surrounding tissue may have prevented the diffusional transport of nutrients and other products in and out of the trapped microcapsules (Winn et al., 1989).

### 6.3 Immune Response

An inflammatory immune response was observed in all dogs except Spot, the animal that received empty microcapsules. This pattern supports the reported biocompatibility of the alginate-poly-L-lysine-alginate microcapsule material (Clayton et al., 1991; DeVos et al., 1997; Klock et al., 1997), but suggests that the encapsulated cells are immunogenic and not fully protected from immune mediators in the dog. Immune responses in the CNS of mice were not investigated in the experiments performed by Ross et al (1999a, 1999b).

While the immune response was not characterized until histological examination, the increase in white blood cell content in the CSF provided a good clinical indication of the cellular response. The microcapsules induced an inflammatory response whether or not the cells were secreting a foreign product. Both acute and chronic [Angus and Buick] reactions were noted upon histological observation of lymphocytes, macrophages, multinucleated giant cells, glial responses and fibroblastic scarring in the brain and spinal cord tissue. The extent and duration of the responses suggest that they were not simply due to mechanical injury from surgery, which should have disappeared with time, as seen in murine CNS microcapsule experiments (Aebischer et al., 1988; Winn et al., 1989).

Casual observation of microcapsules maintained *in vitro* reveals growth of cells at the bottom of the plates suggesting that some cells may be escaping from the capsules. If this is the case, it is possible that this also occurs *in vivo* and may alert the immune system of the presence of foreign cells. Alternatively, the microcapsules simply may not be providing a sufficient immuno-isolation environment for the cells in dogs.

## 6.4 MPS I

The implantation of microcapsules secreting  $\alpha$ -L-iduronidase to the CNS of an MPS I dog did not result in histological correction of the lysosomal inclusions, even in the immediate vicinity of the capsule implantation site. Brain cells remained laden with cytoplasmic inclusions and peripherally located nuclei while degenerating cells were scattered throughout the brain. Delivery of the enzyme has been shown to be sufficient for clearance of the storage bodies (Neufeld and Fratantoni, 1970; Shull et al., 1987; Shull et al., 1988), but enzyme delivery may have been impeded here by the immune disruption described above. Further, since this dog had been previously treated neonatally (Lutzko et al., 1999b) and later with intraperitoneally implanted microcapsules, Quincy's immune system was "primed" to develop antibodies against the enzyme as demonstrated by his rapid increase in antibody titre.

If microcapsule technology is to be used for neurological diseases such as the MPSs, repeated therapy will be necessary since the microcapsules have not yet been developed for long-term (years) treatment (Lindner and Emerich, 1998). It is therefore interesting to note here the effect of the successive procedures. Since  $\alpha$ -L-iduronidase is a foreign enzyme to the MPS I system, antibodies directed towards the protein were observed even with the first treatment (Lutzko et al., 1999b). The immune response appeared to abolish the effect of any enzyme delivery in the first and all subsequent procedures, and is clearly an impediment to treatment, even in the somewhat immuno-privileged CNS.

## 6.5 Areas for Further Research

An area of research that may be beneficial for CNS APA microcapsule treatment is the use of less-immunogenic cell lines. The cells used here were non-autologous canine kidney cells. While non-autologous cells remain the vision for microencapsulation, it may be advantageous to use cells that are intrinsic to the brain environment such as neurons, glia or neural progenitor cells (Fisher, 1997; Pincus et al., 1998).

In other experiments establishing the feasibility of encapsulated cell technology in the CNS of large animals and even humans, xenogeneic cells were used and no inflammatory response was detected (Aebischer et al., 1994a, 1994b; Emerich et al., 1994a; Aebischer et al., 1996b). This suggests, then, that the development of more stable, biocompatible and immuno-protective properties is necessary for APA microcapsules to be used effectively in the brain. Once the microcapsule and cell technologies have been advanced, it may be worthwhile to co-culture the encapsulated cells with cellular immune mediators to establish any immunogenic properties before more *in vivo* experiments are carried out (Kaslow et al., 1998).

With the invasive nature of direct CNS implantation as well as the volume restriction, it would be advantageous to develop a system where only peripheral microcapsule implantation would be necessary to provide neurological treatment (and systemic, when necessary). To circumvent the BBB, it may be interesting to develop a fusion protein that could take advantage of transporter mechanisms at the blood-brain interface and thereby deliver the desired product to the brain. For example, researchers

have exploited the properties of the transferrin receptor at the BBB. With the development of fusion structures composed of neurotrophic factors such as NGF or GDNF combined with the antibody to transferrin, scientists have delivered these factors to the rat CNS (Friden et al., 1993; Backman et al., 1996; Albeck et al., 1997). Such fusion protein constructs have also been created at the DNA level resulting in functional components (Friden et al, 1996; McGrath et al., 1997). It would be interesting to combine this technique with microcapsule technology, that is, constructing a fusion gene containing the protein of interest, transfecting a cell line and encapsulating these cells for *in vivo* systemic implantation.

## **6.6 Conclusion**

At this point, the use of APA microcapsules does not appear to be an effective means of long-term product delivery to the CNS of large animals. The data presented here suggest the need for improved microcapsule structure for enhanced cell protection *in vivo*. Further, the results shed light on the immunological complications that may arise with invasive and repeated treatment in the dog brain.

## APPENDIX A – SOLUTIONS

### Alkaline Phosphatase Developing Solution

5g (1 tablet) Sigma 104 Phosphatase substrate tablets  
5ml DEA

### 1.1% CaCl<sub>2</sub>

11g CaCl<sub>2</sub>  
500ml 0.9% NaCl  
500ml ddH<sub>2</sub>O  
autoclave sterilize

### 10x Citrate Saline Stock

8.08g sodium citrate (trisodium citric acid)  
250ml ddH<sub>2</sub>O  
250ml 0.9% NaCl  
autoclave sterilize

### CHES Stock Solution (pH 8.2)

2g CHES (2-[N-Cyclohexylamino]ethane-sulfonic acid, Sigma, Cat No. C-2885)  
100ml 0.9% NaCl  
autoclave sterilize

### Cresyl Violet (Nissl Stain)

60ml *Cresyl Violet Stock Dye*: 1.2g cresyl violet acetate (Sigma, Cat No.C-1791)  
ddH<sub>2</sub>O to 500ml

470ml *Acetate Buffer*: 6ml 1M acetic acid  
994ml ddH<sub>2</sub>O

30ml *Basic Buffer*: 13.6g sodium acetate  
ddH<sub>2</sub>O to 1000ml

Filter, pH 3.5

### DEA (diethanolamine)

1L ddH<sub>2</sub>O  
102mg 0.5mM MgCl<sub>2</sub>  
96.6ml 1M diethanolamine  
pH 9.8

**0.4M Formate Buffer (pH 3.5)**

4.8ml 88% formic acid

6.8g sodium formate

0.5g  $\text{NaN}_3$

4.5g  $\text{NaCl}_2$

500ml ddH<sub>2</sub>O

**2% Glutaraldehyde**

50ml 4% glutaraldehyde in ddH<sub>2</sub>O

50ml 0.2M sodium cacodylate buffer

**0.5M Glycine/Carbonate Buffer (pH 10.2)**

26.7g glycine

47.1g  $\text{Na}_2\text{CO}_3$

100ml ddH<sub>2</sub>O

**Homogenization Buffer**

700 $\mu$ l  $\beta$ -mecaptoethanol (to final concentration of 10mM)

20ml Tris-Cl, pH 7.5 (to final concentration of 20mM)

28ml 5M NaCl (to final concentration of 140mM)

2.5g Saponin (to final concentration of 0.25%) (Sigma, Cat No. S-1252)

1L ddH<sub>2</sub>O

**4% Paraformaldehyde**

4g paraformaldehyde (Sigma-Aldrich, P-6148)

100ml 0.1M sodium phosphate buffer

filtered

**Periodic Acid Schiff (PAS)**

Commercial preparation – AJP Scientific Inc/Maynard Scientific Co.

**10x PBS (phosphate buffered saline) Stock Solution (pH 7.4)**

40g NaCl

1g KCl

5.75g  $\text{Na}_2\text{HPO}_4 \cdot 7\text{H}_2\text{O}$

0.425g  $\text{KH}_2\text{PO}_4$

480ml ddH<sub>2</sub>O

autoclave sterilized

**PBS/T**

0.2g  $\text{KH}_2\text{PO}_4$  (1.5mM)

2.9g  $\text{Na}_2\text{HPO}_4$  (20mM)

8.0g NaCl (0.14mM)

0.2g KCl (3mM)

1L ddH<sub>2</sub>O

pH to 7.4 then add 0.5ml (0.05%) Tween20 (Polyoxyethylenesorbitan Monolaurate, Sigma, Cat No. P-1379)

**1% PLL (Poly-L-Lysine hydrobromide) Stock Solution**

100mg PLL (Sigma, P-7890)

200ml 0.9% physiological saline

filter sterilized

**2% Potassium Alginate**

4g potassium alginate (Kelco Company)

200ml 0.9% physiological saline

filter sterilize

**Sodium Cacodylate Buffer (pH 7.4)**

42.8g sodium cacodylate

to 1000ml ddH<sub>2</sub>O

**0.1M Sodium Phosphate Buffer (pH 7.4)**

500ml 0.4M sodium phosphate dibasic stock solution in 1500ml ddH<sub>2</sub>O

~150ml 0.4M sodium phosphate monobasic stock solution in 350ml ddH<sub>2</sub>O

**0.4M Sodium Phosphate Dibasic Stock Solution**

227.2g sodium phosphate dibasic (anhydrous) ( $\text{Na}_2\text{HPO}_4$ )

4L ddH<sub>2</sub>O

**0.4M Sodium Phosphate Monobasic Stock Solution**

191.97g sodium phosphate monobasic ( $\text{NaH}_2\text{PO}_4$ )

4L ddH<sub>2</sub>O

**Spurr Resin (firm)**

20g vinylcyclohexane dioxide (ERL)

12g diglycidylether of polypropylene (DER)

52g nonenyl succinic anhydride (NSA)

0.8g dimethylaminoethanol (DMAE)

**Toluidine Blue**

1% toluidine blue (Marivac, Cat No. Ct009-0)

1% sodium borate

ddH<sub>2</sub>O

**2M Tris-HCl**

242.2g Tris base (Boehringer Mannheim, Cat No. 604205)

25ml concentrated HCl

pH to 7.4-8 then add ddH<sub>2</sub>O to 1L

**Trypsin**

10ml 10x stock citrate saline

90ml ddH<sub>2</sub>O

0.125g Trypsin (Sigma, Cat No. T-0134)

filter sterilized

## APPENDIX B

### Rationale

The  $\alpha$ -L-iduronidase enzyme activity assay described in section 2.3.3 was carried out on the CSF, plasma and brain tissue of the dogs implanted with microcapsules in experiment #3. While activity levels were apparent in the brain tissue, only background levels could be detected in the CSF and plasma samples despite attempted changes in the protocol (incubation periods for up to 24 hours, increased sample volume and larger volume of stop buffer). It was suspected that enzyme activity was lost as a result of freezing and thawing of the samples. The following investigation was designed to examine this possibility and confirm that the assay itself is valid.

### Materials and Methods

A fresh sample of CSF was obtained from a tissue dog ("fresh" CSF). A fresh enzyme source was obtained from cell culture media ("fresh" media) as outlined in section 2.3.4. Additionally, CSF from Dana that had been frozen and thawed repeatedly was used as a control (frozen CSF).

Within one hour of obtaining the fresh samples, the activity assay was carried out as described in section 2.3.3 in glass tubes with 1ml stop buffer. 25 $\mu$ l and 50 $\mu$ l samples were used for each and 1, 2 and 4-hour incubation time points were assessed. The CSF samples were then frozen at -70°C and the media at -20°C. The assay was repeated for each sample and time point on days 4 and 8 post-fresh-sample collection.

## Results

The detailed results are presented in table B-1 and figure B-1. Briefly, on day 0, enzyme activity was detected only in the fresh CSF and media. In both cases, the activity increased linearly with time. Further, greater concentrations of enzyme resulted in increased activity. On day 4, the enzyme activity detected in the “fresh” CSF was approximately half the amount seen on day 0, while that detected in the “fresh” media was ~1.4 fold lower than on day 0. The same enzyme activity patterns were noted. On day 8 the activity in the “fresh” CSF decreased by another ~1.2 fold while the activity in the “fresh” media decreased by another ~1.5 fold.

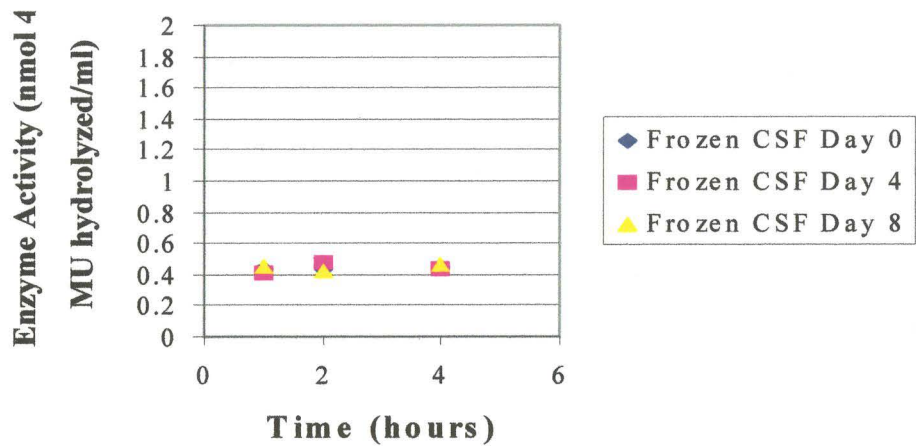
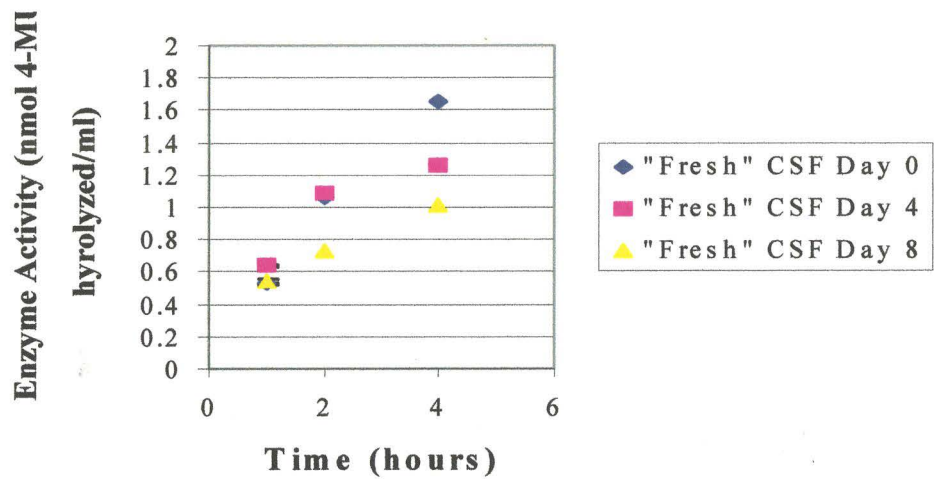
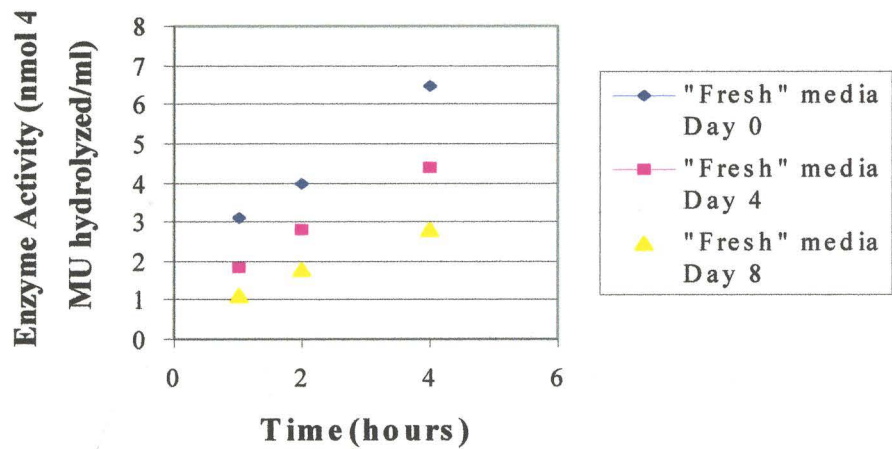
## Conclusions

The enzyme activity assay appears to be valid as normal enzyme kinetics were demonstrated over time and with different enzyme concentrations. Freezing and thawing the samples appears to have a deleterious effect on  $\alpha$ -L-iduronidase activity and provides an explanation for the lack of activity observed in the CSF and plasma of the dogs in experiment #3.

**Table B-1** Results obtained from the examination of freezing and thawing effects on the activity of  $\alpha$ -L-iduronidase in CSF and media. Average enzyme activity is expressed as nmol 4-MU hydrolyzed / ml / hour  $\pm$  SD.

	Day 0		Day 4		Day 8	
	25 $\mu$ l	50 $\mu$ l	25 $\mu$ l	50 $\mu$ l	25 $\mu$ l	50 $\mu$ l
<b>Frozen CSF</b>	0.006 $\pm$ 0.002	0.0088 $\pm$ 0.018	0.0054 $\pm$ 0.001	0.0144 $\pm$ 0.003	0.0054 $\pm$ 0.013	0.0112 $\pm$ 0.256
<b>“Fresh” CSF</b>	0.3628 $\pm$ 0.009	0.5234 $\pm$ 0.015	0.1892 $\pm$ 0.032	0.3317 $\pm$ 0.0042	0.1516 $\pm$ 0.005	0.2439 $\pm$ 0.010
<b>“Fresh” Media</b>	1.1458 $\pm$ 0.040	1.4041 $\pm$ 0.193	0.8441 $\pm$ 0.007	1.055 $\pm$ 0.017	0.5563 $\pm$ 0.010	.07893 $\pm$ 0.037

**Figure B-1** Enzyme activity for each 25  $\mu$ l sample on each day. 50 $\mu$ l samples show the same patterns depicted here. (A) Frozen CSF (B) "Fresh" CSF (C) "Fresh" Media.

**A****B****C**

## REFERENCES

- Aebischer, P, Winn, SR, Galletti, PM. (1988) Transplantation of neural tissue in polymer capsules. *Brain Research*, 488: 364-368.
- Aebischer, P, Tresco, PA, Sagen, J, Winn, SR (1991) Transplantation of microencapsulated bovine chromaffin cells reduces lesion-induced rotational asymmetry in rats. *Brain Research*, 560: 43-49.
- Aebischer, P, Goddard, M, Signore, AP, Timpson, RL. (1994a) Functional Recovery in Hemiparkinsonian Primates Transplanted with Polymer-Encapsulated PC12 Cells. *Experimental Neurology*, 126: 151-158.
- Aebischer, P, Buchser, E, Joseph, JM, Favre, J, de Tribolet, N, Lysaght, M, Rudnick, S, Goddard, M. (1994b) Transplantation in Humans of Encapsulated Xenogenic Cells without Immunosuppression. *Transplantation*, 58(11): 1275-1277.
- Aebischer, P, Ponchon N.A-M, Heyd, B, Deglon, N, Joseph, J-M, Zurn, AD, Baetge, EE, Hammang, JP, Goddard, M, Lysaght, M, Kaplan, F, Kato, AC, Schlupe, M, Hirt, L, Regli, F, Porchet, F, de Tribolet, N. (1996a) Gene Therapy for Amyotrophic Lateral Sclerosis (ALS) Using a Polymer Encapsulated Xenogenic Cell Line Engineered to Secrete hCNTF. *Human Gene Therapy*, 7: 851-860.
- Aebischer, P, Schlupe, M, Deglon, N, Joseph, J-M, Hirt, L, Heyd, B, Goddard, M, Hammang, JP, Zurn, AD, Kato, AC, Regli, F, Baetge, EE. (1996b) Intrathecal delivery of CNTF using encapsulated genetically modified xenogeneic cells in amyotrophic lateral sclerosis patients. *Nature Medicine*, 2(6): 696-699.
- Al-Hendy, A, Hortelano, G, Tannenbaum, GS, Chang, PL. (1995) Correction of the Growth Defect in Dwarf Mice with Nonautologous Microencapsulated Myoblasts – An Alternate Approach to Gomotic Gene Therapy. *Human Gene Therapy*, 6: 165-175.
- Allen, D. (1991) Special Techniques. In *Small Animal Medicine*, Allen, D, Kruth, S, Garvey, M, eds., pp. 1076-1079.
- Bach, G, Friedman, R, Weissman, B, Neufeld, EF. (1972) The Defect in the Hurler and Scheie Syndromes: Deficiency of  $\alpha$ -L-Iduronidase. *PNAS*, 69(8): 2048-2051.
- Barkats, M, Bilang-Bleuel, A, Buc-Caron, H, Castel-Barthe, MN, Corti, O, Finiels, F, Horellou, P, Revah, F, Sabate, O, Mallet, J. (1998) Adenovirus in the Brain: Recent Advances of Gene Therapy for Neurodegenerative Diseases. 55: 333-341.
- Barton, RW and Neufeld, EF. (1971) The Hurler Corrective Factor – Purification and some properties. *Journal of Biological Chemistry*, 246(24): 7773-7779.

- Bastedo, L, Sands, MS, Lambert, DT, Pisa, MA, Birkenmeier, E, Chang, PL. (1994) Behavioral Consequences of Bone Marrow Transplantation in the Treatment of Murine Mucopolysaccharidosis Type VII. *J. Clin. Invest.*, 94: 1180-1186.
- Bielicki, J, Hopwood, JJ, Anson, DS. (1996) Correction of Sanfilippo A Skin Fibroblasts by Retroviral Vector-Mediated Gene Transfer. *Human Gene Therapy*, 7: 1965-1970.
- Blomer, U, Naldini, K, Kafri, T, Trono, D, Verma, IM, Gage, FH. (1997) Highly efficient and sustained gene transfer in adult neurons with a lentivirus vector. *J. Virology*, 71: 6641-6649.
- Boulton, M, Young, A, Hay, Y, Armstrong, D, Flessner, M, Schwartz, M, Johnston, M. (1996) Drainage of CSF through lymphatic pathways and arachnoid villi in sheep: measurement of <sup>125</sup>I-albumin clearance. *Neurpathology and Applied Neurobiology*, 22: 325-333.
- Bradbury, MWB, Cserr, HF. (1985) Drainage of cerebral interstitial fluid and of cerebrospinal fluid into lymphatics. In *Experimental Biology of the Lymphatic Circulation*, Johnston, MG (ed.), pp. 355-394.
- Braun, SE, Pan, D, Aronovich, EL, Jonsson, JJ, McIvor, RS, Whitley, CB. (1996) Preclinical Studies of Lymphocyte Gene Therapy for Mild Hunter Syndrome (Mucopolysaccharidosis Type II). *Human Gene Therapy*, 7: 283-290.
- Breider, MA, Shull, RM, Constantopoulos, G. (1989) Long-Term Effects of Bone Marrow Transplantation in Dogs with Mucopolysaccharidosis I. *Am J Pathol.*, 134(3): 677-692.
- Byrnes, AP, Rusby, JE, Wood, MJA, Charlton, HM. (1995) Adenovirus Gene Transfer Causes Inflammation in the Brain. *Neuroscience*, 66(4): 1015-1024.
- Cervos-Navarro, J, Urich, H. (1995) Disorders of Glycosaminoglycan Metabolism (Mucopolysaccharidoses). In *Metabolic and Degenerative Diseases of the Central Nervous System - Pathology, Biochemistry and Genetics*, Academic Press, Inc. pp. 110-136.
- Chang, PL, Varey, PA, Rosa, NE, Ameen, M, Davidson, RG. (1986) Association of Steroid Sulfatase with One of the Arylsulfatase C Isozymes in Human Fibroblasts. *Journal of Biological Chemistry*, 261(31): 14443-14447.

- Chang, PL, Capone, JP and Brown, GM. (1990) Autologous Fibroblast Implantation Feasibility and Potential Problems in Gene Replacement Therapy. *Mol. Biol. Med.*, 7: 461-470.
- Chang, PL, Shen, N, Wescott, AJ. (1993) Delivery of Recombinant Gene Products with Microencapsulated Cells *In Vivo*. *Human Gene Therapy*, 4: 440-443.
- Chang, PL. (1995) Nonautologous Somatic Gene Therapy. In *Somatic Gene Therapy*, CRC Press, (Chang PL, ed.), pp. 203-223.
- Chang, PL, Van Raamsdonk, JM, Hortelano, G, Barsoum, SC, MacDonald, NC, Stockley, TL. (1999) The *in vivo* delivery of heterologous proteins by microencapsulated recombinant cells. *Trends in Biotechnology*, 17: 78-83.
- Chen, HH, Mack, LM, Kelly, R, Ontell, M, Kockaneck, S, Clemens, PR. (1997) Persistence in muscle of an adenoviral vector that lacks all viral genes. *PNAS*, 94: 1645-1650.
- Clarke, LA, Nasir, J, Zhang, H, McDonald, H, Applegarth, DA, Hayden, MR, Toone, J. (1994) Murine  $\alpha$ -L-Iduronidase: cDNA Isolation and Expression. *Genomics*, 24: 311-316.
- Clarke, LA, Russell, CS, Pownall, S, Warrington, CL, Borowski, A, Dimmick, JE, Toone, J, Jirik, FR. (1997) Murine mucopolysaccharidosis type I: targeted disruption of the murine  $\alpha$ -L-iduronidase gene. *Human Molecular Genetics*, 6(4): 503-511.
- Clayton, HA, London, NJ, Colloby, PS, Bell, PR, James, RF. (1991) The effect of capsule composition on the biocompatibility of alginate-poly-L-lysine capsules. *J. Microencapsulation*, 8(2): 221-233.
- Constantopoulos, G, McComb, RD, Dekaban, AS. (1976) Neurochemistry of the Mucopolysaccharidoses: Brain Glycosaminoglycans in Normals and Four Types of Mucopolysaccharidoses. *Journal of Neurochemistry*, 26: 901-908.
- Constantopoulos, G and Dekaban, AS. (1978) Neurochemistry of the Mucopolysaccharidoses: Brain Lipids and Lysosomal Enzymes in Patients with Four Types of Mucopolysaccharidoses. *Journal of Neurochemistry*, 30: 965-973.
- Constantopoulos, G, Shull, RM, Hastings, NE, Neufeld, EF. (1985) Neurochemical Characterization of Canine  $\alpha$ -L-Iduronidase Deficiency Disease (Model of Human Mucopolysaccharidosis I). *Journal of Neurochemistry*, 45(4): 1213-1217.

- Constantopoulos, G, Scott, JA, Shull, RM. (1989) Corneal Opacity in Canine MPS I – Changes after Bone Marrow Transplantation. *Investigative Ophthalmology & Visual Science*, 30(8): 1802-1807.
- Cserr, HF, Harling-Berg, CJ, Knopf, PM. (1992) Drainage of Brain Extracellular Fluid into Blood and Deep Cervical Lymph and its Immunological Significance. *Brain Pathology*, 2: 269-276.
- Daly, TM, Vogler, C, Levy, B, Haskins, ME, Sands, MS. (1999) Neonatal gene transfer leads to widespread correction of pathology in a murine model of lysosomal storage disease. *PNAS*, 96: 2296-2300.
- Deglon, N, Heyd, B, Tan, SA, Joseph, J-M, Zurn, AD, Aebischer, P. (1996) Central Nervous System Delivery of Recombinant Ciliary Neurotrophic Factor by Polymer Encapsulated Differentiated C<sub>2</sub>C<sub>12</sub> Myoblasts. *Human Gene Therapy*, 7: 2135-2146.
- Dekaban, AS and Constantopoulos, G. (1977) Mucopolysaccharidosis Types I, II, IIIA and V. Pathological and Biochemical Abnormalities in the Neuroal and Mesenchymal Elements of the Brain. *Acta Neuropath.*, 39: 1-7.
- Del Bigio, MR. (1995) The Ependyma: A Protective Barrier Between Brain and Cerebrospinal Fluid. *Glia*, 14: 1-13.
- DeVos, P, DeHaan, B, Van Schilfgaarde, R. (1997) Effect of the alginate composition on the biocompatibility of alginate-polylysine microcapsules. *Biomaterials*, 18(3): 273-278.
- Doering, LC and Chang, PL. (1991) Expression of a Novel Gene Product by Transplants of Genetically Modified Primary Fibroblasts in the Central Nervous System. *Journal of Neuroscience Research*, 29: 292-298.
- During, MJ, Samulski, RJ, Elsworth, JD, Kaplitt, MG, Leone, P, Xiao, X, Li, J, Freese, A, Taylor, JR, Roth, RH, Sladek Jr., JR, O'Malley, KL, Redmond Jr., DE. (1998) In vivo expression of therapeutic human genes for dopamine production in the caudates of MPTP-treated monkeys using an AAV vector. *Gene Therapy*, 5: 820-827.
- Emerich, DF, Winn, SR, Harper, J, Hammang, JP, Baetge, EE, Kordower, JF. (1994a) Implants of Polymer-Encapsulated Human NGF-Secreting Cells in the Nonhuman Primate: Rescue and Sprouting of Degenerating Cholinergic Basal Forebrain Neurons. *Journal of Comparative Neurology*, 349: 148-164.

- Emerich, DF, Hammang, JP, Baetge, EE, Winn, SR. (1994b) Implantation of Polymer-Encapsulated Human Nerve Growth Factor-Secreting Fibroblasts Attenuates the Behavioral and Neuropathological Consequences of Quinolinic Acid Injections into Rodent Striatum. *Experimental Neurology*, 130: 141-150.
- Emerich, DF, Winn, SR, Lindner, MD. (1996a) Continued Presence of Intrastratial but not Intraventricular Polymer-Encapsulated PC12 Cells is Required for Alleviation of Behavioral Deficits in Parkinsonian Rodents. *Cell Transplantation*, 5(5): 589-596.
- Emerich, DF, Lindner, MD, Winn, SR, Chen, E-Y, Frydel, BR, Kordower, JH. (1996b) Implants of Encapsulated Human CNTF-Producing Fibroblasts Prevent Behavioral Deficits and Striatal Degeneration in a Rodent Model of Huntington's Disease. *Journal of Neuroscience*, 16(16): 5168-5181.
- Emerich, DF, Winn, SR, Hantraye, PM, Peschanski, M, Chen, E-Y, Chu, Y, McDermott, P, Baetge, EE, Kordower, JH. (1997) Protective effects of encapsulated cells producing neurotrophic factor CNTF in a monkey model of Huntington's disease. *Nature*, 386: 395-399.
- Englehardt, JF, Ye, X, Doranz, B, Wilson, JM. (1994) Ablation of E2A in recombinant adenoviruses improves transgene persistence and decreases inflammatory response in mouse liver. *PNAS*, 91: 6196-6200.
- Fairbairn, LJ, Lashford, LS, Spooner, E, McDermott, RH, Lebens, G, Arrand, JE, Arrand, JR, Bellantuono, I, Holt, R, Hatton, CE, Cooper, A, Besley, GTN, Wraith, JE, Anson, DS, Hopwood, JJ, Dexter, TM. (1996) Lon-term *in vitro* correction of  $\alpha$ -L-iduronidase deficiency (Hurler syndrome) in human bone marrow. *PNAS*, 93: 2025-2030.
- Fischer, A, Carmichael, KP, Munnell, JF, Jhabvala, P, Thompson, JN, Matalon, R, Jezyk, PF, Wang, P, Giger, U. (1998) Sulfamidase Deficiency in a Family of Dachshunds: A Canine Model of Mucopolysaccharidosis IIIA (Sanfilippo A). *Pediatric Research*, 44(1): 74-82.
- Fisher, LJ and Gage, GH (1993) Grafting in the mammalian central nervous system. *Physiol Rev.*, 73: 583-616.
- Fisher, LJ. (1997) Nerual Precursor Cells: Applications for the Study and Repair of the Central Nervous System. *Neurobiology of Disease*, 4: 1-22.
- Fishman, RA. (1993) *Cerebrospinal Fluid in Diseases of the Nervous System*, 2<sup>nd</sup> ed. W.B. Saunders Company.

Freidmann, TO. (1997) Overcoming the Obstacles to Gene Therapy. *Scientific American*, June: 96-101.

Gabrielli, O, Salvolini, U, Marcotti, M, Mariani, MG, Coppa, GV, Giorgi, PL. (1992) Cerebral MRI in two brothers with mucopolysaccharidosis type I and different clinical phenotypes. *Neuroradiology*, 34: 313-315.

Gehrmann, J, Matsumoto, Y, Kreutzberg, GW. (1995) Microglia: intrinsic immuneffector cell of the brain. *Brain Research Reviews*, 20: 269-287.

Ghadge, GD, Roos, RP, Kang, UJ, Wollmann, R, Fishman, PS, Kalynych, AM, Barr, E, Leiden, JM. (1995) CNS delivery by retrograde transport of recombinant replication-defective adenoviruses. *Gene Therapy*, 2: 132-137.

Ghodsi, B, Stein, C, Derksen, T, Yang, G, Anderson, RD, Davidson, BL. (1998) Extensive  $\beta$ -Glucuronidase Activity in Murine Central Nervous System after Adenovirus-Mediated Gene Transfer to Brain. *Human Gene Therapy*, 9: 2331-2340.

Gielsmann, V. (1995) Lysosomal Storage Diseases. *Biochemica et Biophysica Acta*, 1270: 103-136.

Gitzelmann, R, Bosshard, NU, Superti-Furga, A, Spycher, MA, Briner, J, Wiesmann, U, Lutz, H, Litshi, B. (1994) Feline mucopolysaccharidosis VII due to  $\beta$ -glucuronidase deficiency. *Vet Pathol.*, 31: 435-443.

Graham, F and Van der Eb, AJ. (1973) A New Technique for the Assay of Infectivity of Human Adenovirus 5 DNA. *Virology*, 53: 456-467.

Guffon, N, Souillet, G, Maire, I, Straczek, J, Guibaud, P. (1998) Follow-up of nine patients with Hurler syndrome after bone marrow transplantation. *J. Pediatrics*, 133: 119-125.

Hart, MN and Fabry, Z. (1995) CNS antigen presentation. *Trends Neurosci.*, 18: 475-481.

Haskins, ME, Jezyk, PF, Desnick, RJ, McDonough, SK, Patterson, DF. (1979) Alpha-L-iduronidase Deficiency in a Cat: A Model of Mucopolysaccharidosis I. *Pediatr Res.*, 13: 1294-1297.

Haskins, ME, Aguirre, GD, Jezyk, PF, Patterson, DF. (1980) The pathology of feline model of mucopolysaccharidosis VI. *Am J Pathol.*, 101: 657-674.

Haskins, ME, Aguirre, GD, Jezyk, PF, Desnick, RJ, Patterson, DF. (1983) The Pathology of the Feline Model of Mucopolysaccharidosis I. *Am J. Pathol.*, 112: 27-36.

- Haskins, ME, Desnick, RJ, DiFerrante, N, Jezyk, PF, Patterson, DF. (1984)  $\beta$ -Glucuronidase deficiency in a dog: A model of human mucopolysaccharidosis VII. *Pediatr Res*, 19: 980-984.
- Haskins, ME, Aguirre, GD, Jezyk, PF, Schuchman, EH, Desnick, RJ, Patterson, DF. (1991) Animal Model of Human Disease – Mucopolysaccharidosis Type VII (Sly Syndrome) – Beta-Glucuronidase-Deficient Mucopolysaccharidosis in the Dog. *Am. J. Pathol.*, 138: 1553-1555.
- Hermens, WTJMC and Verhaagen, J. (1998) Viral Vectors, Tools for Gene Transfer in the Nervous System. *Progress in Neurobiology*, 55: 399-342.
- Hickey, WF, Hsu, BL, Kimura, H. (1991) T-Lymphocyte Entro Into the Central Nervous System. *Journal of Neuroscience Research*, 28: 254-260.
- Hobbs, JR, Hugh-Hones, K, Barrett, AJ, Byrom, N, Chambers, D, Henry, K, James, DC, Lucas, CF, Rogers, TR, Benson, PF, Tansley, LR, Patrick, AD, Mossman, J, Young, EP. (1981) Reversal of Clinical Features of Hurler's Disease and Biochemical Improvement after Treatment by Bone Marrow Transplantation. *Lancet*, 2: 709-712.
- Hoffman, D, Breakfield, XO, Short, MP, Aebischer, P. (1993) Transplantation of a Polymer-Encapsulated Cell Line Genetically Engineered to Release NGF. *Experimental Neurology*, 122: 100-106.
- Hopwood, JJ, Muller, V, Smithson, A, Baggett, N. (1979) A Fluorometric Assay Using 4-Methylumbelliferyl  $\alpha$ -L-Iduronide for the Estimation of  $\alpha$ -L-Iduronidase Activity and the Detection of Hurler and Scheie Syndromes. *Clinica Chimica Acta*, 92: 257-265.
- Horellou, P, Bilang-Bleuel, A, Mallet, J. (1997a) *In Vivo* Adenovirus-Mediated Gene Transfer for Parkinson's Disease. *Neurobiology of Disease*, 4: 280-287.
- Horellou, P, Sabate, O, Buc-Caron, M-H, Mallet, J. (1997b) Adenovirus-Mediated Gene Transfer to the Central Nervous System for Parkinson's Disease. *Experimental Neurology*, 144: 131-138.
- Hortelano, G, Al-Hendy, A, Ofosu, FA, Chang, PL. (1996) Delivery of Human Factor IX in Mice by Encapsulated Recombinant Myoblasts: A Novel Approach Towards Allogeneic Gene Therapy of Hemophilia B. *Blood*, 87(12): 5095-5103.
- Huang, M-M, Wong, A, Yu, X, Kakkis, E, Kohn, DB. (1997) Retrovirus-mediated transfer of the human  $\alpha$ -L-iduronidase cDNA into human hematopoietic progenitor cells leads to correction in trans of Huler fibroblasts. *Gene Therapy*, 4: 1150-1159.

- Joseph, JM, Goddard, Mills, J, Padrun, V, Zurn, A, Zielinski, B, Favre, J, Gardaz, JP, Mosimann, F, Sagen, J, Christenson, L, Aebischer, P. (1994) Transplantation of encapsulated bovine chromaffin cells in the sheep subarachnoid space: a preclinical study for the treatment of cancer pain. *Cell Transplantation*, 3: 355-364.
- Kakkis, ED, McEntee, MF, Schmidtchen, A, Neufeld, EF, Ward, DA, Gompf, RE, Kanie, S, Bedolla, C, Chien, S-L, Shull, RM. (1996) Long-Term and High-Dose Trials of Enzyme Replacement Therapy in the Canine Model of Mucopolysaccharidosis I. *Biochemical and Molecular Medicine*, 58: 156-167.
- Kang, UJ. (1998) Potential of Gene Therapy for Parkinson's Disease: Neurobiologic Issues and New Developments in Gene Transfer Methodologies. *Movement Disorders*, 13: 59-72.
- Kaparti, G, Lochmuller, H, Nalbantoglu, J, Durham, H. (1996) The principles of gene therapy for the nervous system. *Trends in Neurosci*, 19(2): 49-53.
- Kaplitt, MG, Leone, P, Samulski, RJ, Xiao, X, Pfaff, DW, O'Malley, KL, During, MJ. (1994) Long-term gene expression and phenotypic correction using adeno-associated virus vectors in the mammalian brain. *Nature Genetics*, 8: 148-154.
- Kaslow, HR, Guo, Z, Warren, DW, Wood, RL, Mircheff, AK. (1998) A method to study induction of autoimmunity in vitro: co-culture of lacrimal cells and autologous immune system cells. *Adv Exp Med Biol*, 438: 583-9.
- Kennedy, PGE. (1997) Potential use of herpes simplex virus (HSV) vectors for gene therapy of neurological disorders. *Brain*, 120: 1245-1259.
- Klock, G, Pfeffermann, A, Ryser, C, Grohn, P, Kuttler, B, Hahn, HJ, Zimmermann, U. (1997) Biocompatibility of mannuronic acid-rich alginates. *Biomaterials*, 18(10): 707-713.
- Kordower, JH, Winn, SR, Liu, Y-T, Mufson, EJ, Sladek Jr, JR, Hammang, JP, Baetge, EE, Emerich, DF. (1994) The aged monkey basal forebrain: Rescue and sprouting of axotomized basal forebrain neurons after grafts of encapsulated cells secreting human nerve growth factor. *PNAS*, 91: 10898-10902.
- Kroll, RA and Neuwelt, EA. (1998) Outwitting the Blood-Brain Barrier for Therapeutic Purposes: Osmotic Opening and Other Means. *Neurosurgery*, 42(5): 1083-1099.
- Lachmann, RH and Efstathiou, S. (1999) Use of herpes simplex virus type I for transgene expression within the nervous system. *Clinical Science*, 96: 553-541.

Lassmann, H. (1997) Basic mechanisms of brain inflammation. *Journal of Neural Transmission*. 50(Suppl): 183-190.

Laquerre, S, Goins, WF, Moriuchi, S, Oligino, TJ, Kriskey, DM, Marconi, P, Soares, MK, Cohen, JB, Gloriosio, JC. (1999) Gene-transfer Tool: Herpes Simplex Virus Vectors in The Development of Human Gene Therapy. Friedmann, T, ed. Cold Spring Harbor Laboratory Press, New York, pp. 173-208.

Lim, F and Sun, AM. (1980) Microencapsulated Islets as Bioartificial Endocrine Pancreas. *Science*, 210(21): 908-910.

Lindner, MD, Winn, SR, Baetge, EE, Hammang, JP, Gentile, FT, Doherty, E, McDermott, PE, Frydel, B, Ullman, MD, Schallert, T, Emerich, DF. (1995) Implantation of Encapsulated Catecholamine and GDNF-Producing Cells in Rats with Unilateral Dopamine Depletions and Parkinsonian Symptoms. *Experimental Neurology*, 132: 62-76.

Lindner, MD and Emerich, DF. (1998) Therapeutic Potential of a Polymer-Encapsulated L-DOPA and Dopamine-Producing Cell Line in Rodent and Primate Models of Parkinson's Disease. *Cell Transplantation*, 7(2): 165-174.

Liu, H-W, Ofosu, FA, Chang, PL. (1993) Expression of Human Factor IX by Microencapsulated Recombinant Fibroblasts. *Human Gene Therapy*, 4: 291-301.

Long, Z, Li, L-P, Grooms, T, Lockey, C, Nader, K, Mychokovsky, I, Mueller, S, Burimski, I, Ryan, P, Kikuchi, G, Ennist, D, Marcus, S, Otto, E, McGarrity, G. (1998) Biosafety Monitoring of Patients Receiving Intracerebral Injections of Murine Retroviral Vector Producing Cells. *Human Gene Therapy*, 9: 1165-1172.

Lowry and Renwick. (1971) Relative Frequency of the Hurler and Hunter syndromes. *N Eng J Med*, 284: 221-2.

Lutzko, C, Kruth, S, Abrams-Ogg, ACG, Lau, K, Li, L, Clark, BR, Ruedy, C, Nanji, S, Foster, R, Kohn, D, Shull, R, Dube, ID. (1999a) Genetically Corrected Autologous Stem Cells Engraft, but Host Immune Responses Limit Their Utility in Canine  $\alpha$ -L-Iduronidase Deficiency. *Blood*, 93(6): 1895-1905.

Lutzko, C, Omori, F, Abrams-Ogg, ACG, Shull, R, Li, L, Lau, K, Ruedy, C, Nanji, S, Gartley, C, Dobson, H, Foster, R, Kruth, S, Dube, ID. (1999) Gene Therapy for Canine  $\alpha$ -L-Iduronidase Deficiency: *In Utero* Adoptive Transfer of Genetically Corrected Hematopoietic Progenitors Results in Engraftment but Not Amelioration of Disease. *Human Gene Therapy*, 10: 1521-1532.

- Lysaght, MJ and Aebischer, P. (1999) Encapsulated Cells as Therapy. *Scientific American*, April: 76-89.
- Martin, JH, Brust, JCM, Hilal, S. (1991) *Principles of Neural Science*, 3<sup>rd</sup> ed. El Sevier Science Publishing Co., Inc. Kandel, ER, Schwartz, JH, Jessell, Tam, eds. pp. 309-324.
- McKusick, VA and Neufeld, EF. (1983) The Mucopolysaccharide Storage Diseases. In *The Metabolic Basis of Inherited Disease*, 5<sup>th</sup> ed. Stanbury, JB, Wyngaarden, JB, Fredrickson, DS, Goldstein, JL, Brown, MS (eds). McGraw Hill, Inc., pp. 751-787.
- Menon, KP, Tiwu, PT, Neufeld, EF. (1992) Architecture of the Canine IDUA Gene and Mutation Underlying Canine Mucopolysaccharidosis I. *Genomics*, 14: 763-768.
- Moskowitz, SM, Dlott, B, Chuang, PD, Neufeld, EF. (1992) Cloning and expression of cDNA encoding the human lysosomal enzyme,  $\alpha$ -L-iduronidase. *FASEB J.*, 6: A77.
- Muenzer, J. (1986) Mucopolysaccharidoses. *Adv. Pediatr.*, 33: 269-302.
- Naldini, L, Blomer, U, Gallay, P, Ory, D, Mulligan, R, Gage, FH, Verma, IM, Trono, D. (1996) In vivo gene delivery and stable transduction of nondividing cells by a lentiviral vector. *Science*, 272: 263-267.
- Naldini, L and Verma, IM. (1999) Lentiviral Vectors in The Development of Human Gene Therapy. Friedmann, T, ed. Cold Spring Harbor Laboratory Press, New York, pp. 47-60.
- Neufeld EF and Fratantoni, JC. (1970) Inborn Errors of Mucopolysaccharide Metabolism. *Science*, 169: 141-145.
- Neufeld EF and Meunzer J. (1989) The Mucopolysaccharidoses. In *The Metabolic Basis of Inherited Disease*. Sriver, CR, Beaudet, AL, Sly, W, Valle, D, eds. McGraw-Hill, New York, pp. 1565-1587.
- Neumann, H, Cavialie, A, Jenne, DE, Wekerle, H. (1995) Induction of MHC Class I Genes in Neurons. *Science*, 269: 549-551.
- Nolte, J. (1993) *The Human Brain – An Introduction to its Functional Anatomy*, Mosby-Year Book, Inc, pp. 33-75.
- O'Connor, LH, Erway, CL, Vogler, Ca, Sly, WS, Nicholes, A, Grubb, J, Holmberg, SW, Levy, b, Sands, MS. (1998) Enzyme Replacement Therapy for Murine Mucopolysaccharidosis Type VII Leads to Improvements in Behaviour and Auditory Function. *J. Clin. Invest.*, 101: 1394-1400.

Ohashi, T, Watabe, K, Uehara, K, Sly, WS, Vogler, C, Eto, Y. (1997) Adenovirus-mediated gene transfer and expression of human  $\beta$ -glucuronidase gene in the liver, spleen and central nervous system in mucopolysaccharidosis type VII mice. *PNAS*, 94: 1287-1292.

Okada, H, Miyamura, K, Itoh, T, Hagiwara, M, Wakabayashi, T, Mizuno, M, Colosi, P, Kurtzman, G, Yoshida, J. (1996) Gene therapy against an experimental glioma using adno-associated virus vectors. *Gene Therapy*, 3: 957-964.

Oliver Jr., JE and Conrad, CR. (1975). Cerebral Ventriculography. In *Radiographic Technique in Small Animal Practice*. Ticer, JW (ed), WB Saunders Company, pp. 271-277.

Oliver, JE, Lorenz, MD. Neurologic Examination. (1983) In *Handbook of Veterinary Neurologic Diagnosis*, WB Saunders Company, pp. 19-54.

Parr, MJ, Wen, PY, Schaub, M, Khoury, SJ, Sayegh, MH, Fine, HA. (1998) Immune parameters affecting adenoviral vector gene therapy in the brain. *Journal of NeuroVirology*, 4: 194-203.

Peirone, MA, Delaney, K, Kwiecin, J, Fletch, A, Chang, PL. (1998) Delivery of Recombinant Gene Products to Canines with Nonautologous Microencapsulated Cells. *Human Gene Therapy*, 9: 195-206.

Peters, C, Balthazor, M, Shapiro, EG, King, RJ, Kollman, C, Hegland, JD, Henslee-Downey, J, Trigg, ME, Cowan, MJ, Sanders, J, Bunin, N, Weinstein, H, Lenarsky, C, Falk, P, Harris, R, Bowen, T, Williams, TE, Grayson, GH, Warkentin, P, Sender, L, Cool, VA, Crittenden, M, Packman, S, Kaplan, P, Lockman, LA, Anderson, J, Krivit, W, Dusenbery, K, Wagner, J. (1996) Outcome of Unrelated Donor Bone Marrow Transplantation in 40 Children with Hurler Syndrome. *Blood*, 87(11): 4894-4902.

Peters, C, Shapiro, EG, Krivit, W. (1998) Hurler syndrome: Past, present and future. *J. Pediatrics*, 133: 7-9.

Pincus, DW, Goodman, RR, Fraser, RAR, Nedergaard, M, Goldman, SA. (1998) Neural Stem and Progenitor Cells: A Strategy for Gene Therapy and Brain Repair. *Neurosurgery*, 42(4): 858-867.

Ponchon, NA-M, Heyd, B, Deglon, N, Joseph, J-M, Zurn, AD, Baetge, EE, Hammang, JP, Goddard, M, Lysaght, M, Kaplan, F, Kato, AC, Schlupe, M, Hirt, L, Regli, F, Porchet, F, DeTribolet, N, Aebischer, P. (1996) Clinical Protocol – Gene Therapy for Amyotrophic Lateral Sclerosis (ALS) Using a Polymer Encapsulated Xenogeneic Cell Line Engineered to Secrete hCNTF. *Human Gene Therapy*, 7: 851-860.

- Poorthuis, BJHM, Romme, AE, Willemsen, R, Wagemaker, G. (1994) Bone Marrow Transplantation Has a Significant Effect on Enzyme Levels and Storage of Glucosaminoglycans in Tissues and in Isolated Hepatocytes of Mucopolysaccharidosis Type VII Mice. *Pediatric Res.*, 36(2): 187-193.
- Ray, J, Bouvet, A, DeSanto, C, Fyfe, JC, Xu, D, Wolfe, JH, Aguirre, GD, Patterson, DF, Maskins, ME, Henthron, PS. (1998) Cloning of the Canine  $\beta$ -Glucuronidase cDNA, Mutation Identification in canine MPS VII and Retroviral Vector-Mediated Correction of MPS VII Cells. *Genomics*, 48: 248-253.
- Raymon, HK, Thode, S, Gage, FH. (1997) Application of *ex Vivo* Gene Therapy in the Treatment of Parkinson's Disease. *Experimental Neurology*, 144: 82-91.
- Ridet, JL and Privat, A. (1995) Gene Therapy in the Central Nervous System: Direct Versus Indirect Gene Delivery. *Journal of Neuroscience Research*, 42: 287-293.
- Robbins, SL, Kumar, V, Cotran, RS. (1994) Robbins Pathologic Basis of Disease, 5<sup>th</sup> ed. Saunders, Philadelphia.
- Rome, LH, Weissmann, BW, Neufeld, EF. (1979) Direct demonstration of binding of a lysosomal enzyme,  $\alpha$ -L-iduronidase, to receptors on cultured fibroblasts. *Proc. Natl. Acad. Sci.*, 76(5): 2331-2334.
- Rosenberg, GA. (1990) In *Brain Fluids and Metabolism*, Oxford University Press, pp. 3-57.
- Ross, CJD, Ralph, M, Chang, PL. (1999a) Delivery of Recombinant Gene Products to the Central Nervous System with Nonautologous Cells in Alginate Microcapsules. *Human Gene Therapy*, 10: 49-59.
- Ross, CJD, Maier, S, Ralph, M, Chang, PL. (1999b) A Novel Treatment for Lysosomal Storage Diseases Using Cell Microencapsulation. In Submission.
- Rosler, K, Neuchrist, C, Kitz, K, Scheiner, O, Kraft, D, Lassman, H. (1992) Expression of Leucocyte Adhesion Molecules at the Human Blood-Brain Barrier (BBB). *Journal of Neuroscience Research*, 31: 365-374.
- Rowland, LP, Fink, ME, Rubin, L. (1991) Cerebrospinal Fluid: Blood-Brain Barrier, Brain Edema, and Hydrocephalus in *Principles of Neural Science*, 3<sup>rd</sup> ed. (Kandel, ER, Schwartz, JH, Jessell, TM, eds.) Elsevier Science Publishing Co., Inc., pp. 1050-1060.
- Russel, PJ. (1996) *Genetics*, 4<sup>th</sup> ed. Harper Collins College Publishers, pp. G8-G9.

Sagot, Y, Tan, SA, Baetge, E, Schmalbruch, A, Kato, AC, Aebischer, P. (1995) Polymer Encapsulated Cell Lines Genetically Engineered to Release Ciliary Neurotrophic Factor Can Slow Down Progressive Motor Neuronopathy in the Mouse. *European Journal of Neuroscience*, 7: 1313-1322.

Samulski, RJ, Sally, M, Muzyczka, N. (1999) Adeno-associated Viral Vectors in The Development of Human Gene Therapy. Friedmann, T, ed. Cold Spring Harbor Laboratory Press, New York, pp. 131-172.

Sands, MS, Barker, JE, Vogler, CA, Levy, B, Gwynn, B, Galvin, N, Sly, WS, Birkenmeier, EH. (1993) Treatment of murine mucopolysaccharidosis type VII by syngeneic bone marrow transplantation in neonates. *Lab. Invest.*, 68: 676-686.

Sands, MS, Vogler, C, Kyle, JW, Grubb, JH, Levy, B, Galvin, N, Sly, WS, Birkenmeier, EH. (1994) Enzyme Replacement Therapy for Murine Mucopolysaccharidosis Type VII. *J. Clin. Invest.*, 93: 2324-2331.

Sands, MS, Vogler, C, Torrey, A, Levy, B, Gwynn, B, Gruff, J, Sly, WS, Birkenmeier, EH. (1997) Murine Mucopolysaccharidosis Type VII: Long Term Therapeutic Effects of Enzyme Replacement and Enzyme Replacement Followed by Bone Marrow Transplantation. *J. Clin. Invest.*, 99(7): 1596-1605.

Sautter, J, Tseng, JL, Braguglia, D, Aebischer, P, Spenger, C, Seiler, RW, Widmer, HR, Zurn, AD. (1998) Implants of Polymer-Encapsulated Genetically Modified Cells Releasing Glial Cell Line-Derived Neurotrophic Factor Improve Survival, Growth and Function of Fetal Dopaminergic Grafts. *Experimental Neurology*, 149: 230-236.

Scott, HS, Litjens, T, Nelson, PV, Thompson, PR, Brooks, DA, Hopwood, JJ, Morris, CP. (1993) Identification of Mutations in the  $\alpha$ -L-Iduronidase Gene (IDUA) That Cause Hurler and Scheie Syndromes. *American Journal of Human Genetics*, 53: 973-986.

Shull, RM, Munger, RJ, Spellacy, E, Hall, CW, Constantopoulos, G, Neufeld, EF. (1982) Canine  $\alpha$ -L-Iduronidase Deficiency – A Model of Mucopolysaccharidosis I. *Am J. Pathol.*, 109(2): 244-248.

Shull, RM, Helman, RG, Spellacy, E, Constantopoulos, G, Munger, RJ, Neufeld, EF. (1984) Morphologic and Biochemical Studies of Canine Mucopolysaccharidosis I. *Am J. Pathol.*, 114: 487-495.

Shull, RM, Hastings, NE, Selcer, RR, Jones, JB, Smith, JR, Cullen, WC, Constantopoulos, G. (1987) Bone Marrow Transplantation in Canine Mucopolysaccharidosis I – Effects within the Central Nervous System. *Journal of Clinical Investigation*, 79: 435-443.

- Shull, RM, Breider, MA, Constantopoulos, GC. (1988) Long-term Neurological Effects of Bone Marrow Transplantation in a Canine Lysosomal Storage Disease. *Pediatr Res.*, 24: 347-352.
- Shull, RM, Kakkis, ED, McEntee, MF, Kanie, SA, Jona, AJ, Neufeld, EF. (1994) Enzyme replacement in a canine model of Hurler Syndrome. *PNAS*, 91: 12937-12941.
- Smidsrod, O and Skjak-Braek, G. (1990) Alginate as immobilization matrix for cells. *TIBTECH*, 8: 71-78.
- Stein, CS, Ghodsi, A, Derksen, D, Davidson, BL. (1999) Systemic and Central Nervous System Correction of Lysosomal Storage in Mucopolysaccharidosis Type VII Mice. *Journal of Virology*, 73(4): 3424-3429.
- Stockley, TL and Chang, PL. (1997) Non-Autologous Transplantation with Immunolocalization in Large Animals – A Review. In *Science Medicine and Technology*. Prokop, A, Hunkeler, D, Cherrington, AD, eds. New York Academy of Sciences, New York, pp. 408-425.
- Stoltzfus, LJ, Sosa-Pineda, B, Moskowitz, SM, Menon, KP, Dlott, B, Hooper, L, Teplow, DB, Shull, RM, Neufeld, EF. (1992) Cloning and Characterization of cDNA Encoding Canine  $\alpha$ -L-Iduronidase-mRNA Deficiency in Mucopolysaccharidosis I Dog. *Journal of Biological Chemistry*, 267(10): 6570-6575.
- Suhr, ST and Gage, FH. (1999) Gene Therapy in the Central Nervous System – The Use of Recombinant Retroviruses. *Arch Neurol.*, 56: 287-292.
- Tai, IA and Sun, AM. (1993) Microencapsulation of recombinant cells: a new delivery system for gene therapy. *FASEB Journal*, 7: 1061-1069.
- Tamura, M, Ikenaka, K, Tamura, K, Yoshimatsu, T, Miyao, Y, Kishima, H, Mabuchi, E, Shimizu, K. (1998) Transduction of glioma cells using a high-titer retroviral vector system and their subsequent migration in brain tumors. *Gene Therapy*, 5: 1698-1704.
- Tandon, V, Williamson, JB, Cowie, RA, Wraith, JE. (1996) Spinal Problems in Mucopolysaccharidosis I (Hurler Syndrome). *Journal of Bone and Joint Surgery*, 78-B(6): 938-944.
- Taylor, RM and Wolfe, JH. (1997a) Glycosaminoglycan Storage in Cultured Neonatal Murine Mucopolysaccharidosis Type VII Neuroglial Cells and Correction by  $\beta$ -Glucuronidase Gene Transfer. *Journal of Neurochemistry*, 68: 2079-2085.
- Taylor, RM and Wolfe, JH. (1997b) Decreased lysosomal storage in the adult MPS VII brain in the vicinity of grafts of retroviral vector-corrected fibroblasts secreting high levels of  $\beta$ -glucuronidase. *Nature Medicine*, 3(7): 771-774.

Tuszynski, MH, Roberts, J, Senut, M-C, U, H-S, Gage, FH. (1996) Gene therapy in the adult primate brain: intraparenchymal grafts of cells genetically modified to produce nerve growth factor prevent cholinergic neuronal degeneration. *Gene Therapy*, 3: 305-314.

Vogler, C, Birkenmeier, EH, Sly, WS, Levy, B, Pegors, C, Kyle, JW, Beamer, WG. (1990) A Murine Model of Mucopolysaccharidosis VII – Gross and Microscopic Findings in Beta-Glucuronidase-Deficient Mice. *Am. J. Pathol.*, 136(1): 207-217.

Vogler, C, Sands, MS, Levy, B, Galvin, N, Birkenmeier, EH, Sly, WS. (1996) Enzyme Replacement with Recombinant  $\beta$ -Glucuronidase in Murine Mucopolysaccharidosis Type VII: Impact of Therapy during the First Six Weeks of Life on Subsequent Lysosomal Storage, Growth and Survival. *Pediatric Research*, 39(6): 1050-1054.

Walkley, SU, Haskins, NE, Shull, RM. (1988) Alterations in neuron morphology in mucopolysaccharidosis type I. A Golgi study. *Acta Neuropathol.*, 75: 611-620.

Watts, REW, Spellacy, E, Kendall, BE, du Boulay, G, Gibbs, DA. (1981) Computed Tomography Studies on Patients with Mucopolysaccharidoses. *Neuroradiology*, 21: 9-23.

Whitley, CB, Belani, KG, Chang, P-N, Summers, CG, Blazar, BR, Tsai, MY, Latchaw, RE, Ramsay, NKC, Kersey, JH. (1993) Long-Term Outcome of Hurler Syndrome Following Bone Marrow Transplantation. *American Journal of Medical Genetics*, 46: 209-218.

Whitley, CB, McIvor, RS, Aronovich, EL, Berry, SA, Blazar, BR, Burger, SR, Kersey, JH, King, RA, Faras, AJ, Latchaw, RE, McCullough, J, Pan, D, Ramsay, NKC, Stroncek, DF. (1996) Retroviral-Mediated Transfer of the Iduronate-2-Sulfatase Gene into Lymphocytes for Treatment of Mild Hunter Syndrome (Mucopolysaccharidosis Type II). *Human Gene Therapy*, 7: 537-549.

Wilkerson, MJ, Lewis, DC, Marks, SL, Prieur, DJ. (1998) Clinical and Morphologic Features of Mucopolysaccharidosis Type II in a Dog: Naturally Occurring Model of Hunter Syndrome. *Vet Pathol.*, 35: 230-233.

Winn, SR, Wahlberg, L, Tresco, PA, Aebischer, P. (1989a) An Encapsulated Dopamine-Releasing Polymer Alleviates Experimental Parkinsonism in Rats. *Experimental Neurology*, 105: 244-250.

Winn, SR, Aebischer, P, Galletti, PM. (1989) Brain tissue reaction to permselective polymer capsules. *Journal of Biomedical Materials Research*, 23: 31-41

Winn, SR, Tresco, PA, Zielinski, B, Greene, LA, Jaeger, CB, Aebischer, P. (1991) Behavioral Recovery following Intrastratial Implantation of Microencapsulated PC12 Cells. *Experimental Neurology*, 113: 322-329.

Winn, SR, Lindner, MD, Lee, A, Haggett, G, Francis, JM, Emerich, DF. (1996) Polymer-Encapsulated Genetically Modified Cells Continue to Secrete Human Nerve Growth Factor for over One Year in Rat Ventricles: Behavioural and Anatomical Consequences. *Experimental Neurology*, 140: 126-138.

Wolfe, JH, Sands, MS, Barker, JE, Gwynn, B, Rowe, LB, Vogler, CA, Birkenmeier, EH. (1992) Reversal of pathology in murine mucopolysaccharidosis type VII by somatic cell gene transfer. *Nature*, 360: 749-753.

Yamada, S, DePasquale, M, Patlak, CS, Cserr, HF. (1991) Albumin outflow into deep cervical lymph from different regions of rabbit brain. *American Journal of Physiology*, 261: H1197-H1204.

Yang, Y, Nunes, FA, Berencsi, K, Furth, EE, Gonczol, E, Wilson, JM. (1994a) Cellular immunity to viral antigens limits E1-deleted adenoviruses for gene therapy. *PNAS*, 91: 4407-4411.

Yang, Y, Nunes, FA, Berencsi, K, Gonczol, E, Englehardt, JF, Wilson, JM. (1994b) Inactivation of E2a in recombinant adenoviruses improves the prospect for gene therapy in cystic fibrosis. *Nature Genetics*, 7: 362-369.

Zlokovic, BV and Apuzzo, MLJ. (1997b) Cellular and Molecular Neurosurgery: Pathways from Concept to Reality – Part I: Target Disorders and Concept Approaches to Gene Therapy of the Central Nervous System. *Neurosurgery*, 40(4): 789-803.

Zlokovic, BV and Apuzzo, MLJ. (1997b) Cellular and Molecular Neurosurgery: Pathways from Concept to Reality – Part II: Vector Systems and Delivery Methodologies for Gene Therapy of the Central Nervous System. *Neurosurgery*, 40(4): 805-812.